THE SPUZZUM PLUTON NORTHWEST OF HOPE, B. C.

by

MARK RICHARD VINING

B.Sc., University of Washington, 1974

A THESIS SUBMITTED IN PARTIAL FULFILLMENT OF

THE REQUIREMENTS FOR THE DEGREE OF

MASTER OF SCIENCE

in

THE FACULTY OF GRADUATE STUDIES

(Department of Geological Sciences)

We accept this thesis as conforming

to the required standard

THE UNIVERSITY OF BRITISH COLUMBIA

April, 1977

In presenting this thesis in partial fulfilment of the requirements for an advanced degree at the University of British Columbia, I agree that the Library shall make it freely available for reference and study. I further agree that permission for extensive copying of this thesis for scholarly purposes may be granted by the Head of my Department or by his representatives. It is understood that copying or publication of this thesis for financial gain shall not be allowed without my written permission.

Department of Geological Sciences

The University of British Columbia
2075 Wesbrook Place
Vancouver, Canada
V6T 1W5

Date 13 April 1977

ABSTRACT

The Spuzzum Batholith underlies an area northwest of Hope, B.C. It is nearly 60 km. long in a northerly direction and 10 to 20 km. across. The southern part of the body is zoned from pyroxene diorite in its core, through hornblende diorite, to biotite-hornblende tonalite. Tonalite forms about two thirds of the pluton's area, forming a nearly continuous rim. The pluton intrudes upper Paleozic Chilliwack Group, the Cretaceous(?) Giant Mascot Ultramafic Body, and Settler Schist of unknown age. K-Ar ages for tonalite and diorite range from 76 to 103 m.y.

Diorite consists of subhedral orthopyroxene and plagioclase (An_{62} to An_{41}), with variable amounts of hornblende and clinopyroxene. Tonalite is largely composed of anhedral quartz and biotite, and subhedral hornblende and plagioclase (An_{50} to An_{32}). Tonalite and some diorites are foliated. These rocks are locally hornblendized, resembling hornblende gabbro. Pods of directionless hornblendite are common in hornblendized rocks.

Foliations and mineralogical zonation outline a crude tongue-like structure, modified by later deformation. Spuzzum diorite appears to have intruded the main part of the Giant Mascot Ultramafic Body but some hornblendites are younger than diorite.

The Giant Mascot Ultramafic Body, 2 by 3 km., is zoned from dunite or peridotite, through pyroxenite, to a rim of hornblendite up to 100 m. across. Hornblendite occurs also as dykes.

Orthopyroxenes of Spuzzum diorite are weakly aluminous hypersthene; those of the contact with Giant Mascot pyroxenite are bronzite. Clinopyroxenes of the same rocks are somewhat more aluminous salites and diopsides. Hornblendites from Spuzzum diorite and the Giant Mascot Ultramafic Body resemble alkali basalt in composition. Hornblende analyses fall into three categories: edenite, pargasite-common hornblende, and thirdly, more iron-rich common hornblende.

It is concluded that Spuzzum diorite and tonalite originated by crystal settling from quartz diorite magma at depth, followed by diapiric rise of a zoned pluton composed of residual tonalite liquid cored by drawn-up dioritic cumulate. A mathematical test shows the compositions of diorite and tonalite to be consistent with this hypothesis. The rising pluton subsequently engulfed the Giant Mascot Ultramafic Body. Hornblendites may have formed by metasomatism of these rocks and adjacent diorite or tonalite as a consequence of the second boiling of tonalite and the coursing of resultant hydrothermal fluid through the nearly solid pluton.

CONTENTS

APPENDICES

LIST OF TABLES

LIST OF FIGURES

LIST OF FIGURES

LIST OF PLATES

ACCOMPANYING MAPS

(in pocket)

Geology Between the Fraser River and Emory Creek, Northwest of Hope, B. C.

Mineralogical Zonation in the Spuzzum Pluton (on same sheet)

I. INTRODUCTION

A. General Statement

The object of this thesis was to examine and describe that part of the Spuzzum Pluton that lies between American Creek and Emory Creek near Hope, B. C., and also to determine the contact relationships between the Giant Mascot Ultramafic Body and the surrounding Spuzzum Pluton.

B. Location and Access

The thesis area, about 11 by 12 kilometres, is approximately centred on the Giant Mascot Copper-Nickel Mine 10 kilometres northwest of Hope. Mapping was carried on mainly within the American Creek and Emory Creek watersheds, and, to a lesser extent, in the north part of the Garnet Creek watershed (fig. 1). Much of the area, except the upper part of Stulkawhits Creek, has been extensively logged within the last several years. Networks of logging roads cover the countryside except at high elevation. Although most of these roads are in very poor repair, making even poor foot trails, they were very useful during mapping.

Elevations range from near sea level at the Fraser River to just over 1500 metres; valley bottoms in the thesis area lie from 600 to 1070 metres. Areas not logged are heavily forested except for occasional open areas on ridgetops. Outcrop is generally scarce and difficult to place on the map except in logged areas or on ridgetops.

C. Previous Work

The Spuzzum Intrusions, hornblende tonalite and minor diorite, were first studied by Morris (1955), and later by McTaggart and Thompson (1967),

Fig. 1
GENERAL LOCATION MAP OF THE GREATER HOPE AREA, B. C.
(thesis area outlined in dashed line)

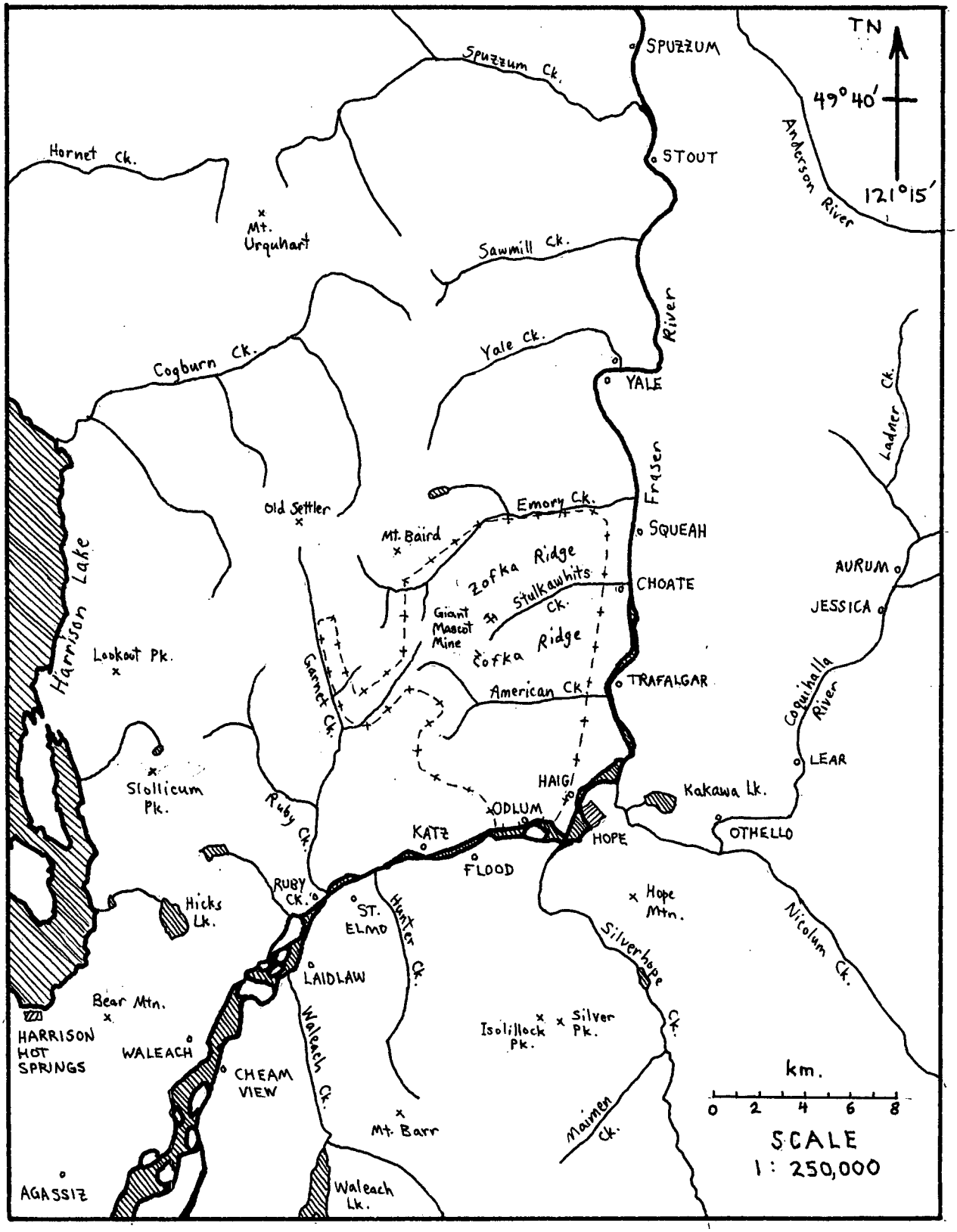

the type area being near Spuzzum, north of Yale, B. C. At that time the plutonic rocks in the area of this thesis were included in the Chilliwack Batholith (Cairnes, 1944). McTaggart and Thompson (1967) also distinguished the Yale Intrusions, sills and stocks of granodiorite to tonalite, and considered them to be younger than type Spuzzum tonalite. Roddick and Hutchinson (1970) described the Scuzzy Pluton of leucocratic granodiorite northwest of Yale. The most comprehensive effort to sort out plutonic rocks near Hope was by T. A. Richards (Richards and White, 1970; and Richards, 1971). He assigned to the Spuzzum Intrusions the rocks that are the subject of this study, and distinguished several other stocks and plutons south of Hope which had previously been assigned to the Chilliwack Batholith. His work has been recently revised and condensed (Richards and McTaggart, 1976).

The Giant Mascot Ultramafic Body was studied in detail by Aho (1956), but little was done to relate his findings to regional geology. McLeod (1975) studied ore genesis in a drift of the Giant Mascot Mine. Lowes (1971) studied in detail the structure and metamorphism of rocks between the Fraser River and Harrison Lake. In more recent exploratory efforts by Giant Mascot Mines Ltd. and the B. C. Department of Mines and Petroleum Resources, the ultramafic rocks between the Fraser River and Harrison Lake have been remapped (Eastwood, 1971; and unpublished material by Giant Mascot Mines, Ltd.). Detailed studies of schists in contact with Spuzzum tonalite include Read (1960), Richards (1971), Lowes (1971), and Pigage (1973).

D. Present Investigation

Field work for this thesis was carried on mostly during the summer months of 1975, and laboratory work during the winter and spring of 1976.

Mapping was done on 20 chain airphotos made by the government of British Columbia and enlarged sections on 1:50,000 National Topographic Series maps. For the vicinity of the Giant Mascot property a 1:3600 map was made available by Giant Mascot Mines, Ltd.

E. Acknowledgements

This thesis was prepared under the supervision of K. C. McTaggart, to whom I am thankful for guidance, encouragement, and field assistance. Thanks are given to Mr. F. W. Holland of Giant Mascot Mines, Ltd., for lodging at the mine; to Dr. P. A. Christopher of the B. C. Department of Mines and Petroleum Resources for initiating the project, financial support, and field assistance; to Mr. C. L. Hronek of Vancouver, B. C., for assistance on some traverses; and to Mr. Allen Doherty of the University of New Brunswick for invaluable field assistance through August 1975. The B. C. Department of Mines and Petroleum Resources provided field equipment and a special research grant.

II. GENERAL GEOLOGY

A. Introduction

The mid-Cretaceous Spuzzum Pluton lies on the southeastern margin of the Coast Plutonic Complex in the axial belt of the Northern Cascades structural system (Monger, 1970). It intrudes Settler Schist primarily (fig. 2), but also the Chilliwack Group in the southwest, and in the northwest, gneiss which may be the migmatized equivalent of Settler Schist (McTaggart and Thompson, 1967). Non-plutonic rocks in this region include: (1) Custer (Skagit) Gneiss east of the Hope Fault, a high grade migmatitic complex of layered gneiss and schist; (2) Upper Paleozoic Hozameen Group east of the Yale Fault, composed of ribbon chert, pelite, basic volcanics, and minor limestone; (3) Upper Paleozoic Chilliwack Group to the west, composed of pelite, sandstone with minor conglomerate, pyroclastics, basic volcanics, limestone, and minor chert; (4) Jurassic Ladner Group northeast of the Hozameen Fault, composed of pelite, volcanic sandstone, and minor conglomerate and volcanics; and (5) Eocene conglomerate and minor sandstone adjacent to the Hope Fault on the east, forming a narrow belt that pinches out north of the thesis area (McTaggart and Thompson, 1967; Monger, 1970; McTaggart, 1970).

Ultramafic rocks occur in a crudely northwest-trending belt with its southern end at the Giant Mascot Mine. These rocks consist of gabbro to partly serpentinized peridotite and, except for the Giant Mascot Ultramafic Body, have been considered alpine type (McLeod, 1975). The Coquihalla Serpentinite Belt stretches along the Hozameen Fault east of the Fraser River.

Fig. 2
GENERAL GEOLOGY MAP OF THE GREATER HOPE AREA, B. C.

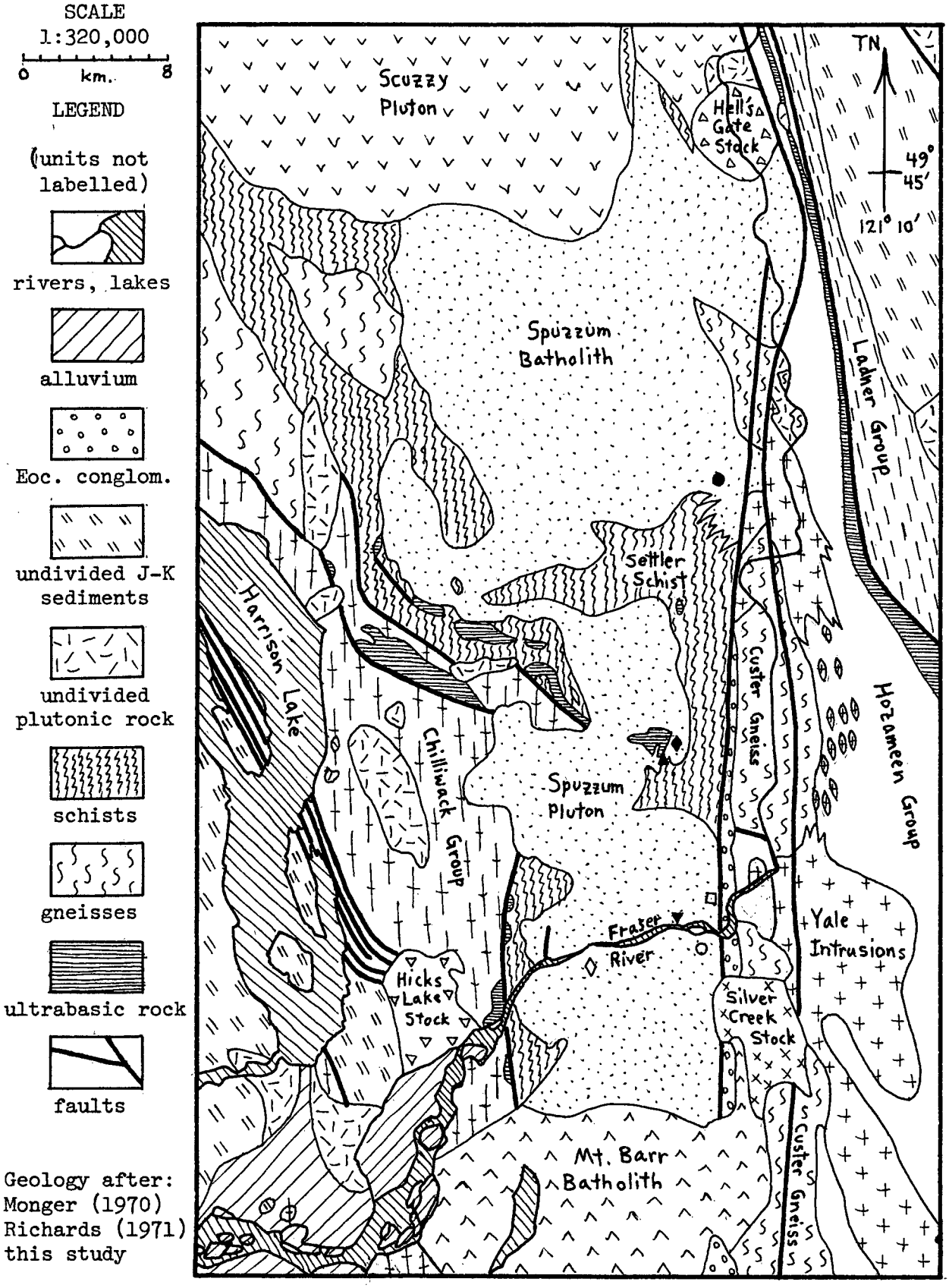

Intrusive rocks neighboring the Spuzzum Pluton include: (1) Scuzzy Pluton of uncertain age to the northwest, composed of coarse leucocratic granodiorite with minor tonalite; (2) Eocene and Paleocene Yale Intrusions forming a north-trending belt east of the Fraser Canyon, a heterogeneous assemblage ranging from granite to gabbro, granodiorite being most abundant; (3) Early Oligocene Silver Creek Stock south of Hope, composed of homogeneous mesocratic tonalite; (4) Early Oligocene Hell's Gate Stock at Hell's Gate, composed of fine-grained granodiorite or trondhjemite; and (6) Middle Miocene Mount Barr Batholith to the south, a four phase complex ranging from tonalite to quartz monzonite (Roddick and Hutchinson, 1970; and Richards, 1971). The Hicks Lake Stock west of Ruby Creek, composed of mafic tonalite, is correlated with phase 1 of the Mount Barr Batholith (Richards, 1971).

B. Settler Schist

North of Emory Creek, Settler Schist consists of layered pelitic schist, graphitic pelitic schist, quartzofeldspathic schist, micaceous quartzite, and minor calc-silicate layers and talc-anthophyllite pods. Pelitic assemblages are typical of staurolite through sillimanite zones of the Barrovian facies series. Pelitic and calc-silicate assemblages indicate pressures and temperatures of 5.5 to 8 kilobars and 550 to 700° during regional metamorphism (Pigage, 1973).

Richards (1971) described upgrading near the contact with Spuzzum tonalite thus:

> "A later contact metamorphic aureole some 1000 yards wide was superimposed on the regionally metamorphosed schists. In the schists close to the contact with the tonalite, fibrolite and sillimanite occur with muscovite and biotite while further away coarse porphyroblasts of muscovite and chlorite pseudomorph staurolite. Thus, it appears that the tonalite has truncated the earlier-formed regional metamorphic isograds and superimposed a younger thermal metamorphism upon the older regional metamorphism." (p. 30)

Richards concluded that contact metamorphism took place at a pressure of about 4.5 kilobars, which corresponds with a depth of about 13 kilometres.

C. Giant Mascot Ultramafic Body

An irregular shaped body, zoned crudely from hornblendite to peridotite, is situated at the Giant Mascot Copper-Nickel Mine. The 2 by 3 kilometre body consists of pipes of olivine pyroxenite or dunite surrounded by pyroxenite which is the most common rock type. This is in turn surrounded by a remarkable marginal zone of coarse pegmatitic hornblendite up to 100 metres across. The southwest half of the body is a highly varied hornblendic assemblage that contains many bodies of feldspathic rocks, hornblendite dykes, and various other rocks. Copper and nickel orebodies are in this part of the ultramafic body (Aho, 1956).

The different varieties of ultramafic rocks are closely related; most of their mutual contacts are gradational, but some are sharp locally. The body as a whole is in line with, and may be related to, a string of gabbro or hornblendite to pyroxenite or dunite bodies in schist to the northwest (Lowes, 1971). The associated feldspathic rocks, mainly hypersthene-augite-hornblende diorites but also gabbroic rocks and

norite, appear to have conflicting age relationships, cutting and being cut by one another and the ultramafic rocks. A large degree of contemporaneity between them and the ultramafic rocks is suggested (Aho, 1956).

Potassium-argon ages of ultramafic rocks of orebodies range from 104 to 119 million years. Hornblendite dykes have an age of 95 million years and are the youngest ultramafic rocks (McLeod, 1975).

Aho (1956) interpreted the mineralogical zonation in orebodies, that is pyroxenite to dunite, as resulting from conversions between orthopyroxene and olivine by hydrothermal addition or subtraction of SiO_2. Many of the mutually crosscutting relationships in these rocks support this hypothesis. McLeod (1975) preferred to explain the overall zonation pattern and interstitial sulphides by diapiric intrusion of an ultramafic crystal - sulphide melt mush that may have preceded the Spuzzum Pluton. Similarities in mineral compositions between ultramafic rocks and surrounding feldspathic rocks, as well as the intimate field relationships among them, support this view (Aho, 1956; McTaggart, 1971; and McLeod, 1975).

D. Spuzzum Pluton

Diorite and tonalite of the Spuzzum Intrusions (McTaggart and Thompson, 1967), or the Spuzzum Batholith (Richards and McTaggart, 1976), extend for many kilometres along the west side of the Fraser River north of Hope, forming one of the large plutons of the Coast Plutonic Complex (fig. 2). In the north it consists mainly of biotite-hornblende tonalite, and fairly common hornblende diorite with occasional hornblendite bodies (McTaggart and Thompson, 1967). In the south tonalite remains the same, but diorite has a distinct mineralogical zonation. This zonation is concentric and

characterized by pyroxene diorite in the middle grading continuously to pyroxene-hornblende diorite at the contact with tonalite, but these types are nearly the same chemically (Richards, 1971). Tonalite in the south forms an outer sheath to the intrusion, containing the zoned diorite core. Tonalite is gneissoid in all parts of the batholith; diorite in the south, however, may be directionless or weakly foliated. The southern part of the batholith appears to have a tongue-shaped structure, and may have been intruded as a pluton separate from the northern part but contemporaneous with it.

In the north tonalite shows a gradational and conformable contact with metamorphic rocks correlated by McTaggart and Thompson (1967) with the Hozameen Group. In the south the Spuzzum Batholith intrudes Settler Schist and Giant Mascot ultramafic rocks (Richards, 1971; and McLeod, 1975). Small to large xenoliths of gneiss and schist are included in tonalite in all parts. In some places schist and marble xenoliths occur in diorite in the south.

Potassium-argon ages from all parts of the batholith are listed in table I, and their localities are shown in fig. 2. Ages range from 76 to 103 million years, some determinations being concordant between hornblende and biotite. There is not a clear separation between ages of tonalite and diorite, but tonalite ages are generally younger. Considering that this area has undergone considerable metamorphism, plutonism, and deformation, resetting is easily possible and these ages should be considered minimum (Monger, 1970). Tonalite was considered to be younger than diorite (Richards, 1971), intruding it along its contact with country rock. In this study the hypothesis that diorite and tonalite were intruded as a single zoned pluton is favoured. Both Richards and this author have considered only the

TABLE I

COMPILATION OF K-AR AGE DETERMINATIONS

FOR THE SPUZZUM BATHOLITH

Symbol in fig. 2	Reference	Age (m.y.)	Mineral	Rocktype
● <	McTaggart and Thompson (1967)	76 ± 4	Bio	tonalite
		76 ± 3	Hbd	tonalite
◊ <	Richards and White (1970)	103 ± 5	Bio	tonalite
		103 ± 5	Bio	tonalite
□ <	"	79 ± 4	Hbd	tonalite
	"	81 ± 4	Bio	tonalite
○	"	83 ± 4	Bio	tonalite
♦ <	McLeod (1975)	85.1 ± 2.8	Hbd	tonalite
	"	79.4 ± 2.5	Bio	tonalite
▲	"	89.6 ± 3.1	Hbd + Px	diorite
▼	"	89.5 ± 2.8	Hbd	diorite

southern part of the larger Spuzzum Batholith, this author hereafter referring to that part only as the Spuzzum Pluton.

E. Regional Structure

> " The structure of the Cascade Mountains, as detailed by Misch (1966), in northern Washington State and Southern British Columbia, is that of a central north-northwesterly trending gneiss complex, comprising rocks of the Skagit Metamorphic Suite, flanked by thrust plates that overlie autochthonous Mesozoic rocks."
> (Lowes, 1971, p. 6)

The Skagit Metamorphic Suite (Custer Gneiss) disappears in the Fraser Canyon; in Washington it is bounded on the west by the Straight Creek Fault and on the east by the Ross Lake Fault (Misch, 1966). A narrow graben, formed by the Hope and Yale Faults, extends from the international border northward through Hope, and onward for about 250 kilometres. This graben may be part of a major tectonic boundary extending into Yukon Territory (Price and Douglas, 1972).

The steeply dipping Hozameen Fault bounds the Hozameen Group on the east in southern British Columbia. In the North Cascades of Washington the fault is called the Ross Lake Fault Zone (Misch 1966) and is a west-dipping thrust fault. The Hozameen Fault appears to cross the Fraser Canyon Fault Zone (Hope and Yale Faults) and east of the Fraser Canyon is marked by a conspicuous belt of serpentinite. McTaggart and Thompson (1967) regarded the fault as being older than the Fraser Canyon Fault Zone, extending northwestward from it at a low angle near Keefers, B. C.

West of the metamorphic core the Church Mountain Thrust Plate, mainly Chilliwack Group, overlies Mesozoic rocks. This is in turn overlain by the Shuksan Thrust Plate of phyllite and greenschist of uncertain age in Washington (Misch, 1966). The Church Mountain Thrust extends northward

and passes beneath Harrison Lake, where Chilliwack Group rocks are in faulted contact with Mesozoic rocks to their west. Faultbound and sheared mafic and ultramafic rocks in Settler Schist west of the Spuzzum Pluton may mark the northward extension of the root zone of the Shuksan Thrust (Lowes, 1971).

Folding and faulting in this region are the result of several episodes of deformation, some involving metamorphism and plutonism. McTaggart and Thompson (1967) summarized the deformational periods in south central British Columbia thus:

> "1. Northwest-trending folding and faulting during the development of the Custer Gneiss, affecting both Custer and Hozameen rocks (late Paleozoic or early Mesozoic?).
> 2. Northeasterly folding and thrusting (mid-Cretaceous?).
> 3. Deformation associated with the Hozameen Fault (mid Cretaceous?).
> 4. Folding and metamorphism of the Hozameen Group northwest of Hope [Settler Schist] and northwest of Stout, with accompanying emplacement of the Spuzzum Intrusions (late Late Cretaceous).
> 5. North-south folding and faulting along Fraser River (Eocene and earlier?).
> 6. Deformation (slight) accompanying emplacement of the Chilliwack batholithic rocks (Miocene and earlier?)." (p. 1222)

III. SPUZZUM PLUTON

A. Introduction

Richards (1971) divided the Spuzzum Pluton south of American Creek, into two major units, biotite-hornblende tonalite and diorite. He further subdivided diorite into three types separated by gradational contacts: (1) hypersthene-augite diorite, (2) augite-hypersthene-hornblende diorite, and (3) biotite-hypersthene-hornblende diorite. North of American Creek rapid variation in amounts of biotite and pyroxenes makes Richards' types difficult to map and, in addition, the area is complicated by the occurrence of another distinctive type. Therefore Spuzzum diorite "proper" is subdivided in this study on the criterion of relative abundance of hydrous versus anhydrous mafic minerals. Two major categories are defined: pyroxene diorite and hornblende diorite depending on whether or not pyroxene > hornblende + biotite (+ chlorite). Tonalite is characterized by lack of pyroxene and abundance of quartz. These rocks occur in a concentrically zoned pattern with pyroxene diorite in the core surrounded by hornblende diorite, in turn surrounded by tonalite (map in pocket). Rocks believed to have formed by the hornblendization of diorite or tonalite, characterized by abundance of hornblende, with plagioclase and perhaps quartz and biotite, but no pyroxene, fall into a fourth category. This type grades to normal diorite or tonalite. Small ultramafic bodies, widespread and locally very abundant, are closely associated with hornblendized rocks. Small bodies of tonalitic and rarer dioritic pegmatite occur throughout the Spuzzum Pluton.

B. Petrography

1. Zoned Diorite and Tonalite

Since diorite and tonalite are considered to be closely related genetically and to form a single intrusive body, they are treated as a single unit. In general these rocks are weakly seriate porphyritic, medium-grained, and leuco- to mesocratic. Average modes and optically determined plagioclase compositions for pyroxene diorite, hornblende diorite, and tonalite are listed in tables IIa and b and shown in fig. 3. Modes and mineralogical data for individual specimens are listed in appendix I. The interpreted crystallization sequences for these rocks are shown in fig. 4.

Plagioclase becomes less calcic and decreases in amount from pyroxene diorite to tonalite. Small grains are anhedral and larger ones are dominantly subhedral. Small grains are generally unzoned but larger grains consistently have sub- to euhedral weakly oscillatory normal zoning, with superimposed weak to strong patchy zoning. Carlsbad twins, many showing syneusis, are abundant in larger grains. Deformational albite and rarer pericline polysynthetic twins are abundant in all grains, except in tonalite in which fine grains have little or no twinning. Plagioclase of most pyroxene diorite is unaltered and minute inclusions (hematite?) commonly give it a pink colour. Some large grains are bent or polygonized. In hornblende diorite the pink colour is rare, and large grains are commonly bent, occasionally broken, and enclosed in finer subgranoblastic matrix. Plagioclase of tonalite is white and some contains muscovite and epidote. Grains are commonly bent, broken, or polygonized, and recrystallized mortar is abundant.

TABLE IIa

AVERAGE MODES OF THE SPUZZUM PLUTON

Mineral	Hornblendized Rocks	Transition	Pyroxene Diorite	Hornblende Diorite	Tonalite
Qz	.6	1.7	1.4	7.2	15.7
Plag	53.1	56.7	64.5	60.4	51.3
Opx	0	10.5	16.9	7.4	0
Cpx	0	tr	10.3	2.6	0
Hbd	44.7	30.5	5.4	14.6	22.1
Bio	1.0	.3	.5	6.6	9.5
Chl	0	0	0	0	.8
Ep	0	0	0	0	.2
Ap	.1	tr	.1	tr	tr
Opaque	.7	.3	.9	1.2	.5
Total	100.2	100.0	100.0	100.0	100.1
Colour index	46.3	41.6	34.1	32.4	33.0
No. in average	12	3	16	5	12

TABLE IIb

AVERAGE OPTICALLY DETERMINED PLAGIOCLASE COMPOSITIONS

	Hornblendized Rocks	Transition	Pyroxene Diorite	Hornblende Diorite	Tonalite
high	65.8	69.7	62.1	53.8	50.0
low	43.5	46.3	43.7	41.2	32.5
average	54.7	58.0	52.9	47.5	41.3
No. in average	8*	3	14	5	10

* two of the twelve analyses have no plagioclase determinations

Note: Values are compiled from appendix I; abbreviations are the same. "Transition" refers to a type transitional between fully hornblendized and normal diorites. Where more than five plagioclase determinations are available, high and low values are discarded.

Fig. 3

MODAL VARIATION DIAGRAM FOR THE SPUZZUM PLUTON

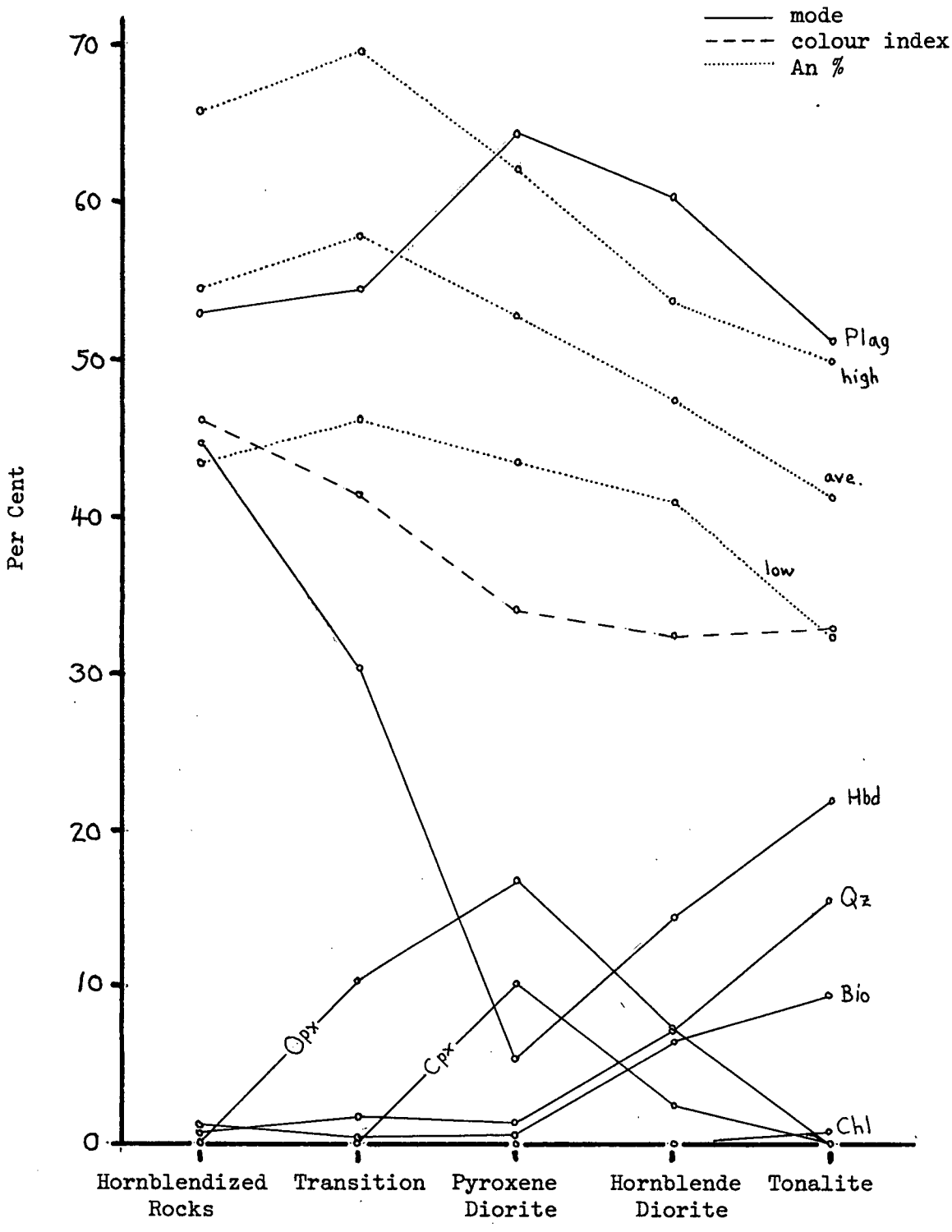

Fig. 4

CRYSTALLIZATION SEQUENCES FOR ROCKS

OF THE SPUZZUM PLUTON

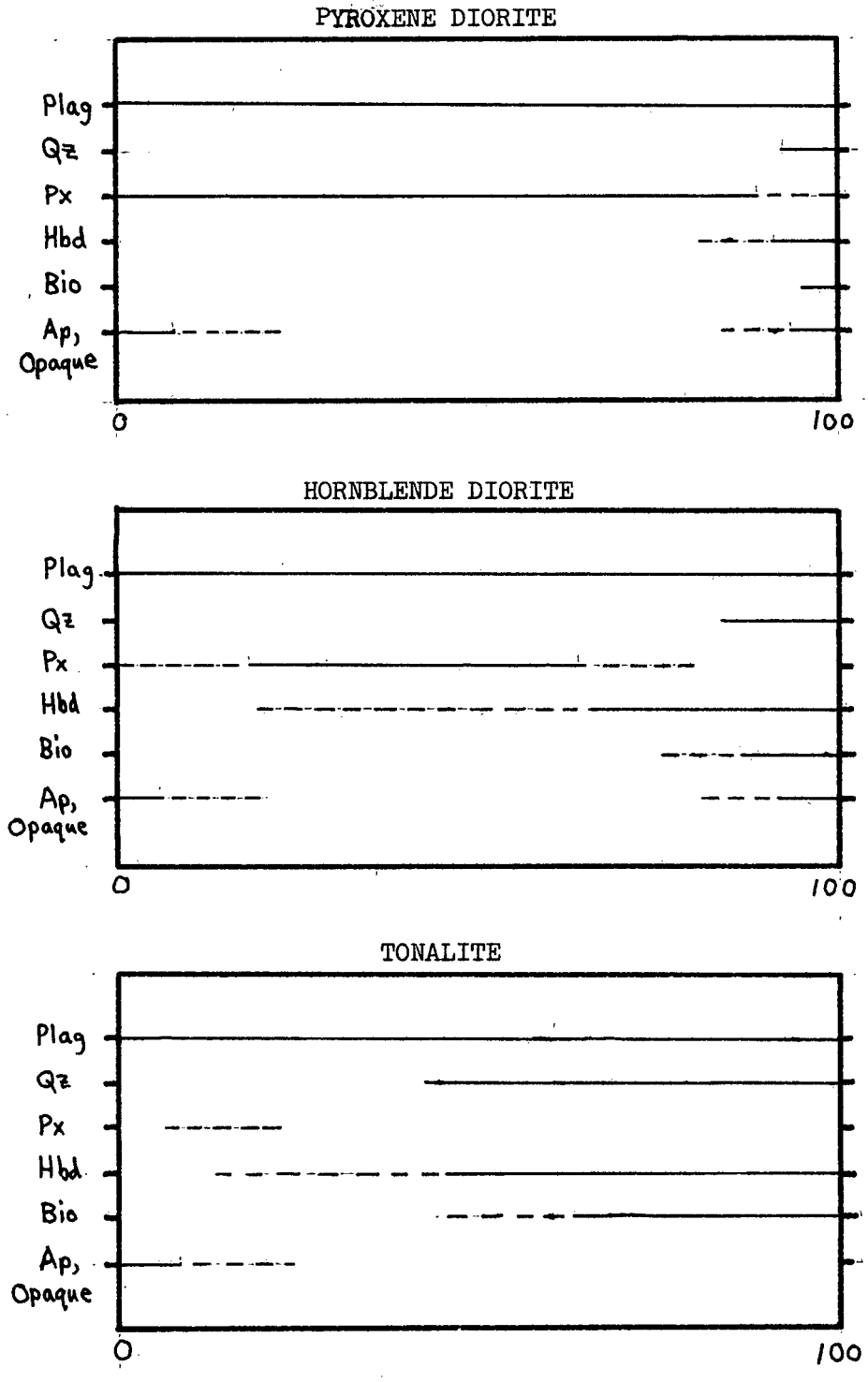

Quartz is fine- to medium-grained, anhedral, and interstitial. Large rounded grains occur in tonalite, but in pyroxene diorite it is confined to clusters of pyroxenes. Strain shadows and polygonization are increasingly abundant from pyroxene diorite to tonalite. Annealing has occurred in some specimens.

Pyroxenes are present in diorite, but not in tonalite. Augite is more severely corroded than hypersthene, in many cases appearing "moth eaten." Both varieties are fine- to medium- or coarse-grained, dominantly subhedral and elongate, with large grains tending to cluster together. Many specimens are coarsely glomeroporphyritic, some specimens having finer-than-average plagioclase. Fine lamellar exsolution is abundant in both pyroxenes on (100), commonly with exsolved blebs in cores of larger grains. Platelets of hematite (?) oriented on (100) and possibly other planes are almost ubiquitous. Augite has abundant simple twinning on (100). As the amount of hornblende increases, augite becomes mottled with tiny structurally continuous blebs of the amphibole. This replacement follows simple zoning in some augite crystals.

Hornblende ($2V_{\alpha} \approx 80^{\circ}$, $\delta \approx .024$; $\gamma \wedge c \approx 18^{\circ}$) is fine- to coarse-grained, anhedral and generally interstitial. The amphibole is pleochroic: $\beta = \gamma > \alpha$, α = pale yellow, β = brownish olive, γ = olive green In tonalite and some hornblende diorite, rims or whole crystals may have β = green and γ = bluish green. In diorite it rims, embays, and encloses pyroxenes. It appears to pseudomorph pyroxene glomerocrysts in some hornblende diorites and one tonalite specimen (24/7/75/1). Irregular clouds of oriented opaque inclusions suggest replacement of pyroxene with hematite platelets. Clouds of worm-like quartz inclusions, common in

tonalite and seen in some hornblende diorites, also suggest replacement of pyroxene. Colourless amphibole ($2V \approx 90^\circ$, $\delta \approx .028$, $\gamma \wedge c \approx 19^\circ$), occurs as skin against hypersthene inclusions in hornblende in diorite, or as irregular patches in hornblende of hornblende diorite or tonalite.

Biotite is fine- to medium-grained (coarser in tonalite), anhedral, and interstitial. It has pale yellow to deep or reddish brown pleochroism. Biotite generally occurs with hornblende, the two together rimming pyroxene in diorite. In diorite it is generally undeformed, but it is commonly bent, pinched, or kinked in tonalite. Chlorite replaces biotite slightly in hornblende diorite, and abundantly in tonalite.

Accessories include small elongate to large irregular apatite, rounded to skeletal or acicular opaques and fibres of rutile (?, length slow, straight extinction, high relief) in quartz. Opaque minerals are primarily pyrite and pyrrhotite with variable amounts of hematite from weathering. Tourmaline (ω = dark bluegrey, ϵ = pink, $\delta \approx .035$) occurs in one tonalite as bundles of euhedral acicular crystals. Epidote is common in small amounts in most tonalites, occurring in a few specimens as euhedral inclusions in biotite and plagioclase, and as scattered clusters of fine grains.

Several specimens have textures that appear metamorphic. In one hornblende diorite specimen (30/7/75/2a), hypersthene poikiloblastically encloses hornblende and biotite and is anhedral. It contains no hematite platelets. Bands of recrystallized mortar are abundant. Several pyroxene diorites have granoblastic plagioclase-hornblende-pyroxene matrices, and large plagioclase grains contain rounded to subhedral pyroxene or hornblende inclusions. One of these has large skeletal hypersthene crystals among ordinary pyroxene grains. Quartz is unstrained in these specimens.

In several pyroxene diorites and one hornblende diorite, large skeletal individual sulphide grains enclose and embay pyroxene and plagioclase. Anhydrous silicates and sulphide are separated by a monocrystalline, thin but continuous, skin of hornblende. This texture is not abundant, but widespread and conspicuous.

2. Hornblendized Rocks

Hornblendized rocks resembling gabbro with hornblende as the only major mafic mineral and showing strong textural evidence of replacement, are irregularly distributed through the Spuzzum Pluton, superimposed on the typical zonation. This type is found in all diorites, and in a few localities appears in tonalite. Contact with surrounding rock is gradational over distances of centimetres to tens of metres. It is clearly associated with hornblende veins and hornblendite pods seen most commonly in diorite. Pigage (1975, personal communication) reported gradual variation from tonalite to hornblendite north of Emory Creek. McTaggart and Thompson (1967) described diorite of the Spuzzum Batholith near Spuzzum, B. C., thus:

> "Medium-grained diorite in which hornblende approaches 50% of the rock is fairly common and hornblendite is seen occasionally." (p. 1211)

Hornblendized rocks are interpreted to result from alteration of diorite or tonalite contemporaneous with the formation of hornblendite dykes, pods, and veins which are described in the next section.

Three specimens of hornblendized diorite are classified as transitional to diorite. Two tonalite specimens are unusually mafic and may also be hornblendized. Averaged modes and plagioclase compositions for the three hornblendized diorites are listed in tables IIa and b and shown in fig. 3. Modes and mineralogical data for individual specimens are listed in appendix I.

Rocks of this unit are meso- to melanocratic, medium-grained, and inequigranular. Plagioclase compositions range widely and average slightly higher than the average of pyroxene diorite. Smaller grains are anhedral, and larger ones are an- to subhedral and commonly altered with inclusions of epidote minerals, sericite, or hornblende. Small grains are commonly unzoned but large ones have abundant strong patchy zoning, with relict an- to subhedral oscillatory normal zoning. Carlsbad twins are common in larger grains, and deformational albite and pericline twinning is abundant. Phenocrysts commonly appear polygonized or bent, enclosed in a subgranoblastic matrix of plagioclase and hornblende.

Hornblende (similar to that in tonalite) is fine- to coarse-grained and an- to subhedral, forming dense decussate clots or stringers. Small an- to subhedral crystals are commonly superimposed on large interlocked irregular grains. Simple and lamellar twinning are common on (100), but in some sections rims are untwinned. Cores of clots commonly contain patches of colourless amphibole (see previous section) suggesting replacement of hypersthene. In one specimen hornblende appears to form pseudomorphs after glomeroporphyritic pyroxenes (20/8/75/3). In general, hornblende embays and includes corroded remnants of plagioclase. In some specimens fine-grained subgranoblastic plagioclase is replaced and pseudomorphed by hornblende, while large plagioclase graqns are relatively unchanged.

Biotite is fine- to medium-grained, occurring as scattered flakes with hornblende. Chlorite occurs as small irregular flakes or bundles in hornblende clots. Opaque minerals form small blebs in hornblende clots, or dusty patches, some oriented, in large hornblende crystals. Small round to euhedral grains of apatite are generally in hornblende clots.

Quartz forms rare anhedral grains with plagioclase. It may or may not have strain shadows. Pyroxenes are found in transitions to diorite. Most of these are hypersthene and occur as corroded relics in hornblende clots.

3. Ultramafic Bodies

Richards (1971) reported 1/2 to 2 inch thick pyroxenite replacement bodies in pyroxene diorite south of the Fraser River. In this study pyroxenite bodies were found only at the head of the north fork of American Creek. These are under 10 centimetres in longest dimension and irregular in shape, occurring in directionless pyroxene diorite with metamorphic textures (specimen 10/7/75/3; see above, page 20).

Hornblendite occurs at many localities as rounded to irregular, commonly complexly interconnected pods less than one metre in largest dimension (plates 1 and 2). These, with few exceptions, have sharp contacts and occur exclusively in hornblendized diorite or tonalite. In some localities pods are elongate in the foliation of the host, but are not foliated internally (plate 3); in other places the foliation is truncated or contorted by irregular pods. More commonly the host rock is directionless.

Hornblendite also occurs as dyke- or pipe-like bodies up to several metres in width, which are accompanied by small pods. Northwest of Odlum, large parallel slabs of hornblendized diorite with extremely sharp contacts are surrounded by hornblendite (fig. 5a). A schist xenolith is divided into three parts by the confluence of two hornblendite dykelets (fig. 5b). In the same pipe-like body are rounded to angular, equant to irregular

inclusions of hornblendized diorite, some appearing displaced (fig. 5a), others having their foliation concordant with the surrounding foliation suggestive of replacement. Common domelike protrusions of hornblendite into hornblendized diorite, and irregular sutured contacts suggest resorption or assimilation of the latter (figs. 5c and d). Several of these relationships occur in a pipe-like body of hornblendite south of the fork in American Creek (plates 10 and 11).

Hornblendite forms stringers parallel to the foliation in large schist xenoliths (fig. 5e), northwest of Odlum, and to a lesser degree at the Giant Mascot Mine. In several places, but especially well exposed northwest of Odlum, pegmatite dykelets and veins appear to be replaced by hornblendite (plate 8). These are accompanied by very thin veins of hornblende, and host diorite grades to hornblendized diorite close to these veins. This is especially well displayed in pyroxene diorite on the southwestern flank of Zofka Ridge (plates 12 and 13).

Hornblendites from the Spuzzum Pluton are medium- to coarse-grained, inequigranular, and decussate. They contain scattered anhedral chlorite, and rare corroded plagioclase. Most large hornblende grains are poikilitic, containing small sub- to anhedral ones. Optical properties appear the same as hornblende of hornblendized rocks, except that hornblende of thin veins is entirely bluegreen whereas hornblende from larger bodies is olive with bluegreen rims. A specimen from northwest of Odlum has oriented opaque platelets in a large minority of hornblende grains, suggestive of pyroxene replacement.

Plate 1. Irregular hornblendite pods in hornblendized diorite, south fork of American Creek. (19/6/75/5)

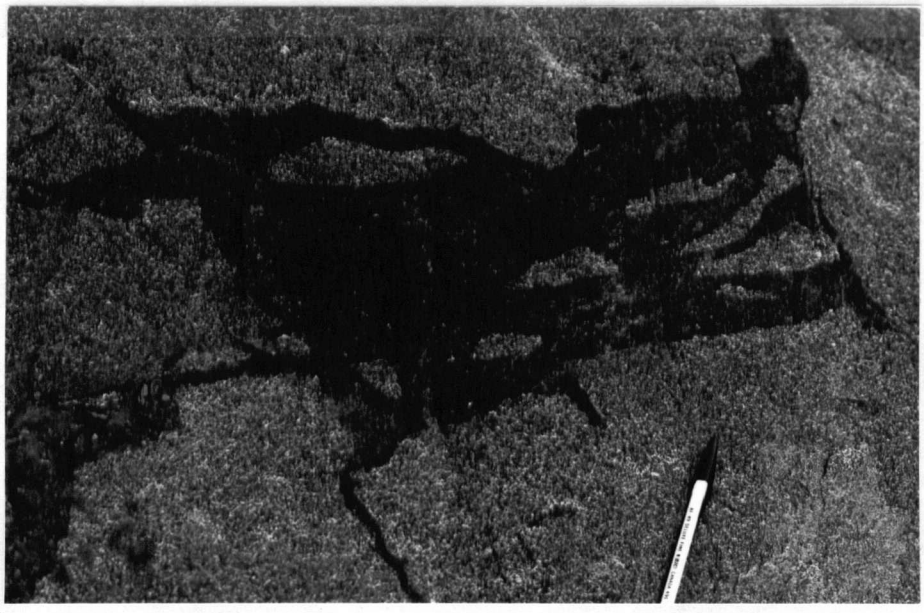

Plate 2. Hornblendite body in pyroxene diorite southwest of location in plate 1. Hornblende stringers appear to follow fractures in diorite. Note diorite xenoliths. (1/7/75/6)

Plate 3. Hornblendite pod elongated in the foliation of hornblendized diorite. Note leucocratic patches and fault offset. (20/6/75/6)

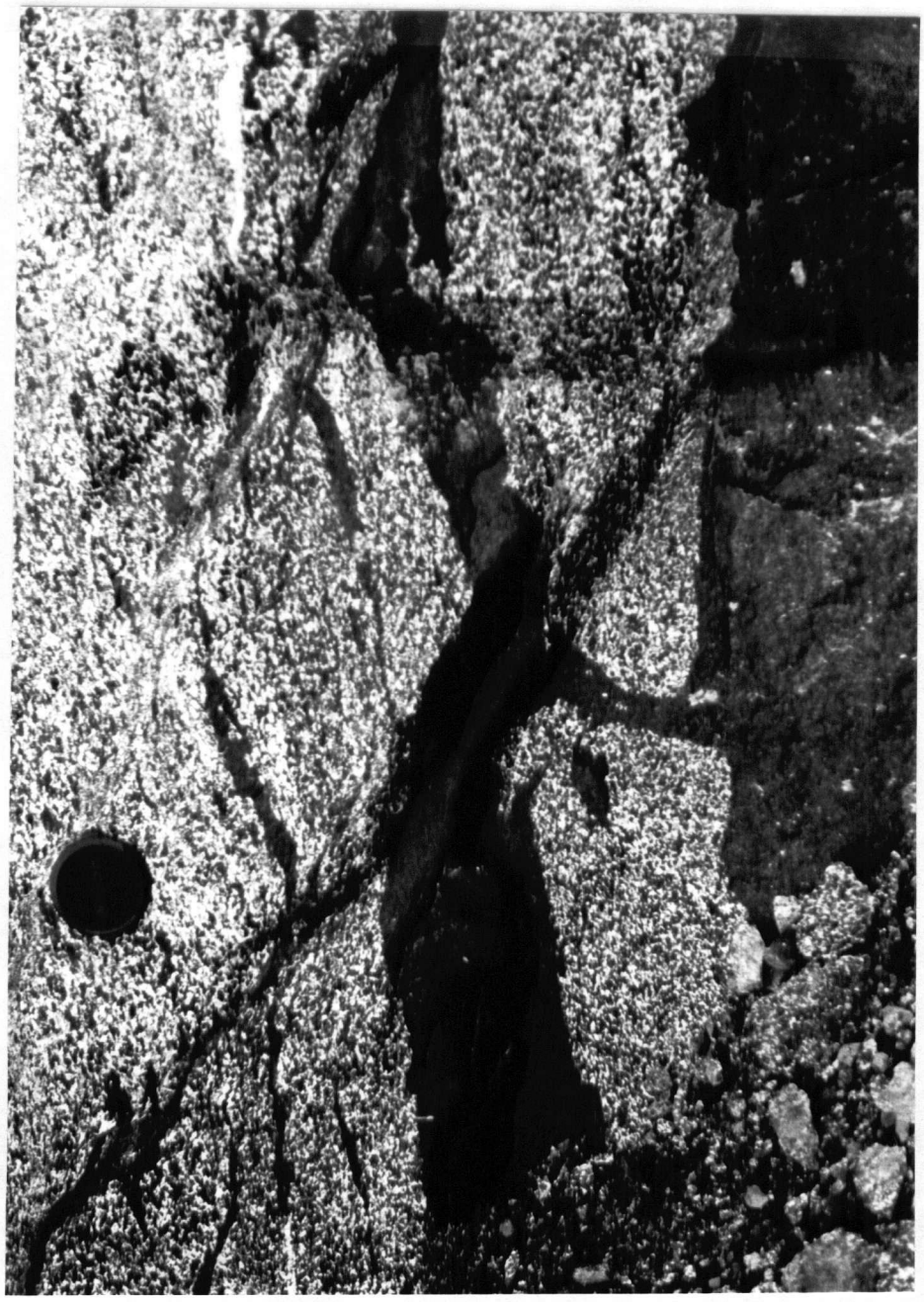

Plate 4. Dykelets and stringers of hornblendite in hornblendized diorite near Odlum. (AM#2)

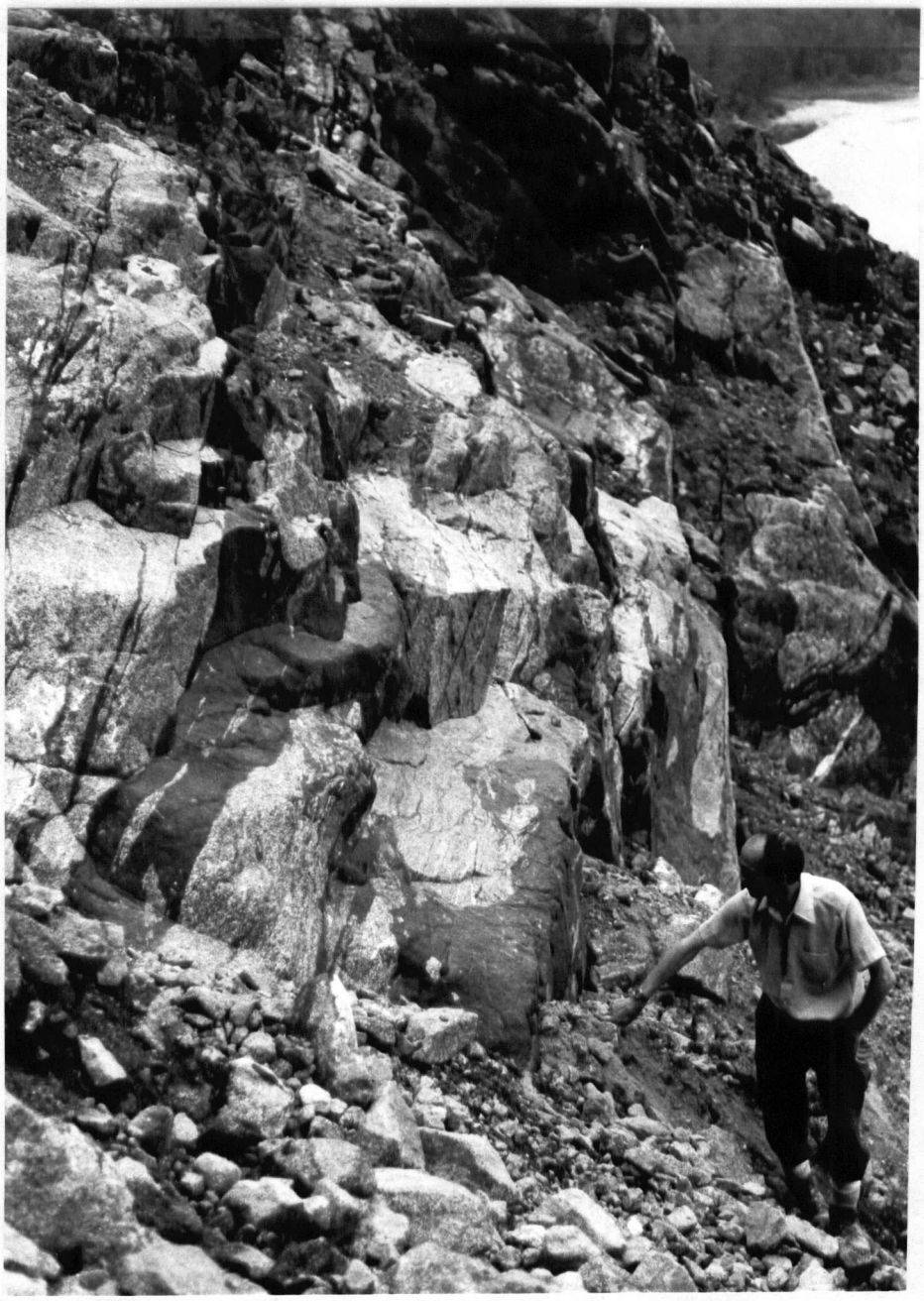

Plate 5. Same as Plate 4. Note large hornblendite body in centre background.

Plate 6. Lower part of large hornblendite body in Plate 5. Note xenoliths of hornblendized diorite.

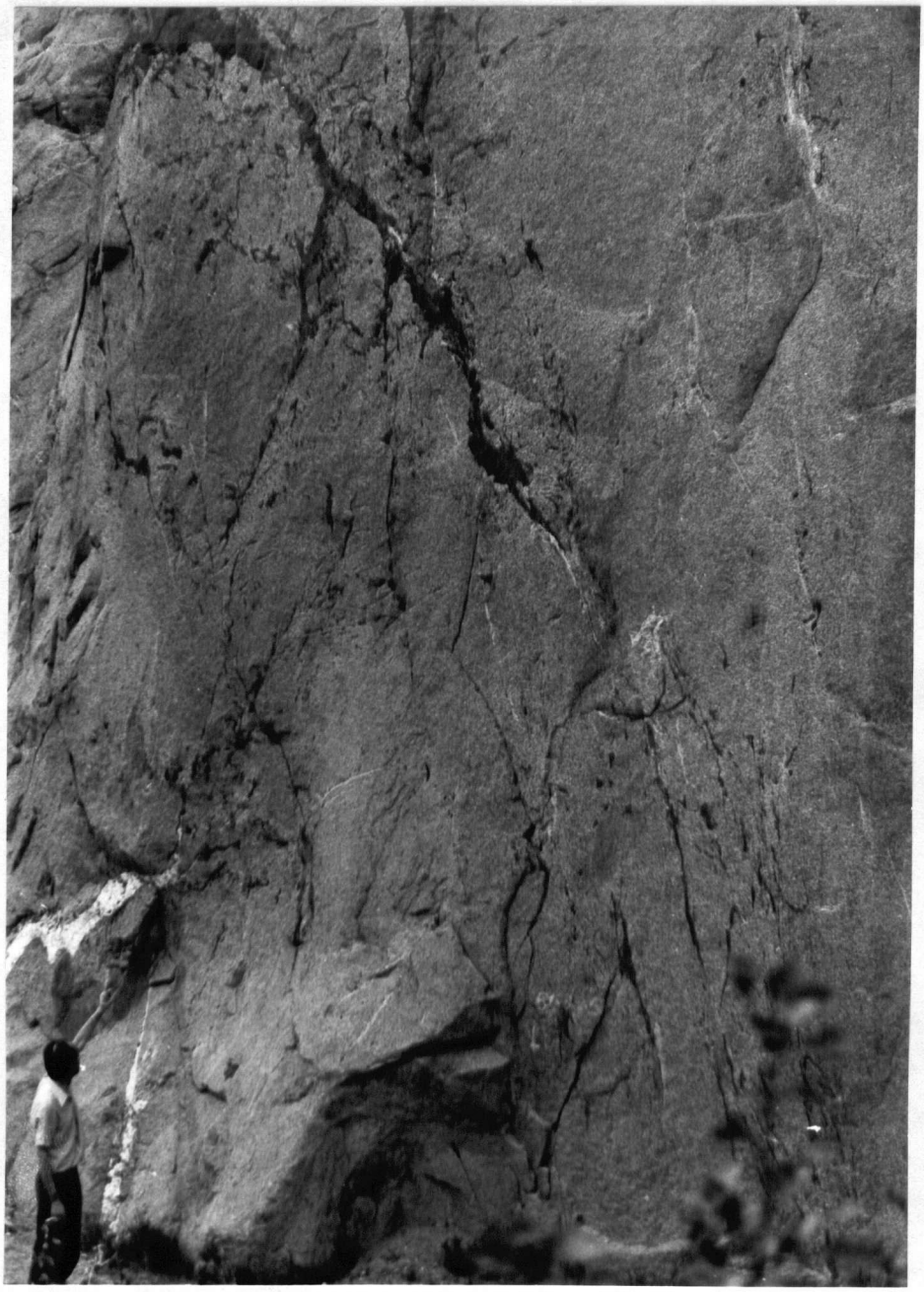

Plate 7. Hornblendite veins and pods in hornblendized diorite near Odlum. Note pegmatite dykelets at lower left. (AM#2)

Plate 8

Pegmatite dykelet or vein replaced by hornblendite. (AM#2)

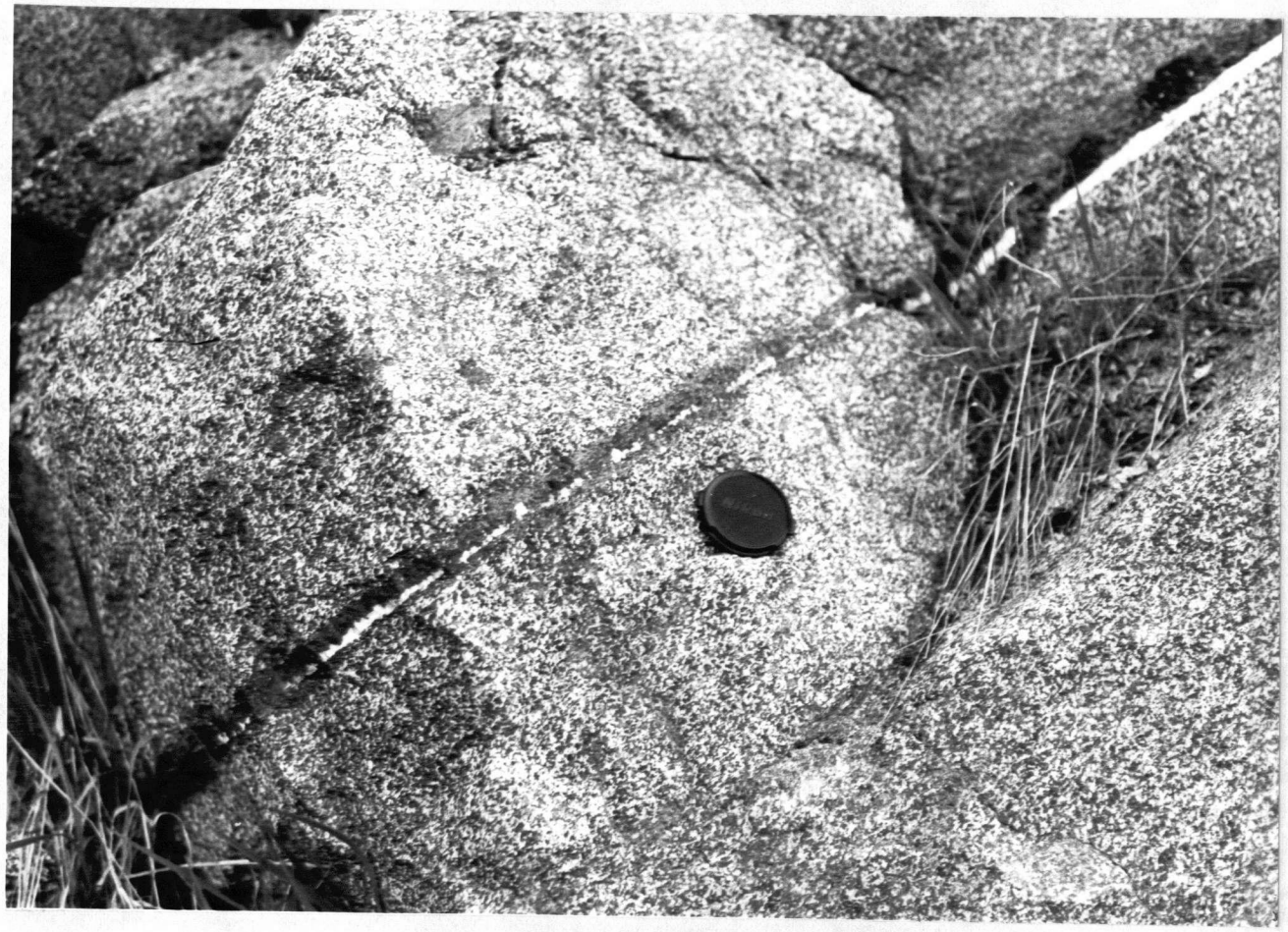

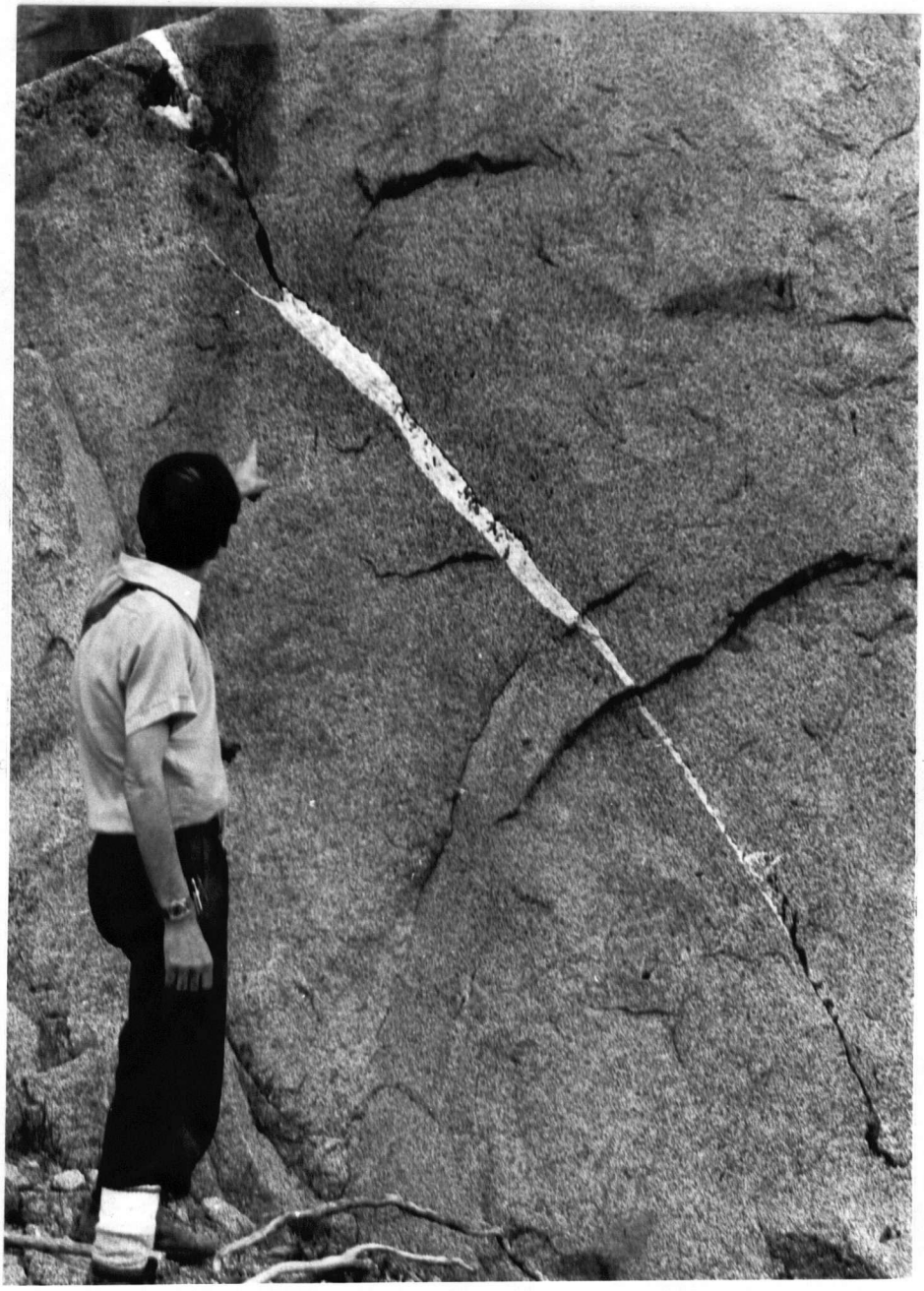

Plate 9. Same as Plate 8.

Plate 10 (above)

Hornblendite dykelet in hornblendized pyroxene diorite, south fork of American Creek. Note fine-grained margin and very coarse-grained, plagioclase-cored hornblende centre. (1/7/75/5b)

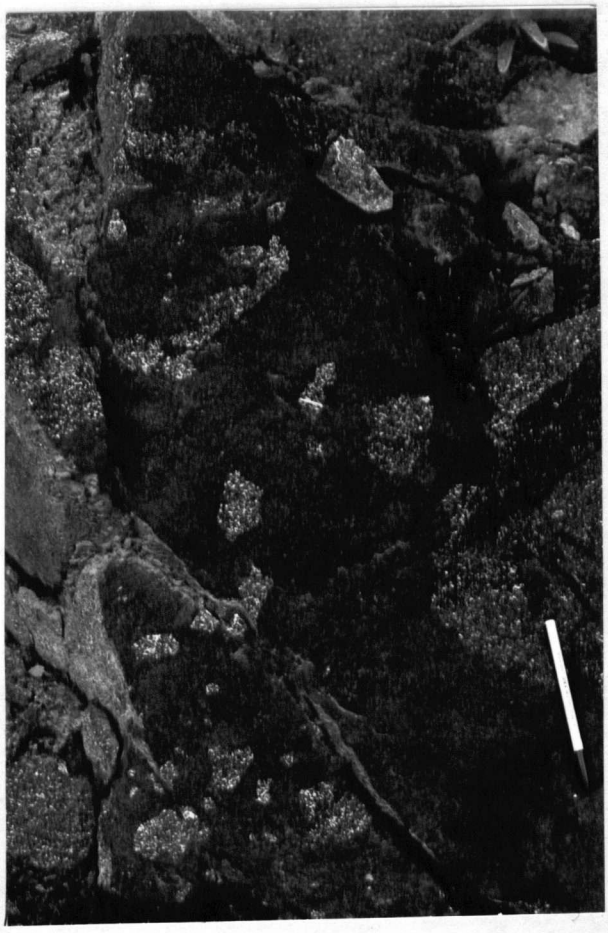

Plate 11 (left)

Hornblendite body containing xenoliths of hornblendized diorite, south fork of American Creek. (19/6/75/5)

Plate 12. Localized metasomatism producing hornblende along fractures in pyroxene diorite, and replacing pegmatite and mafic dykelet. Note also layering in diorite. (29/7/75/1)

Plate 13. Same as Plate 12. Note hornblendization of diorite and mafic dykelet near pegmatite dykelet, and parallel fractures.

Fig. 5a

MULTIPLE PARALLEL HORNBLENDITE DYKES IN HORNBLENDIZED DIORITE

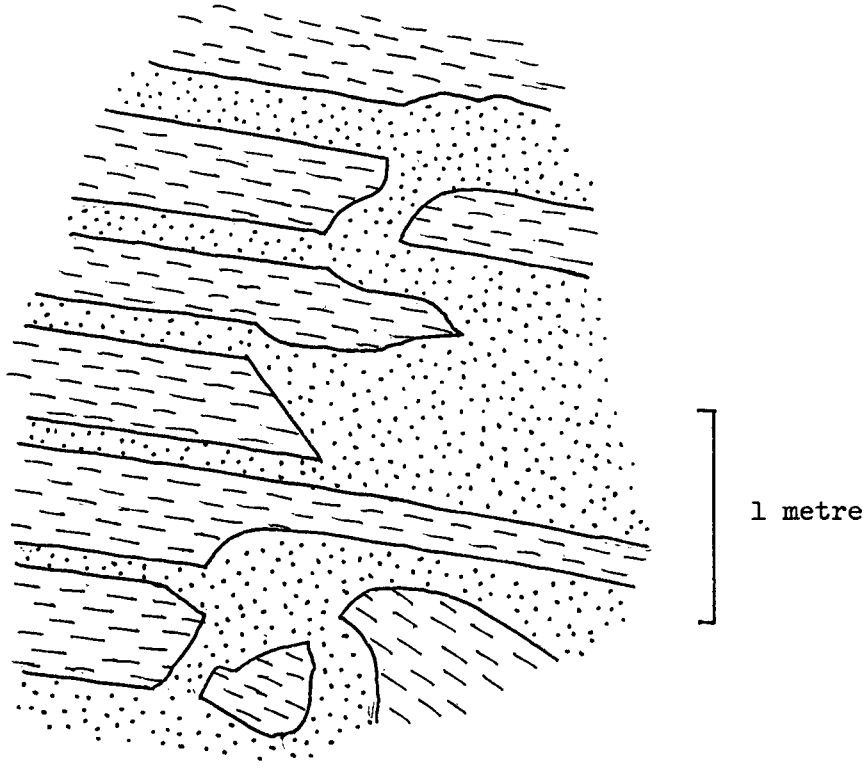

Fig. 5b

FRAGMENTED SCHIST XENOLITH IN HORNBLENDIZED DIORITE,
CUT BY HORNBLENDITE DYKELETS

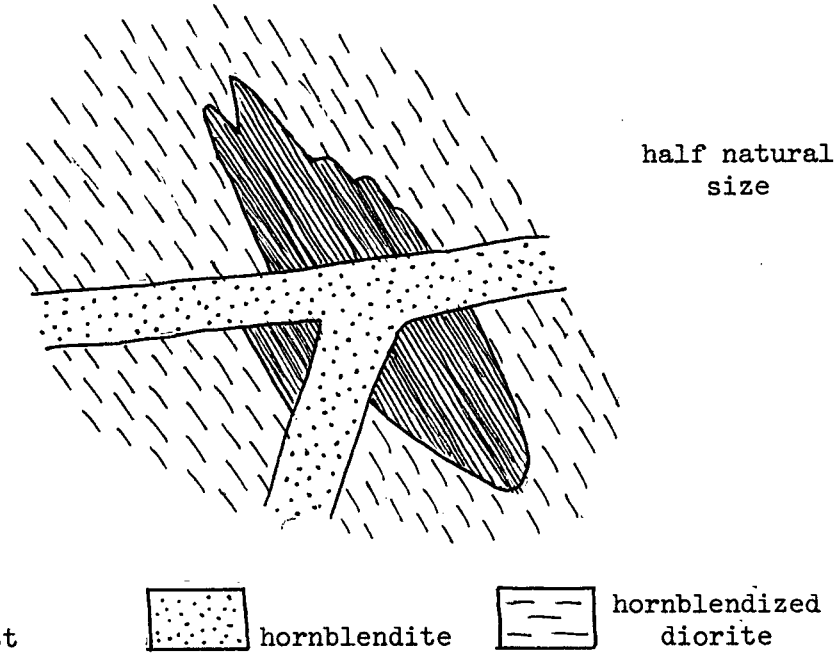

Fig. 5c

DOMELIKE PROTRUSION OF HORNBLENDITE
INTO HORNBLENDIZED DIORITE

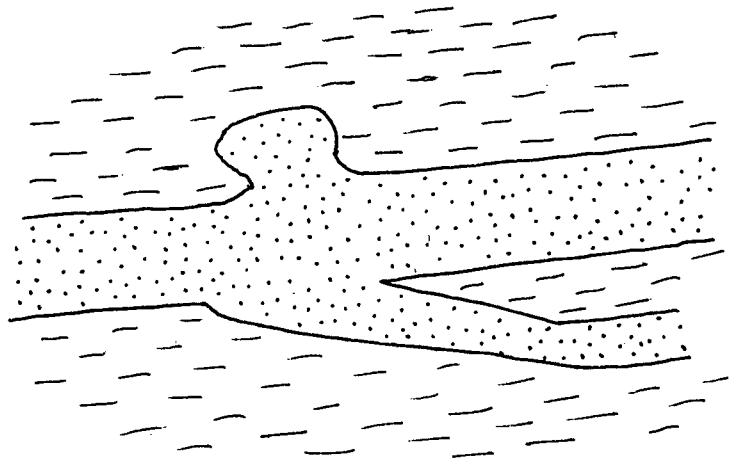

one fourth
natural
size

Fig. 5d

IRREGULAR CONTACT OF HORNBLENDITE
AGAINST HORNBLENDIZED DIORITE

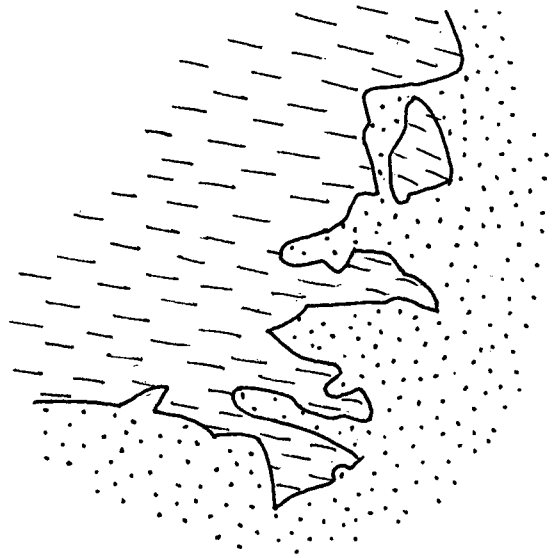

1 metre

hornblendite

hornblendized diorite

Fig. 5e

INJECTION OF DIORITE AND

INVASION OF HORNBLENDITE INTO

A SCHIST XENOLITH

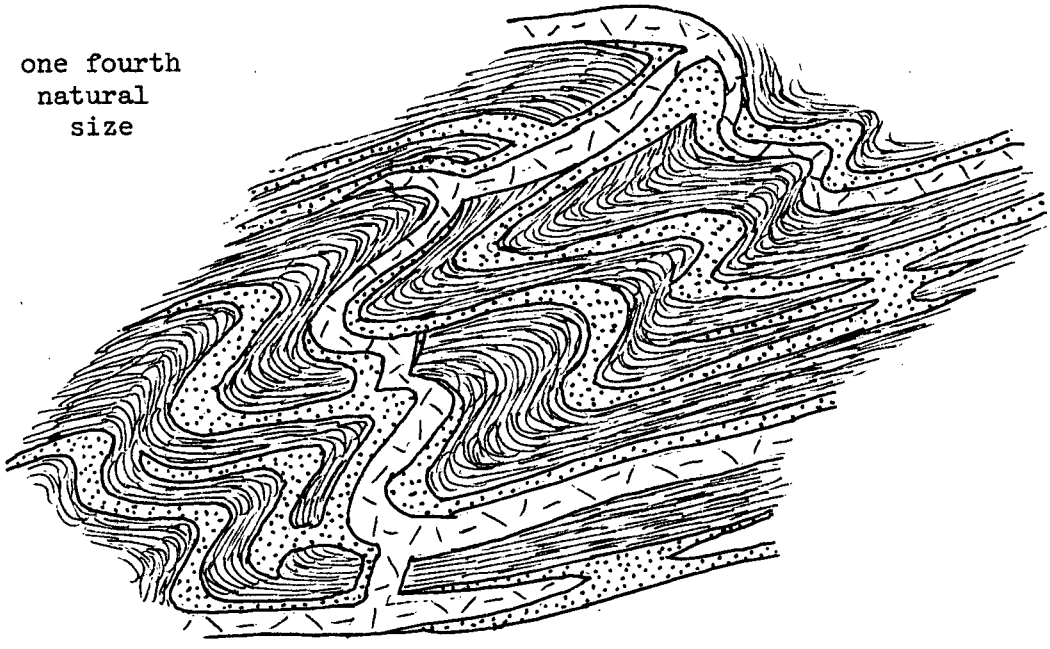

schist hornblendite hornblendized diorite

This author concludes that Spuzzum hornblendite is younger than diorite and tonalite. Emplacement of it appears to be partly magmatic as suggested by dilational features and angular xenoliths, but also partly metasomatic as suggested by vein-like and pod-like bodies and associated hornblendized rocks.

C. Structure

1. Internal Structure

Richards (1971) described the foliation pattern of diorite south of American Creek as suggesting "the presence of two crude domes, one north of the Fraser River and the other south of Flood" (p. 28). The foliation of tonalite is dominantly steep and northerly striking. His map shows a large dioritic core, crudely rectangular in shape and elongate northward, with about 40 per cent of the foliations dipping steeply and striking north to northwest, and a somewhat smaller fraction dipping rather shallowly northward. A more detailed map (Richards and McTaggart, 1976), shows two cores of pyroxene diorite within hornblende diorite, roughly corresponding to Richards' dome pattern. Structural data and mineralogical variation are not clearly related, but some correlation can be seen.

North of American Creek this correlation becomes less pronounced. Foliations, some with lineation, are developed as aligned tabular plagioclase crystals in tonalite and diorite, and aligned elongate pyroxenes in diorite. Cataclastic rocks contain biotite and hornblende strung out in shears, and bands rich in recrystallized mortar. The overall distribution of diorite and tonalite is consistent with a pattern of concentric zonation from pyroxene diorite in the core, through hornblende diorite, to tonalite (see map in pocket). Near the Giant Mascot Ultramafic Body

the rim of tonalite is discontinuous and hornblende diorite may be absent, leaving pyroxene diorite in close proximity to tonalite, ultramafic rocks, and schist. Foliations in general do not parallel contacts within the pluton, and only crudely parallel those with surrounding units (fig. 6). The foliation data suggest at least two generations, one a "swirled" flow structure and the other a superimposed northwest striking cataclastic foliation, both being discontinuously developed.

Richards (1971) recognized that subdivision of Spuzzum diorite is somewhat arbitrary, for variation within the unit as a whole is gradational. He believed the tonalite unit to intrude diorite, and described its contact at Hunter Creek southwest of Hope as a "100 foot wide zone between diorite and tonalite . . ." in which "rapid transition from type III diorite to tonalite across this zone is striking and abrupt" (p. 24). North of American Creek continuously exposed gradation from hornblende diorite to tonalite was not found, nor was found a sharp contact of tonalite with diorite. The nearest seen outcrops of clearly recognizable diorite and tonalite are over 30 metres apart.

Richards described the evidence of the age of tonalite relative to diorite as inconclusive but suggestive that diorite is older. The fact that large pelitic and calc-silicate schist xenoliths occur in diorite near its margin in a few places lends support of his hypothesis, but this, with the presence of schist xenoliths in tonalite, could also be explained by the intrusion of diorite and tonalite as a single unit into schist. Radiometric ages of tonalite (table I) average four million years younger than those of diorite (which are few in number), but tonalite ages range from 76 to 103 million years. This spread in values is perhaps indicative of resetting, as they are all potassium-argon determinations using biotite or hornblende

Fig. 6

FOLIATION PATTERNS IN THE SPUZZUM PLUTON

Scale 1:125,000

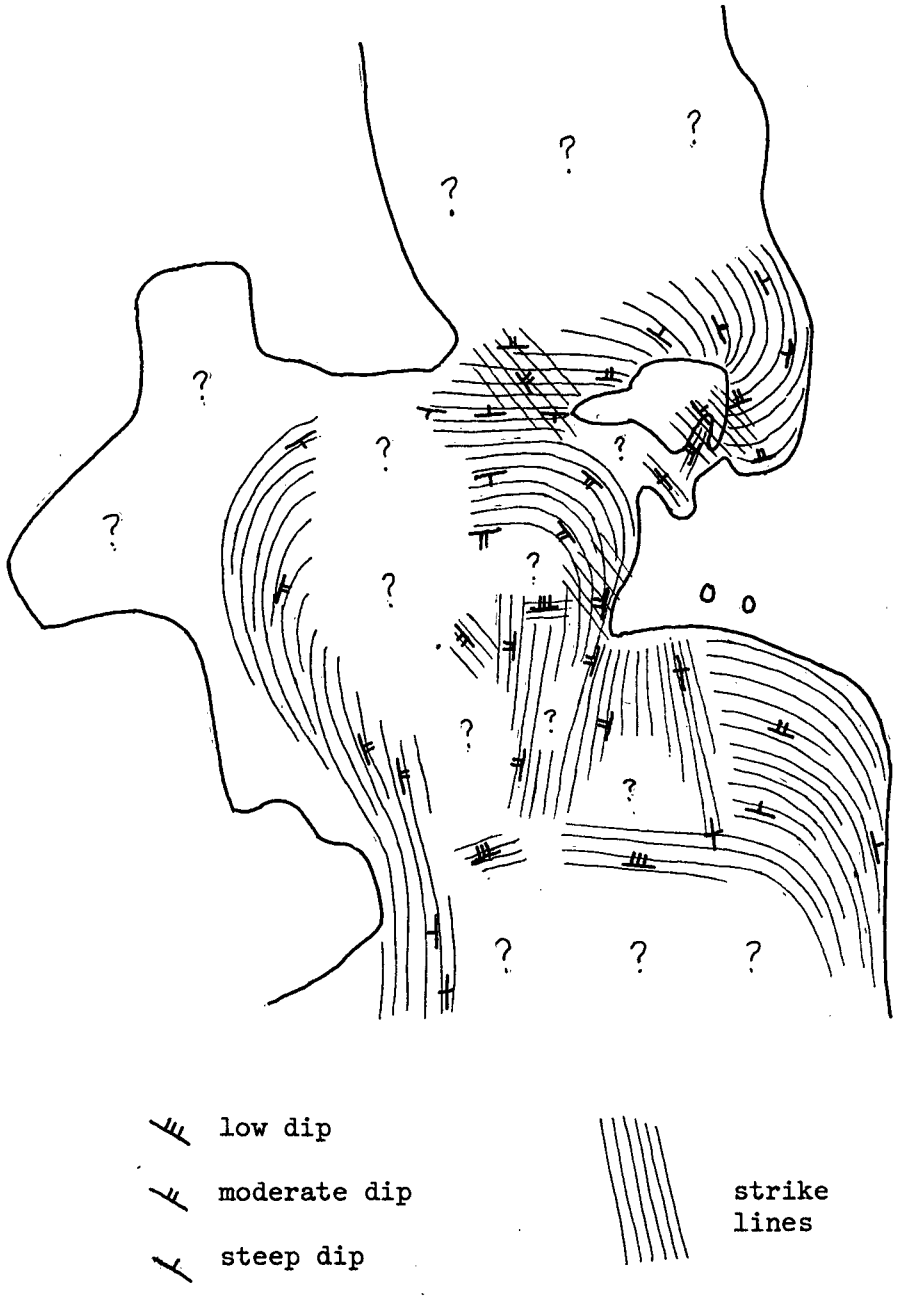

from rocks in which hornblendite is common.

Tonalite of the Spuzzum Pluton is regionally homogeneous, whereas diorite shows continuous variation in mineralogy (south of Emory Creek). Richards (1971) reported that the foliation of tonalite appears to truncate that of diorite in a few places, and structural data from his map show a high angle discordance at one locality. At this locality tonalite is shown in a more detailed map (Richards and McTaggart, 1976) to truncate the mineralogical zonation in diorite, tonalite being in contact with pyroxene diorite rather than separated from it by hornblende diorite. This author believes these facts are the strongest which suggest diorite is older than tonalite. They, however, do not prove this to be so, and in fact can be explained by a model of fractional crystallization followed by diapiric emplacement of a single pluton of tonalite cored by diorite (discussion in later sections). Local truncation of structural features can be expected, especially if emplacement occurred in a spasmodic fashion. Further juxtaposition could have been developed as a result of regional disturbances which appear to have affected the northern extension of the Spuzzum Batholith (McTaggart and Thompson, 1967).

2. Contact Relationships

Diorite and tonalite intrude schist. Small dykes and bodies of tonalite can be found in several places, and xenoliths of schist from a few centimetres to at least automobile size are common. Most larger ones retain many of their metamorphic characteristics except that they are generally coarser grained. Small ones tend to lose their identity, being thoroughly recrystallized as hornblende-biotite-quartz-plagioclase granofels.

Richards (1971) reported calc-silicate xenoliths in diorite but not in tonalite. Calc-silicate layers are found in pelitic xenoliths in both diorite and tonalite north of American Creek. Pigage (1973) described similar calc-silicate layers in schists north of Emory Creek. Read (1960) described sillimanite grade contact metamorphism superimposed on Barrovian regional metamorphism in the large re-entrant which composes the southern arm of Zofka Ridge. The southwest contact of this re-entrant is against diorite and exhibits a wide variety of contact metamorphic rocks not considered in detail in this study.

There is considerable uncertainty as to the time relationships between Giant Mascot ultramafic rocks and certain gabbroic and dioritic rocks at the Giant Mascot Mine (Aho, 1956; and McLeod, 1975). These latter rocks can be found intimately associated with all types of ultramafic rocks, but only a few are similar to Spuzzum diorite or tonalite. Pyroxene diorite at the mine, however, closely resembles that of the Spuzzum Pluton. Clean contact between these rocks and ultramafic rocks other than hornblendite was seen in three places (fig. 7):

(a) The first is about 400 metres east of the mill, where hornblende pyroxenite is in contact with pyroxene diorite (specimens 27/8/75/2a, b, and c). Alternation between diorite and pyroxenite is discontinuously exposed along a streambed for about 100 metres, the upstream end of which is close to a mutual contact with schist. Contact of diorite with pyroxenite is generally very sharp, but close to schist a heterogeneous, discontinuous "mixed" zone separates them.

Pyroxenite consists of medium-grained, subequigranular, hypidiomorphic augite and bronzite in approximately equal amounts, with abundant sub- to

Fig. 7
LOCAL GEOLOGY MAP OF THE GIANT MASCOT MINE

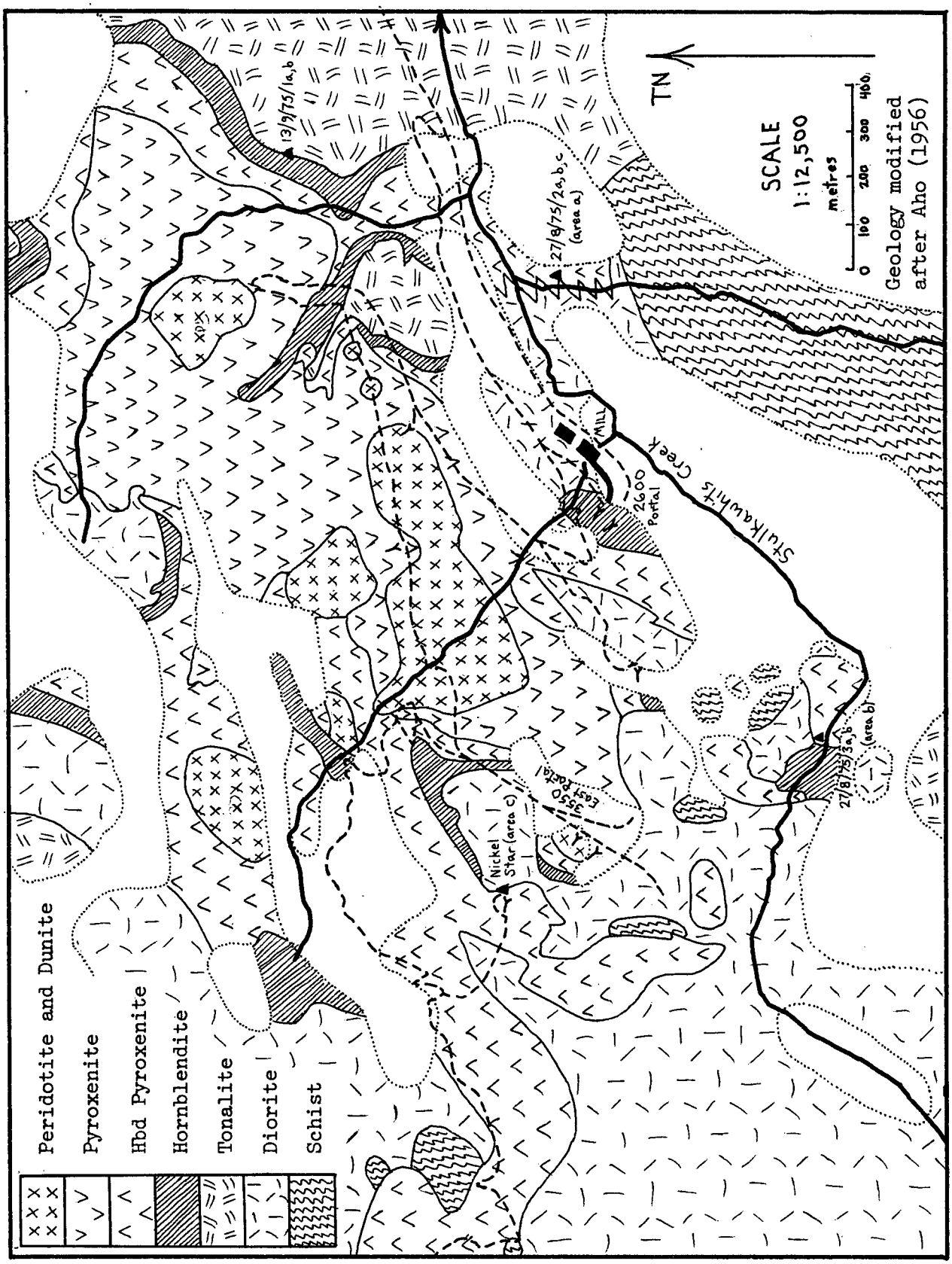

euhedral large poikilitic hornblende crystals, and minor interstitial plagioclase and quartz. Hornblende also forms skins around pyroxenes and invades them along cleavages, augite being more strongly replaced.

Diorite is largely composed of medium-grained, subequigranular, an- to euhedral, plagioclase (zoned An 52 to 82) with sutured grain boundaries, vague relic euhedral zoning in larger grains, superimposed strong patchy zoning, and irregular ragged-looking Carlsbad and albite twinning. Pyroxenes, augite being less abundant than bronzite, are fine- to medium-grained, sub- to euhedral, and loosely clustered. Hornblende forms large anhedral poikilitic grains among pyroxene clusters and interstitial to plagioclase and pyroxenes, and replaces pyroxenes as in pyroxenite.

The "mixed" zone is gabbroic in composition and heterogeneous in texture. In general it is composed of large, anhedral, poikilitic plagioclase crystals (zoned An 40 to 61) with abundant albite twinning and with rare subhedral normal and strong patchy zoning. Bronzite is sub- to euhedral, commonly forming complex skeletal grains included in plagioclase. Augite is an- to euhedral. Hornblende replaces pyroxenes and forms irregular grains as in diorite. It also forms pseudomorphs after pyroxene. This zone appears to pinch and swell along the contact of diorite and pyroxenite, but a thin contact zone of altered pyroxenite appears to be continuous. It contains hornblende crystals similar to those in pyroxenite, as well as sub- to euhedral, fine- to medium-grained pyroxenes in large anhedral poikilitic plagioclase grains (zoned An 68 to 90). This zone appears to grade into unaltered pyroxenite by a steady decrease in amount of plagioclase, but is sharp against diorite.

These relationships could be interpreted as assimilation of solid diorite by pyroxenite liquid, forming the mixed zone between them. In

this case diorite could be basified by local metasomatism from the crystallizing pyroxenite, causing the prominent alteration and mild recrystallization textures. On the other hand, intrusion of diorite liquid into solid pyroxenite could equally well basify diorite by assimilation of pyroxenite. Local metasomatism could produce the mixed zone. Temperatures of equilibration of pyroxenes (later section) are about 1000° C which supports the latter case.

(b) The second contact area is about 800 metres southwest of the mill where round xenoliths of hornblende-rich ultramafic rock can be seen in glomeroporphyritic hornblende diorite (27/8/75/3b). Exposure is along a series of waterfalls and is continuous. Diorite is in sharp contact with coarse hornblendite and hornblende pyroxenite, but these contacts are inconclusive. Xenoliths range from 2 to 30 centimetres in long dimension and are generally ovoid. Several thin, fine-grained hornblendite dykelets cut diorite and appear to cut ultramafic rock as well. These dykelets show that some hornblendite is younger than both diorite and other ultramafic rocks, and the xenoliths show that diorite is younger than these ultramafic rocks.

(c) The third contact area is about 150 metres in elevation above the 3550 east portal, where typical hornblende-rich pyroxene diorite is closely associated with pyroxenite, but contacts are not exposed. Xenoliths identical to those described above can be seen in outcrop, and large pieces of float (produced during road building) show fairly large (30 centimetres or so) and angular xenoliths clearly composed of pyroxenite. Thin fine-grained hornblendite dykelets up to several centimetres wide cut diorite and pyroxenite, one cutting what appears to be a xenolith in plate 14. A dykelet of hornblende diorite 15 centimetres wide cuts pyroxenite with

sharp contacts, but its extension toward diorite is covered. This dykelet has hornblende textures similar to comb-layering described by Moore and Lockwood (1973), suggestive of rapid growth in a volatile-rich environment. These rocks show again that hornblendite is younger than diorite and that pyroxenite is older than diorite.

Coarse, pyroxene-bearing hornblendite is cut by a fine-grained pyroxene-free hornblende diorite dykelet at the 2600 portal. This hornblendite is not clearly the same as that of small dykelets seen elsewhere to cut diorite, but the diorite dykelet appears much like the matrix of glomeroporphyritic Spuzzum diorite. This relationship suggests that either the pyroxene hornblendite is older than Spuzzum diorite,or that old pyroxenite may have been hornblendized during emplacement of the Spuzzum Pluton.

A well exposed but inconclusive contact of tonalite against coarse hornblendite lies about 100 metres in elevation above the switchbacks in the mine access road (about 1.0 kilometre northeast of the mill). Moderately foliated tonalite and coarse hornblendite are separated by a fairly continuous, pinching and swelling band of plagioclase-bearing pegmatitic hornblendite (specimens 13/9/75/1a and b) up to at least one metre wide. This contact phase is composed mostly of coarse- to very coarse-grained, idiomorphic, somewhat poikilitic hornblende crystals set in an interstitial matrix of medium-grained plagioclase (An 42), augite, and hornblende. Augite forms rounded to elongate, clustered grains included in and among fine- to coarse-grained, interstitial plagioclase grains with weak patchy zoning and rare deformational twinning. Matrix hornblende occurs with clusters of augite, and rims and replaces augite

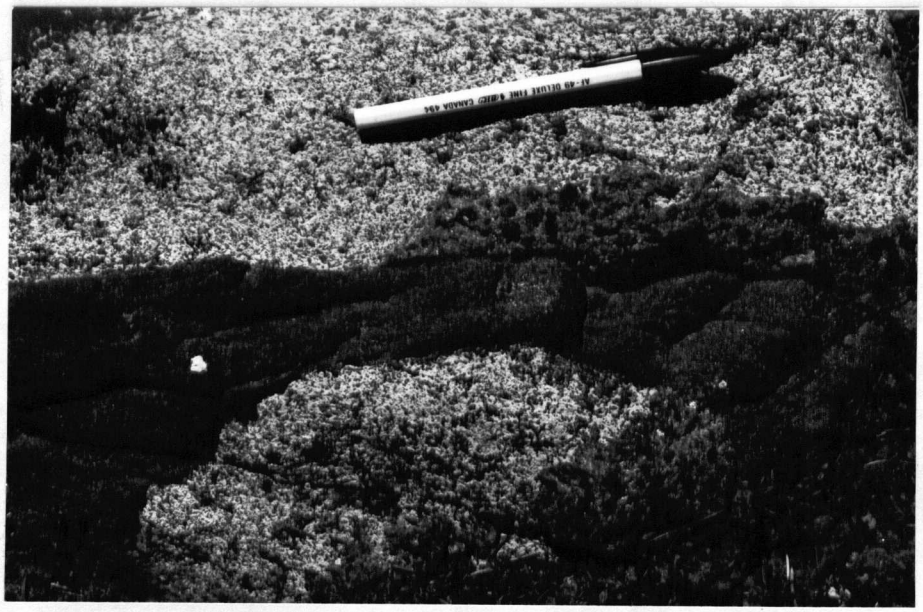

Plate 14. Hornblendite dykelet cutting pyroxene diorite and pyroxenite at the Giant Mascot Mine. Note offset and rounded form of pyroxenite body. (28/8/75/1a,b)

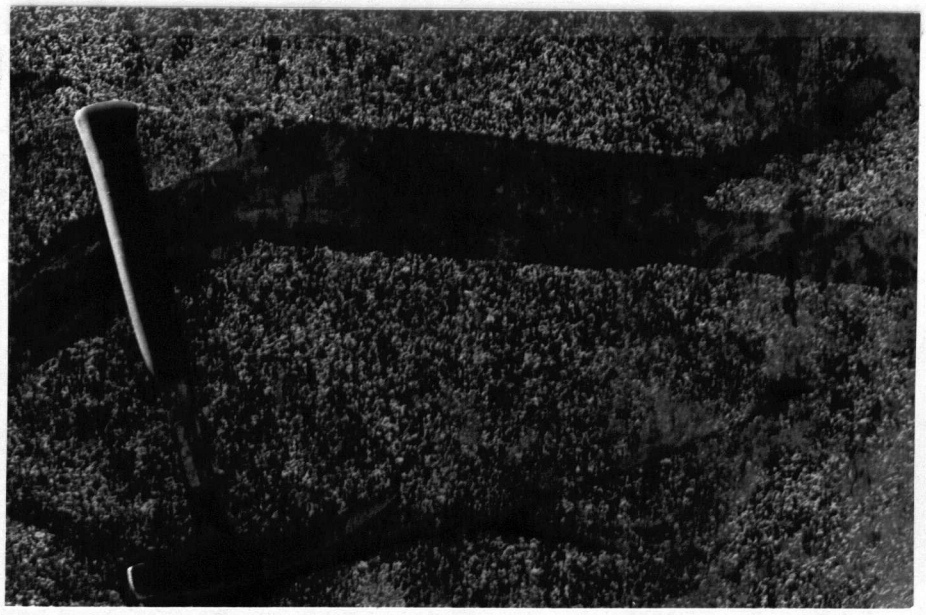

Plate 15. Mafic dyke in diorite. Note sharp contacts and dilational separation of walls. (29/7/75/6)

along cleavages. This contact zone generally grades to coarse hornblendite by a decrease in amount of plagioclase, but its contact with tonalite is sharp.

From the evidence of the paragraphs above it is concluded that the Spuzzum Pluton intrudes the Giant Mascot Ultramafic Body. The relations of other dioritic and gabbroic rocks, not clearly part of the Spuzzum Pluton, are unknown.

IV. MINOR INTRUSIONS

A. Mafic Dykes and Pipes

Fine-grained dykes ranging in composition from mesocratic pyroxene or hornblende diorite to melanocratic amphibolite intrude Spuzzum diorite at several localities and tonalite in at least one locality. They also intrude ultramafic rocks at the Giant Mascot Mine. These dykes have sharp contacts and show dilational features (plate 15), the walls of host rock commonly appearing to fit together. Some hornblende-rich varieties have weak to strong alignment of subhedral hornblende with polygonal, equant plagioclase.

An amphibolitic body near the mill at the mine (fig. 7) has large rounded poikiloblastic plagioclase with hornblende-rich and hornblende-free patches within individual crystals. Hornblende forms a decussate matrix. This texture is also seen in some dykes. The body contains xenoliths of hornblendized rocks, diorite, tonalite, hornblendite, schist, and pyroxenite, forming a conspicuous intrusive breccia. Plagioclase is strongly normal zoned (An 50 to 80), but poikiloblasts are weakly reverse zoned or unzoned with compositions between An 50 and An 70. Hornblende is olive or brown with $2V \approx 90°$, $\delta \approx .026$, and $\gamma \wedge c \approx 17°$.

B. Pegmatite Dykelets and Veins

Coarse-grained chlorite-hornblende-quartz-plagioclase pegmatite cuts tonalite, diorite and mafic dykes. Accessory rutile and tourmaline may be present as rounded crystals or acicular bundles. Northwest of Odlum and north of American Creek (plates 8, 9, 12 and 13) this pegmatite is replaced

by hornblende.

Along Stulkawhits Creek veins of plagioclase pegmatite cut hornblendized tonalite and hornblendite stringers and pods. This pegmatite contains biotite, hornblende, and quartz in small quantities.

Dioritic hornblende-plagioclase pegmatites cut and grade into pyroxene or hornblende diorite at several localities. These may be associated with cooling and contraction of Spuzzum diorite during or just after emplacement.

C. Tonalite Aplite Dykelets

Fine-grained, garnetiferous, muscovite-biotite-quartz-plagioclase aplite intrudes tonalite and schist and cuts dykelets of pegmatite. Small euhedral garnets are poikiloblastic, some with inclusion-free pink cores. Biotite is weakly to strongly aligned forming a foliation, but muscovite forms anhedral unoriented grains. Plagioclase has complex oscillatory zoning, ranging in composition from An 32 to about An 60. It forms fine- to medium-grained equant crystals with abundant deformational and Carlsbad twinning. Quartz and fine-grained plagioclase form a granoblastic groundmass.

In tonalite these dykelets appear undeformed except for their foliation and plagioclase twinning, but in schist they appear contemporaneous with broad open folding on northwest trending axes. Some of these dykelets are folded yet cut the foliation of schist, while other dykelets cut them and are planar. Dykelets of these two styles appear identical in all other respects. The fact that rocks younger than Spuzzum tonalite are foliated and folded, strongly suggests a deformational event postdating the Spuzzum Pluton. Metamorphic textures in diorite and tonalite could be a result of this event.

V. HORNBLENDITE ASSOCIATED WITH THE GIANT MASCOT ULTRAMAFIC BODY

Coarse hornblendite forms a discontinuous rim around the main body of the Giant Mascot Ultramafic Body, separating it from surrounding Spuzzum diorite and tonalite. In only a few places does diorite come in contact with pyroxenite, and in those places the latter is hornblendic, hornblende appearing to form porphyroblasts. Aho (1956) described this hornblendite thus:

> "In several localities south of the underground workings and at 2400 feet within the 3550 level, hornblendite can be seen in all stages of replacement of the anhydrous ultrabasics. Pyroxene cores, relict textures, contact relations, and even plagioclase content are preserved in some rocks while in others the pyroxenes have been fully replaced and the pseudomorphs and relict textures have been reconstituted to form a medium-grained, hypidiomorphic-textured hornblendite composed essentially of prismatic brown hornblende full of small magnetite inclusions. Other bodies of pegmatitic, panidiomorphic textured hornblendite, composed of stubby hornblende crystals up to two inches across, have apparently been formed by similar replacement but perhaps at higher temperatures. These pegmatitic hornblendites such as those forming the reaction zone around the main ultrabasic intrusion, grade imperceptibly into the pyroxenites and peridotites at most places. All stages of replacement can be traced, yet many of the hornblendite bodies and even the hornblendic pyroxenites show lineation, sharp contacts, inclusions, contact alteration, and dike apophyses suggestive of intrusion into the surrounding, more anhydrous ultrabasics. Subpoikilitic phenocrysts of labradorite (An 60), labradorite-rich schlieren, and dike-like pegmatitic bodies grading into hornblende gabbro are common near inclusions and contacts of the hornblendites . . ." (p. 452-3)

A detailed map of the Giant Mascot Ultramafic Body and vicinity is shown in fig. 7. This map is primarily the work of Aho (1956), but is modified in outlying areas after the work of this study.

Aho interpeted the rim of hornblendite as a reaction zone between a solid-state intrusion of dry ultrabasic rock into wetter diorite and schist. McLeod (1975) interpreted it also as a reaction zone, but believed that diorite was intrusive into dry ultrabasic rocks. This author is in agreement with the latter.

VI. CHEMISTRY

A. Introduction

Pyroxenes, plagioclase, and hornblende from several localities (table III) were analyzed by electron microprobe. One specimen of pyroxene diorite was run on two occasions and offers a test of consistency in pyroxene analyses. Elements determined are Si, Ti, Al, Fe (as Fe^{+2}only), Mg, Mn, Ca, Na, and K. Where possible, pairs of ortho- and clinopyroxene from the same specimen were used to calculate approximate temperatures of equilibration according to the method of Wood and Banno (1973). Hornblende analyses from hornblendites were used to calculate C.I.P.W. norms for comparison with basic igneous rocks and other known hornblendite. Since the electron probe does not distinguish the oxidation state of iron, hornblende and pyroxene, analyses were approximately corrected by comparison with analyses from literature.

B. Plagioclase

Results of plagioclase microanalyses are listed in table IV. Analyses are arranged in order according to distance from the contact with country rock. Those designated "contact" are from the contact between Spuzzum diorite and pyroxenite at the Giant Mascot Mine (fig. 7). Results agree well with optically determined compositions. Specimens 27/8/75/2a and c have strong patchy zoning and microanalyses may not show the entire range of composition.

C. Pyroxene

Wood and Banno (1973) provide a semi-empirical equation for determining

TABLE III

KEY TO SPUZZUM AND GIANT MASCOT MINERAL ANALYSES

Symbols	Spec. No.	Mineral Analyses Plag.	Hbd	Cpx	Opx	Occurrence and Locality
●[1]	74-7(Feb.1975)*	--	--	3	6	Hornblendite dykelet, Giant Mascot Mine
●[2]	74-7(Apr.1976)	--	--	1	1	--
□	15/6/75/6	2	1	3	4	Px diorite, S side Fraser Canyon, west of Hope
△	17/6/75/15	1	2	3	3	Px diorite, 200 m. E. of mill, Giant Mascot Mine
◇	18/7/75/5	--	--	2	2	Px diorite, 1.25 km. NW of mill, G. M. Mine
▼	18/7/75/7a	--	5	6	--	Hornblendite dykelet, 200 m. NE of 3550 portal, Giant Mascot Mine
▽	24/7/75/11	1	1	4	2	Px diorite, summit of Zofka Ridge, SW of Giant Mascot Mine
◁	27/8/75/2a	1	3	2	2	Pyroxenite, contact with diorite 400 m. east of mill, Giant Mascot Mine
D	same	1	1	2	2	Diorite at same contact
X +	27/8/75/2c	6	6	7	2	Diorite several m. away from same contact
▲	AM#2**	--	1	--	--	Hornblendite, several 100 m. NW of Odlum
■	13/9/75/1a	--	5	--	--	Contact of tonalite with UM rocks 900 m. northeast of mill, Giant Mascot Mine
◆	2600	--	5	--	--	Hornblendite, rim zone of UM rocks, 2600 portal, Giant Mascot Mine

* donated by K. C. McTaggart

** donated by K. Nielson

TABLE IV

PLAGIOCLASE COMPOSITIONS FROM SPUZZUM ANALYSES

Locality	far		far	near	contact	
No.	15/6/75/6		24/7/75/11	17/6/75/15	27/8/75/2a	
Molar fraction	core	rim				
Orthoclase	.0175	.0176	.0182	.0151	.0125	.0006
Albite	.4990	.5231	.5140	.5241	.2685	.4019
Anorthite	.4835	.4593	.4678	.4608	.7190	.5975
An/(An + Ab)%	49.21	46.75	47.65	46.79	72.81	59.78
Optical An %	42 - 48		48-50	--	55 - 77	

No.	27/8/75/2c (contact)					
Molar fraction						
Orthoclase	.0041	.0075	.0047	.0084	0	.0047
Albite	.3840	.3480	.3091	.3005	.2825	.2727
Anorthite	.6119	.6445	.6862	.6911	.7175	.7226
An/(An + Ab) %	61.44	64.93	68.94	69.69	71.75	72.60
Optical An %			52-82			

the equilibration temperature of coexisting ortho- and clinopyroxene as a function of distribution of elements in the two pyroxenes. The equation is derived from a model of ideal mixing in the octahedral (M1) and cubic (M2) sites of each pyroxene, fitted by additional Mg:Fe terms to experimental data from various sources. The equation is:

$$T = \frac{-10202}{\left[\ln\left(\frac{a^{En}_{Cpx}}{a^{En}_{Opx}}\right) + 3.88X^2 - 7.65X - 4.60\right]} - 273.15$$

where T = temperature (°C)

$X = Fe^{+2}/(Mg + Fe^{+2})$ in Opx

and

$$a^{En}_{Opx} = \left(\frac{Mg^{M2}}{Mg^{M2} + Fe^{M2} + Ca + Mn + Na}\right) \cdot \left(\frac{Mg^{M1}}{Mg^{M1} + Fe^{M1} + Fe^{+3} + Cr + Ti + Al + Si - 2}\right)$$

in Opx,

a^{En}_{Cpx} = the same in Cpx

where M1 and M2 are site designations.

Analyses in this study do not include chromium, and the equation above does not provide for potassium, therefore these elements are neglected in the assignment of formulas and the above calculation. Some ambiguity exists in the discussion of Wood and Banno as to assignment of elements to sites. It is readily apparent that for six oxygens there need not be exactly four electropositive atoms. Wood and Banno do not provide for this situation precisely. For this reason the tetrahedral site is first filled with silicon and aluminum until occupancy equals two atoms or until aluminum is consumed (less than two atoms). The octahedral site (M1) is then filled with all remaining Al, Fe^{+3}, Ti, (Cr), and equal amounts of Fe^{+2} and Mg until its occupancy reaches unity. At this state Mg^{M1} and Mg^{M2} are

determined. All remaining Fe, Mg, Mn, Ca, and Na atoms comprise the cubic site (M2), which usually will have occupancy unequal to unity. This is done for consistency because structural data for site occupancy is not available.

Ortho- and clinopyroxene microanalyses are listed in tables Va and b, and shown in fig. 8 in a C-F-M diagram. For estimation of ferric iron, analyzed pyroxene pairs from various sources were compared with Spuzzum pyroxenes. This comparison shows that chromium-poor pyroxene pairs from Stillwater (Hess, 1960), Skaergaard (Brown, 1957), and Bushveld (Hess, 1960; and Atkins, 1969) are most similar to Spuzzum pyroxenes. Analyses of these pyroxenes and a key to sources, types of pyroxenes, and their general modes of occurrence are given in Appendix II. Fe^{+3} contents of these pairs are plotted against Mg/(Mg + Fe) in fig. 9, and estimated curves are drawn for Spuzzum pyroxenes. Corrected formulas are listed for Spuzzum pyroxenes in tables Va and b. Equilibration temperatures calculated from corrected formulas are listed in table VI.

Temperatures calculated from corrected analyses range from .53° to 5.54° higher than those from uncorrected ones and average 920°C. Wood and Banno (1973) caution that use of their equation with rocks differing appreciably in composition from those used to derive it may introduce sizable error. Pyroxene pairs they used were mostly from ultrabasic assemblages, but acid volcanic and basaltic compositions were used also, therefore pyroxenes from Spuzzum diorite should produce results within the given tolerance bracket. Further, the simplifications associated with their thermodynamic treatment are of uncertain consequence. The authors suggest a tolerance of 70 degrees. Correction for Fe^{+3} therefore is of no significance. The overall temperature range is about 100 degrees. Considering the tolerance limitation it can be said with reasonable confidence

TABLE Va

SPUZZUM ORTHOPYROXENE ANALYSES

AND FORMULAS

SYMBOL	●[1]	●[2]	□	△	◊	▼	◖	◗	×
SiO_2	53.20	49.21	51.92	51.51	50.47	52.04	53.13	53.83	53.11
TiO_2	.06	.08	.13	.10	.17	.07	.17	.17	.04
Al_2O_3	.91	.59	1.05	1.23	1.47	1.24	2.98	2.88	1.81
FeO	23.59	22.67	23.76	24.27	20.85	21.31	12.53	13.74	16.33
MgO	21.94	21.16	20.72	20.06	22.22	21.89	27.95	27.62	26.03
MnO	.46	.48	.40	.53	.44	.37	.21	.24	.29
CaO	.72	.72	.77	.72	.98	.88	1.12	.84	.64
Na_2O	.01	.00	.00	.01	.01	.00	.02	.00	.00
K_2O	.00	.00	.00	.00	.00	.00	.00	.00	.00
Total	100.89	94.91	98.75	98.43	96.61	97.80	98.11	99.32	98.25
M2 Site	.9926	1.0438	.9857	.9855	1.0049	.9818	.9918	.9900	.9897
Na	.0008	.0	.0	.0010	.0004	.0	.0011	.0	.0
Ca	.0285	.0305	.0312	.0293	.0402	.0355	.0435	.0323	.0250
Mn	.0144	.0161	.0129	.0171	.0142	.0117	.0063	.0073	.0087
Mg	.6028	.6335	.5832	.5688	.6336	.6155	.7644	.7539	.7197
Fe+2	.3461	.3637	.3584	.3693	.3165	.3191	.1765	.1965	.2363
M1 Site	1	1	1	1	1	1	1	1	1
Mg	.6064	.6110	.5847	.5695	.6357	.6166	.7406	.7204	.7025
Fe+2	.3482	.3507	.3594	.3698	.3176	.3198	.1711	.1878	.2307
Fe+3	.0359	.0359	.0359	.0359	.0359	.0359	.0319	.0329	.0349
Al	.0080	.0	.0164	.0219	.0060	.0257	.0519	.0550	.0308
Ti	.0015	.0024	.0036	.0029	.0048	.0020	.0045	.0039	.0011
Tetrahedral Site	2	1.9748	2	2	2	2	2	2	2
Al	.0315	.0275	.0306	.0336	.0604	.0294	.0751	.0667	.0476
Si	1.9685	1.9473	1.9694	1.9664	1.9396	1.9706	1.9249	1.9333	1.9524

TABLE Vb

SPUZZUM CLINOPYROXENE ANALYSES

AND FORMULAS

SYMBOL	●[1]	●[2]	□	△	◇	▼	▽	◖	◗	×
SiO_2	52.14	49.18	51.71	50.65	49.96	52.35	51.62	52.13	51.27	52.41
TiO_2	.39	.44	.31	.41	.48	.22	.33	.35	.47	.30
Al_2O_3	2.83	3.04	1.73	2.54	2.98	2.45	2.07	3.06	3.69	2.52
FeO	7.99	8.45	10.01	10.96	7.58	6.10	9.33	5.35	5.87	5.94
MgO	14.42	13.85	13.08	12.56	14.78	15.67	13.78	14.91	14.92	15.05
MnO	.15	.15	.17	.26	.17	.14	.16	.11	.14	.16
CaO	22.06	20.33	20.92	20.45	20.20	21.07	20.08	21.30	21.21	22.14
Na_2O	.48	.45	.41	.47	.46	.25	.43	.49	.41	.32
K_2O	.00	.00	.00	.00	.00	.00	.00	.00	.00	.00
Total	100.46	95.89	98.34	98.30	96.61	98.25	97.80	97.70	97.98	98.84
M2Site	1.0037	1.0108	.9881	.9990	1.0072	.9826	.9844	.9767	.9868	.9856
Na	.0341	.0338	.0304	.0350	.0337	.0183	.0316	.0355	.0297	.0230
Ca	.8717	.8439	.8501	.8357	.8277	.8404	.8159	.8523	.8491	.8803
Mn	.0048	.0049	.0054	.0084	.0053	.0044	.0051	.0035	.0044	.0049
Mg	.0736	.0988	.0740	.0833	.1129	.1015	.0988	.0736	.0879	.0657
Fe+2	.0195	.0294	.0282	.0366	.0276	.0180	.0330	.0118	.0157	.0117
M1 Site	1	1	1	1	1	1	1	1	1	1
Mg	.7168	.6987	.6632	.6288	.7271	.7656	.6778	.7539	.7408	.7642
Fe+2	.1900	.2075	.2525	.2762	.1777	.1361	.2261	.1203	.1319	.1367
Fe+3	.0369	.0369	.0369	.0369	.0369	.0359	.0369	.0349	.0359	.0359
Al	.0454	.0441	.0385	.0462	.0445	.0564	.0498	.0811	.0783	.0548
Ti	.0109	.0128	.0089	.0119	.0138	.0060	.0094	.0098	.0131	.0084
Tetrahedral Site	2	2	2	2	2	2	2	2	2	2
Al	.0776	.0947	.0387	.0683	.0898	.0510	.0426	.0534	.0840	.0554
Si	1.9224	1.9053	1.9613	1.9317	1.9102	1.9490	1.9574	1.9466	1.9160	1.9446

Fig. 8

C-F-M DIAGRAM FOR SPUZZUM AND

GIANT MASCOT PYROXENES AND HORNBLENDES

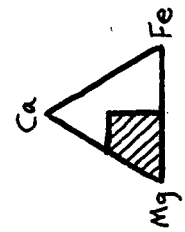

Horizontal scale: Ca/(Ca + Mg + Fe)
Vertical scales: Mg/(Mg + Fe)

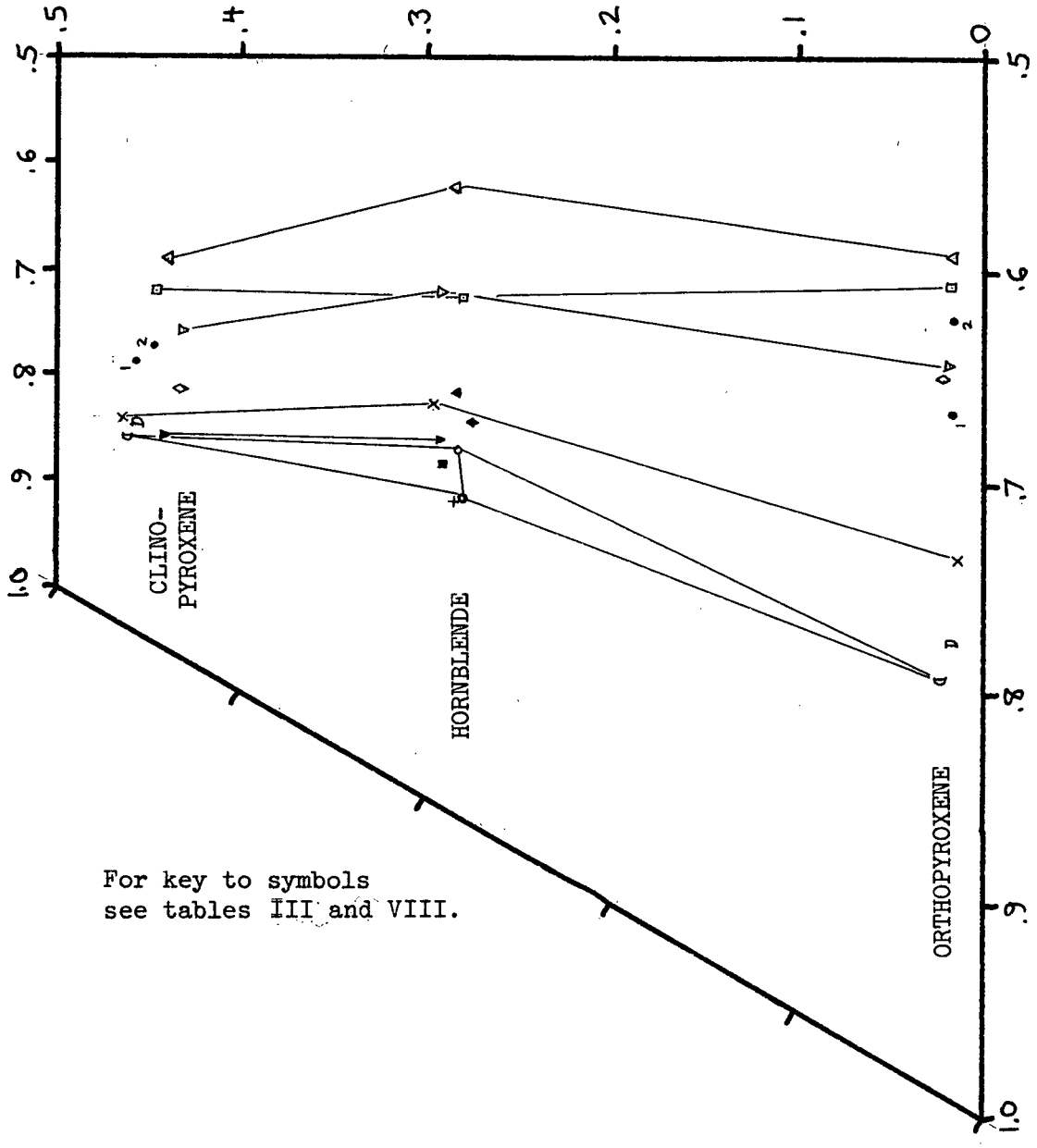

For key to symbols
see tables III and VIII.

Fig. 9

FE^{+3} ATOMS PER FORMULA UNIT

IN SPUZZUM AND GIANT MASCOT PYROXENES

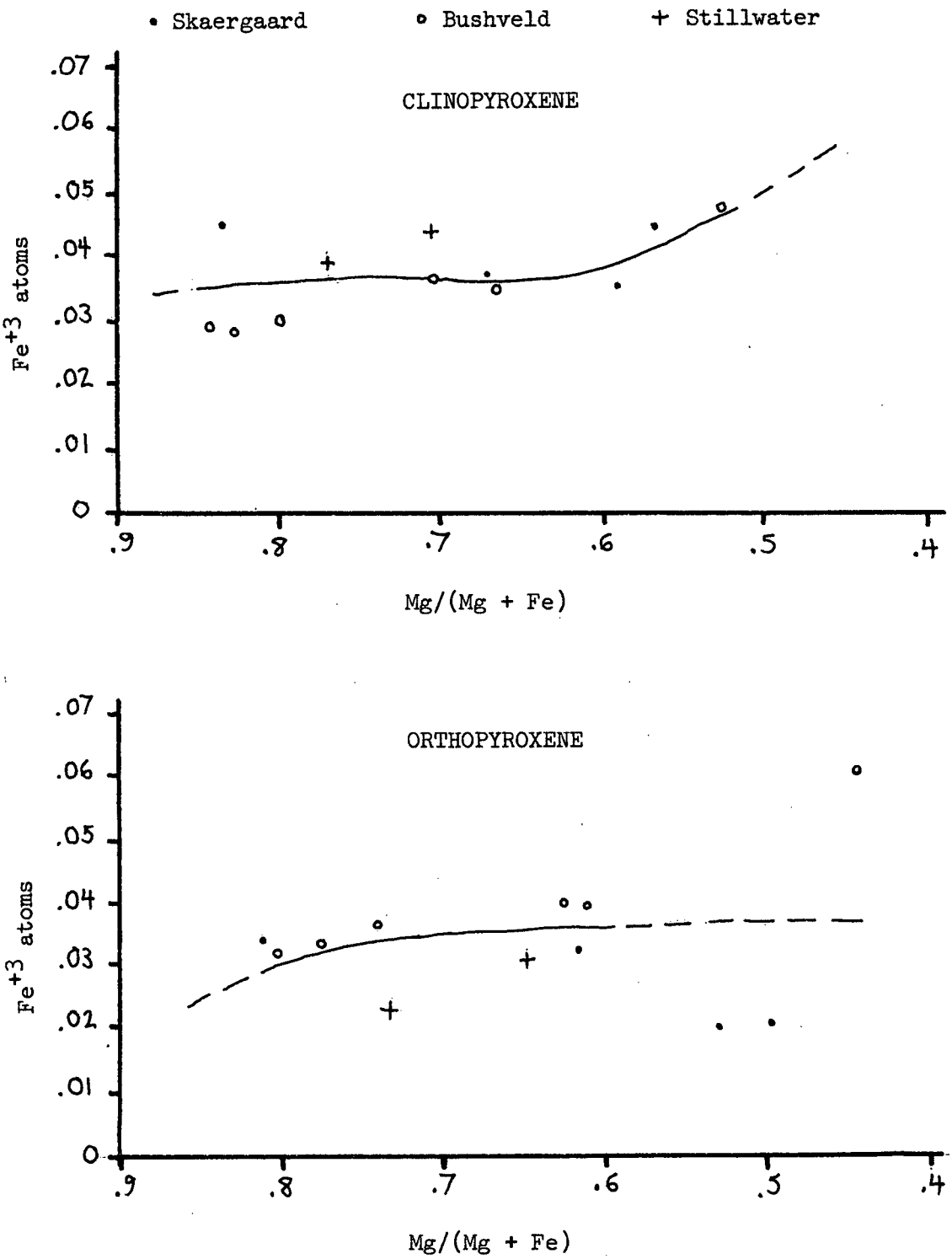

TABLE VI

CALCULATED EQUILIBRATION TEMPERATURES OF SPUZZUM PYROXENE PAIRS

No.	Temperature (°C) from Uncorrected formula	Corrected formula
74-7 (Feb. 75)	882.99	883.52
74-7 (Apr. 76)	913.56	917.94
15/6/75/6	873.17	874.30
17/6/75/15	877.43	880.11
18/7/75/5	948.87	954.41
24/7/75/11	922.81	927.55
27/8/75/2c	917.03	918.49
27/8/75/2a (pyroxenite)	965.62	970.15
27/8/75/2a (contact)	975.57	981.04
Range	102.40	106.74

that pyroxenes at the contact of Spuzzum diorite with Giant Mascot pyroxenite equilibrated at a somewhat higher temperature than pyroxenes in diorite far from this contact.

McLeod (1975) presented microanalyses for 18 pairs of coexisting ortho- and clinopyroxenes from ultramafic rocks from the 3050 level crosscut in the Giant Mascot Mine. These analyses include chromium in addition to elements analysed in this study, and iron is presented as FeO only. Equilibration temperatures calculated as described above average 1026°C and are listed in ascending order in table VII. Histograms of temperature data for Spuzzum and Giant Mascot pyroxene pairs are shown in fig. 10. The properties of these histograms are typical for the data compared to histograms using larger or smaller intervals, or with interval boundaries adjusted higher or lower. The peak at 1120 to 1160°C in the Giant Mascot histogram appears to be real. Whether it results from collecting bias or shows true temperature distribution is not known.

Pyroxenes of diorite are strongly exsolved. A few thin sections of ultramafic rocks show pyroxene to be moderately exsolved. In this study, and that of McLeod (1976, personal communication), care was taken during microanalysis to avoid parts of pyroxene grains rich in exsolution lamellae. If these grains were completely in equilibrium with exsolved pyroxene (when exsolution ceased), then the "clearer" areas should ultimately yield the composition of a single exsolved phase rather than the original pyroxene composition (prior to exsolution). The decrease in calculated temperature in diorite with increased distance from the Giant Mascot Ultramafic Body can be explained by equilibration of pyroxene by exsolution to lower temperatures during post-crystallization cooling. This may have been aided in diorite by increased water content or decreased cooling rate farther

TABLE VII

CALCULATED EQUILIBRATION TEMPERATURES

OF GIANT MASCOT PYROXENE PAIRS

Analysis No.	Temperature (°C)
3	910.39
27	950.44
8	971.34
28	974.87
22	989.07
19	999.50
11	1000.05
15	1007.88
7	1008.90
4	1010.25
2	1018.34
1	1040.21
18	1043.88
25	1003.09
17	1087.59
10	1129.10
16	1130.18
9	1132.59

Pyroxene analyses from McLeod (1975).

Fig. 10

HISTOGRAMS OF EQUILIBRATION TEMPERATURES

FOR PYROXENE PAIRS

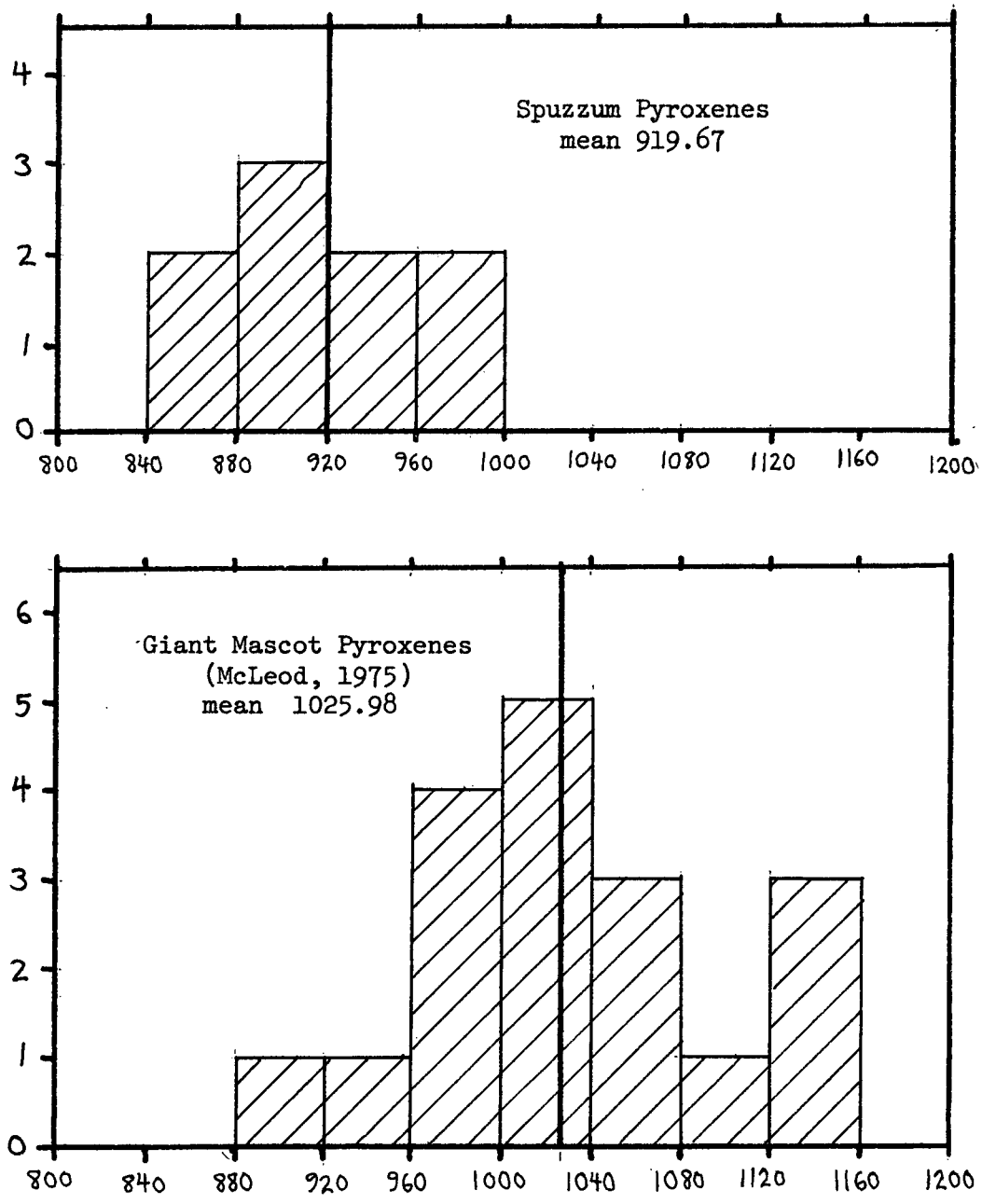

from the ultramafic rocks (which are near a wall of the pluton).

High calculated temperatures in ultramafic rocks may be relict from their original crystallization. Partial to complete re-equilibration of ortho- and clinopyroxenes by exsolution to lower temperatures may have been facilitated by engulfment in the hot Spuzzum Pluton. Deep penetration of magmatic fluids into the ultramafite is suggested by almost ubiquitous development of secondary hornblende in it (Aho, 1956). If temperatures in the ultramafite approached that of surrounding magma, a histogram of equilibration temperatures might be expected to show a maximum approximating the magma temperature, provided further re-equilibration with decreasing temperature is minor (unlike the model suggested for diorite). The Giant Mascot histogram (fig. 10) has such a peak at 1000 to 1040°C. The high temperature peak (1120 to 1160°C) may represent pyroxene pairs unaffected by reheating.

D. Hornblende

A key to hornblende analyses listing symbols, specimen numbers, and modes of occurrence is given in table VIII. Analyses and formulas are listed in table IX. Since volatiles were not determined, the ideal two hydrogens for 24 oxygens are assumed in the formula unit. Assignment of elements to sites is as follows: Tetrahedral sites - Si and Al adding to eight atoms or less if Al is insufficient. Octahedral sites - all remaining Al, Ti, Fe^{+3}, and Mg adding to five atoms or less if Mg is insufficient. If Mg is insufficient, Fe^{+2} is added to five atoms or until it is consumed. Cubic sites - all remaining Mg, Fe^{+2}, Mn and Ca adding to two atoms or less if Ca is insufficient. If Ca is insufficient, Na is added to two atoms or until it is consumed. Alkali sites - all remaining Ca, Na, and K. As with

TABLE VIII

KEY TO SPUZZUM AND GIANT MASCOT

HORNBLENDE ANALYSES

SYMBOL	SPEC. NO.	DESCRIPTION
		SPUZZUM HORNBLENDITE:
▲	AM#2	Type II; homogeneous, medium-grained hornblendite body in diorite
		GIANT MASCOT HORNBLENDITES:
▼	18/7/75/7a	Type II; pyroxene-bearing medium-grained hornblendite dykelet (average 5)
♦	2600	Type II; pyroxene-bearing coarse-grained hornblendite of ultramafic complex (average 5)
■	13/9/75/1a	Type I; plag-bearing very coarse-grained hornblendite adjacent to tonalite (average 5)
		"NORMAL" DIORITES:
□	15/6/75/6	Anhedral grains and rims of pyroxene in pyroxene diorite
△	17/6/75/15	Same as above (average 2)
▽	24/7/75/11	Same as above
		PYROXENITE-DIORITE CONTACT:
○	27/8/75/2a	Large subhedral porphyroblast(?) in pyroxenite 2 cm. from altered diorite (average 2)
○	27/8/75/2a	Different place in same crystal (average 2)
×	27/8/75/2c	Large anhedral brown-cored crystal in altered diorite (average 2)
+	27/8/75/2c	Replacing pyroxene as rims and pale green blades with pyroxene (average 4)

TABLE IX

SPUZZUM AND GIANT MASCOT HORNBLENDE ANALYSES AND FORMULAS

SYMBOL	▲	▼	♦	■	□	△	▽	o–	–o	×	+
SiO_2	44.58	43.82	45.65	50.09	46.65	43.75	45.99	48.27	43.23	42.73	50.06
TiO_2	1.65	1.43	1.36	.72	.78	2.14	.94	1.12	2.43	2.63	.46
Al_2O_3	12.00	11.91	11.03	7.17	8.89	9.81	9.57	7.84	11.50	12.48	8.05
FeO	10.11	8.61	9.87	8.76	12.84	14.69	12.30	7.77	8.45	9.17	7.80
MgO	14.55	14.88	15.62	16.61	13.78	11.68	13.24	16.49	14.87	14.16	16.80
MnO	.09	.07	.15	.14	.10	.16	.14	.10	.09	.07	.11
CaO	11.15	11.37	11.17	12.40	11.39	11.04	11.52	11.29	10.72	11.25	11.71
Na_2O	2.32	2.19	2.30	1.71	.90	1.39	.96	1.26	1.93	1.75	.73
K_2O	.16	.14	.32	.28	.44	.84	.59	.32	.34	.25	.17
Total	96.61	94.42	97.47	97.88	95.77	95.50	95.25	94.46	93.56	94.49	95.89
Alkali Site	.538	.537	.578	.425	.295	.428	.299	.258	.466	.439	.126
K	.030	.026	.058	.051	.083	.162	.112	.060	.065	.047	.031
Na	.508	.511	.520	.374	.212	.267	.187	.198	.402	.392	.095
Cubic Site	2	2	2	2	2	2	2	2	2	2	2
Na	.147	.118	.123	.096	.046	.140	.089	.159	.157	.112	.108
Ca	1.739	1.804	1.725	1.887	1.803	1.784	1.833	1.768	1.716	1.790	1.796
Mn	.011	.009	.018	.016	.013	.020	.018	.012	.011	.009	.013
Fe^{+2}	.104	.069	.134	.0	.139	.056	.060	.060	.115	.089	.082
Octahedral Site	5	5	5	4.940	5	5	5	5	5	5	5
Mg	3.147	3.275	3.346	3.507	3.026	2.618	2.922	3.582	3.302	3.126	3.574
Fe^{+2}	.912	.793	.836	.836	1.202	1.511	1.222	.694	.739	.841	.659
Fe^{+3}	.215	.204	.219	.205	.246	.286	.246	.195	.202	.209	.192
Al	.546	.568	.452	.316	.440	.342	.505	.406	.484	.531	.525
Ti	.181	.159	.148	.077	.087	.243	.105	.123	.273	.294	.050
Tetrahedral Site	8	8	8	8	8	8	8	8	8	8	8
Al	1.513	1.511	1.422	.884	1.108	1.402	1.170	.945	1.541	1.654	.834
Si	6.487	6.489	6.578	7.116	6.892	6.598	6.830	7.055	6.459	6.346	7.166

pyroxenes this scheme is not thoroughly supported by structural evidence. Fe^{+2} is preferentially placed in the cubic site over Mg because it is larger, yet has the same charge as Mg, and perhaps forces Mg to take the smaller octahedral site. This assignment of atoms is based on an admittedly simplistic argument.

Because further calculations were made with hornblende analyses, an estimation of Fe^{+3} content was desired. The same procedure used to estimate Fe^{+3} in pyroxenes was used for hornblende. Hornblende analyses from Deer, Howie, and Zussman (1963) most similar to Spuzzum hornblende analyses were selected for an Fe^{+3} vs. Mg/(Mg + Fe) diagram (fig. 11). Analyses of these hornblendes, and their formulas calculated by the above scheme, are listed in Appendix III. A curve was drawn to represent Fe^{+3} in Spuzzum hornblende. Formulas given in table IX have been corrected.

Several analyses of ultramafic, alkaline, and mafic igneous rocks have been gathered from literature for comparison with that of Spuzzum hornblendite. One analysis of a hornblendite dykelet from South Africa is also included. A key to references, rock types analyzed, and modes of occurrence is given in table X. Analysis 4 is the average of AM#2 and 18/7/75/7a (which are very similar) with Fe_2O_3 calculated from formulas in table IX. Analyses as they appear in their respective sources are listed in table XI with C.I.P.W. norms. Norms were calculated after neglecting volatile elements and normalizing to 100 per cent; effective weight per cent SiO_2 is also listed. Analyses 1 and 2 show a SiO_2 deficiency that cannot be satisfied by forming leucite, and just enough silica has been added to these analyses to satisfy the deficiency (under 5% added). C.I.P.W. norms are shown in simplified form in fig. 12. It can be readily seen that analyses 3, 8, 9, and 10 are most similar to Spuzzum hornblendite. Good

Fig. 11

FE^{+3} ATOMS PER FORMULA UNIT

IN SPUZZUM AND GIANT MASCOT HORNBLENDES

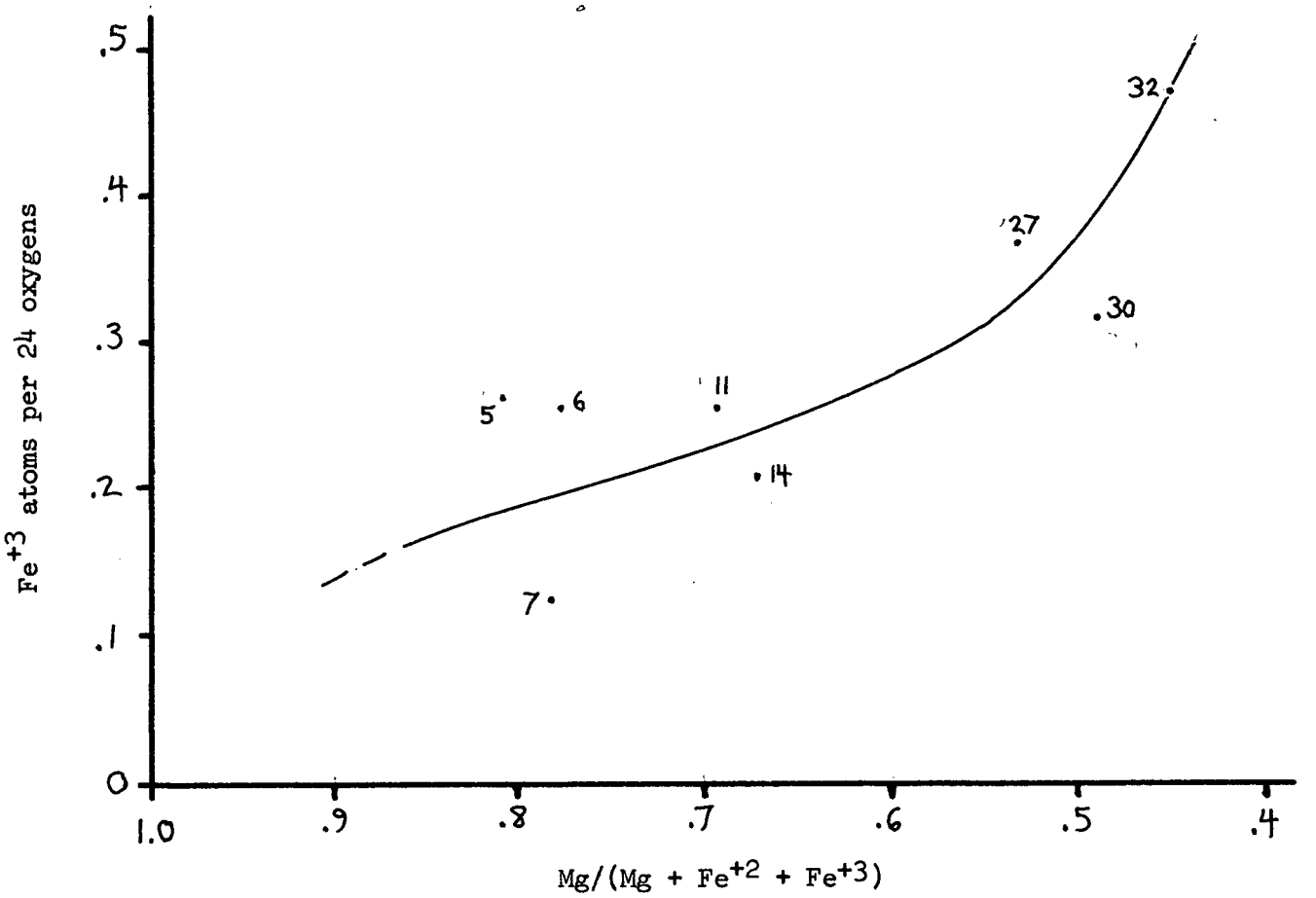

TABLE X

KEY TO WHOLE-ROCK ANALYSES FROM LITERATURE

NO.	REFERENCE	ROCK TYPE	OCCURRENCE
1*	Hyndmann, 1972	mafic alkaline	average of 105 analyses
2*	Hyndmann, 1972	alkaline ultramafic	average of 12 analyses
3	Verhoogen, et al., 1970	nepheline basalt	Honolulu Series, Oahu, Hawaii
4	this study	hornblendite	dykelets, average of 2 analyses
5	Richards, 1971	hornblende diabase	gabbroic complex
6	Verhoogen, et al., 1970	high-Al_2O_3 basalt	Medicine Lake highlands, N. E. California
7	Krauskopf, 1967	peridotite	average of many analyses
8	Richards, 1971	olivine gabbro	gabbroic complex, analysis est. from mode
9	Krauskopf, 1967	olivine basalt	average of many analyses
10	Verhoogen, et al., 1970	olivine basalt	Haleakala Volcano, Maui, Hawaii
11	Verhoogen, et al., 1970	olivine tholeiite	Thingmuli Volcano, Iceland
12	McIver, 1972	hornblendite	dykelet in Bushveld Main Zone Gabbro, S. Africa

* SiO_2 content increased slightly in norm.

TABLE XI

WHOLE-ROCK ANALYSES AND ADJUSTED C.I.P.W. NORMS OF ROCKS FOR COMPARISON WITH SPUZZUM HORNBLENDITE

NO.	1	2	3	4	5	6	7	8	9	10	11	12
SiO_2	41.10	40.28	42.86	46.20	45.70	48.27	43.89	46.14	48.19	48.04	47.07	51.38
TiO_2	2.80	3.67	2.94	1.58	1.49	.89	.81	2.11	1.66	1.83	1.66	.18
Al_2O_3	13.90	6.77	11.46	12.50	18.80	18.28	4.02	11.72	11.91	12.04	14.86	4.57
Fe_2O_3	5.30	4.85	3.34	2.01	1.90	1.04	2.53	--	2.33	2.35	4.08	2.87
FeO	5.30	4.59	9.03	7.96	6.50	8.31	9.92	9.79	9.86	8.80	7.20	10.46
MgO	6.90	21.88	13.61	15.39	7.30	8.96	34.27	20.30	14.15	14.41	8.52	14.86
MnO	.20	.31	.13	.08	.14	.17	.21	--	.15	.17	.17	.24
CaO	15.30	9.92	11.24	11.77	10.60	11.32	3.49	7.78	9.35	8.76	11.47	11.99
Na_2O	5.00	1.22	3.02	2.36	2.70	2.80	.56	1.59	1.67	1.60	2.24	1.14
K_2O	3.20	3.93	.93	.15	.70	.14	.25	.58	.54	.30	.20	.26
P_2O_5	1.10	.70	.52	--	.27	.07	.05	--	.19	.12	.18	.10
Others	1.46	2.61	.86	--	2.13	.22	--	--	--	1.63	2.25	2.39
Total	101.56	100.73	99.94	100.00	98.23	100.47	100.00	100.01	100.00	98.30	99.90	100.44
Lc	14.29	18.04	0.	0.	0.	0.	0.	0.	0.	0.	0.	0.
Ne	22.09	5.51	10.81	3.94	.56	.31	0.	0.	0.	0.	0.	0.
Or	0.	0.	5.55	.88	4.31	.83	1.48	3.43	3.19	1.80	1.21	1.60
Ab	0.	0.	5.84	12.70	22.74	23.07	4.74	13.45	14.13	13.76	19.41	9.82
An	5.81	1.38	15.11	23.06	38.60	36.81	7.72	23.13	23.41	25.19	30.62	6.71
Wo	5.19	0.	0.	0.	0.	0.	0.	0.	0.	0.	0.	0.
Di	37.63	33.33	30.13	28.21	11.54	15.27	7.35	12.36	17.49	14.56	21.23	43.08
Hy	0.	0.	0.	0.	0.	0.	15.32	4.58	20.13	27.97	14.49	33.41
Ol	0.	26.88	20.83	25.29	15.78	20.37	58.08	39.06	14.67	9.45	3.33	.56
Mt	7.40	5.13	4.88	2.92	2.87	1.51	3.67	0.	3.38	3.46	6.06	4.25
He	0.	1.25	0.	0.	0.	0.	0.	0.	0.	0.	0.	0.
Il	5.13	6.89	5.63	3.00	2.94	1.69	1.54	4.01	3.15	3.54	3.23	.34
Ap	2.46	1.59	1.21	0.	.65	.16	.12	0.	.44	.28	.43	.23
	100.00	100.00	99.99	100.00	100.00	100.02	100.00	100.02	100.00	100.01	100.01	100.00
%Mg/(Mg+Fe)	95.33	100.00	82.83	82.69	74.48	68.82	88.05	82.05	77.10	80.33	78.92	74.07
%An	100.00	100.00	70.91	63.13	61.54	60.06	60.55	61.85	60.96	63.31	59.79	39.19
Wt.%SiO_2 in norm	43.14	42.80	43.26	46.20	47.55	48.15	43.89	46.14	48.19	48.81	48.20	52.40

Fig. 12

VARIATION DIAGRAM OF C.I.P.W. NORMS OF WHOLE-ROCK ANALYSES

FOR COMPARISON WITH SPUZZUM HORNBLENDITE

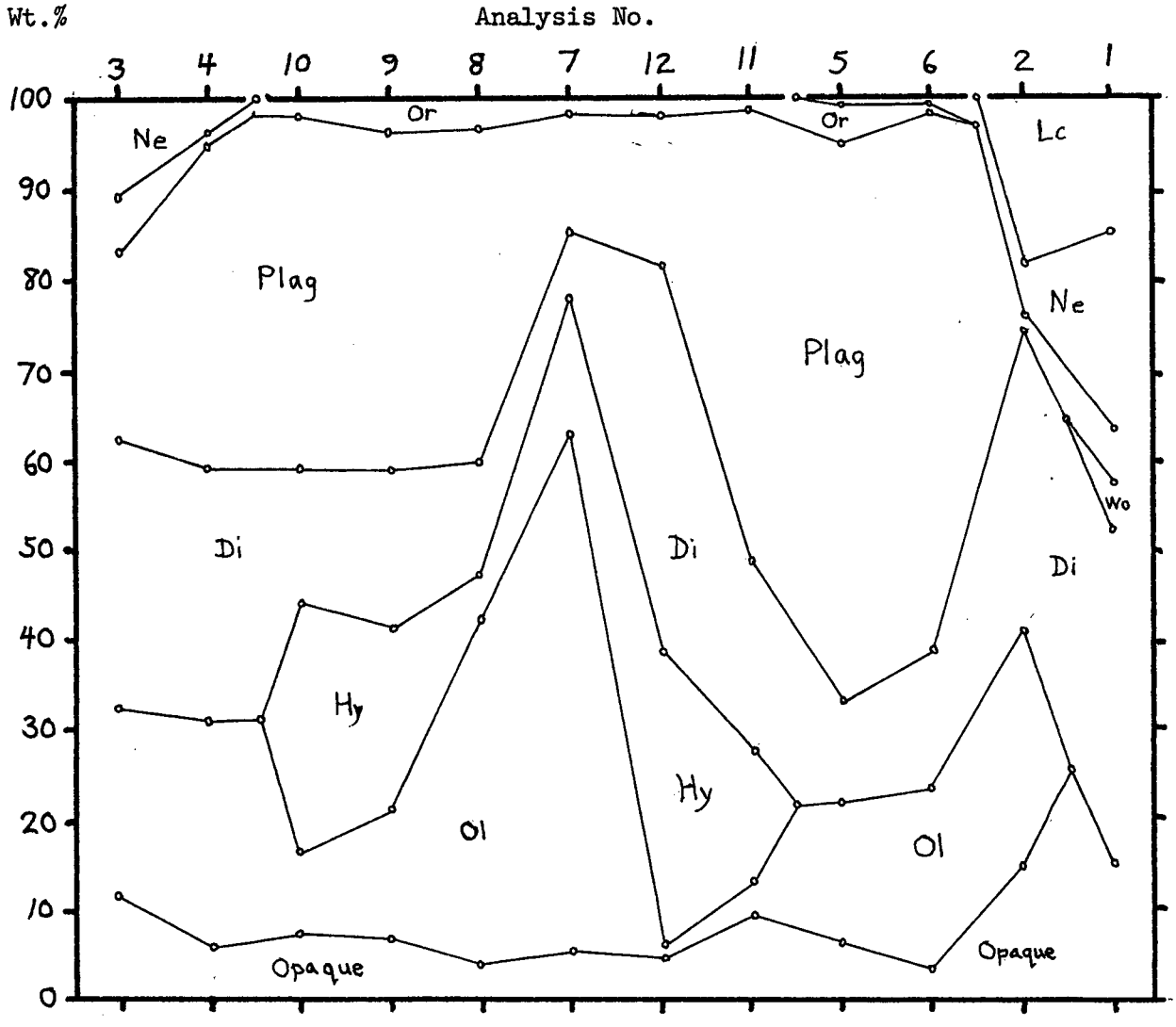

agreement among anorthite content of plagioclase, Mg:Fe in silicates, and effective SiO_2 supports this choice.

It is interesting that all four of the most similar analyses are of moderately to strongly undersaturated basaltic composition. This relationship suggests that Spuzzum hornblendite could be the result of crystallization of basaltic magma under elevated water pressure (McIver, 1972). One possible source of such a "magma" is the reaction of Spuzzum diorite or tonalite with the Giant Mascot Ultramafic Body which is the centre of much hornblendite development (McLeod, 1975). This would require that Spuzzum hornblendite be equal in age to, or slightly younger than, the Spuzzum Pluton. Another possible correlation of Spuzzum hornblendite is with the gabbroic complex of the Yale Intrusions (Richards, 1971), which is contained within the Coquihalla quartz monzonite stock (K-Ar age of 41 m.y.) east of Hope. The gabbroic complex appears to be intruded by quartz monzonite. Analyses 5 and 8 in table XI are from this complex.

Hornblendites of this study (table VIII, page 68) appear chemically related to hornblendes in pyroxenite of the Giant Mascot Ultramafic Body and in Spuzzum diorite in contact with it (pages 43 - 45). Hornblende analyses are plotted with pyroxene analyses in fig. 8, a C-F-M atomic porportions diagram. The most obvious features of this diagram are (1) the compositional parallelism between pyroxenes and coexisting hornblende, and (2) the fact that hornblendites and hornblendes of Giant Mascot pyroxenite and adjacent altered diorite are together in a loose cluster, whereas those of "normal" diorites are more Fe-rich. In fig. 13, Mg/(Mg + Fe) and Al are plotted against Si (atomic proportions in the formula unit). Again hornblendes of pyroxenite and altered diorite cluster around hornblendites.

Two distinct types of hornblendite can be recognized, one Si-rich and the other Si-poor, and the Si content of hornblendes of normal diorite falls between them. The Si-rich hornblendite (type I) occurs as a coarse pegmatite adjacent to tonalite at the east margin of the Giant Mascot Ultramafic Body (fig. 7). The Si-poor hornblendite (type II) occurs as dykelets in Spuzzum diorite and Giant Mascot ultramafic rocks. Hornblendite from the south margin of the ultramafic body, adjacent to diorite, corresponds with type II (fig. 13). Large zoned crystals from pyroxenite have compositions ranging from type I to type II hornblendite. Large poikilitic anhedral crystals from altered diorite group with type II hornblendite, whereas rims of pyroxenes and small subhedral grains among pyroxenes group with type I.

The graphical relationships above suggest that Spuzzum hornblendite (pages 23 - 39) and some Giant Mascot hornblendites (pages 52 - 53) are genetically related. Further, Giant Mascot hornblendites are also related to the large poikiloblasts/phenocrysts of pyroxenite and altered diorite, as well as to hornblende that replaces pyroxenes in altered diorite. It has been suggested that the hornblendite rim around the Giant Mascot Ultramafic Body originated by reaction with diorite or tonalite (Aho, 1956; and McLeod, 1975). The chemical relationships shown above are consistent with this hypothesis in that hornblendite adjacent to tonalite is richer in Si than that adjacent to diorite. Also the amounts of Al and Si in diorite and tonalite show the same relationship as the amounts in corresponding hornblendites (✳ in fig. 13). In this diagram, Al from diorite is plotted against the number of Si in the formula unit of type II hornblende (6.5). The same has been done for tonalite and type I

Fig. 13

MG/(MG + FE) AND AL VERSUS SI PER FORMULA UNIT

IN SPUZZUM AND GIANT MASCOT HORNBLENDES

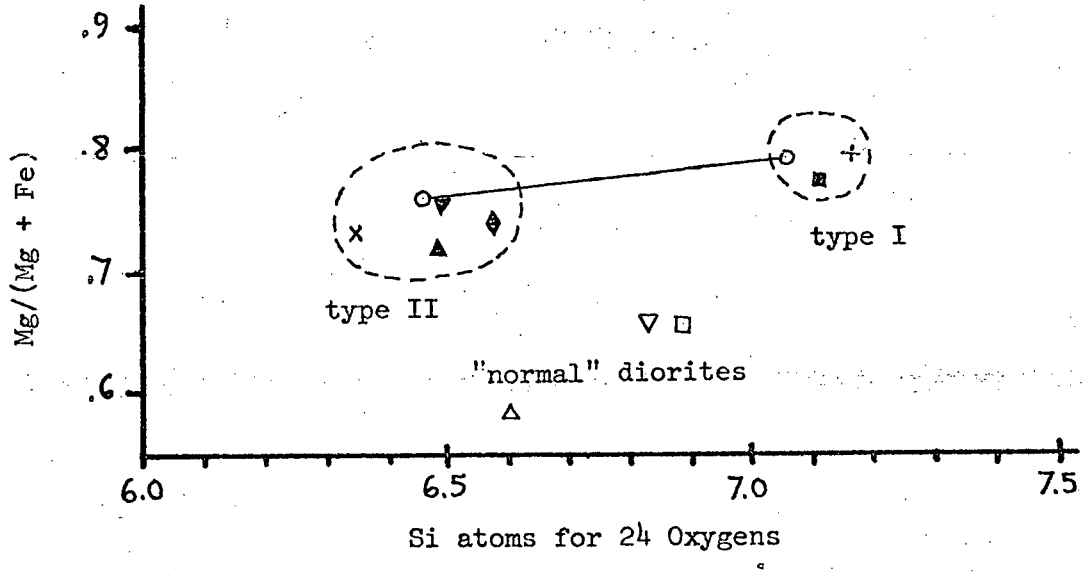

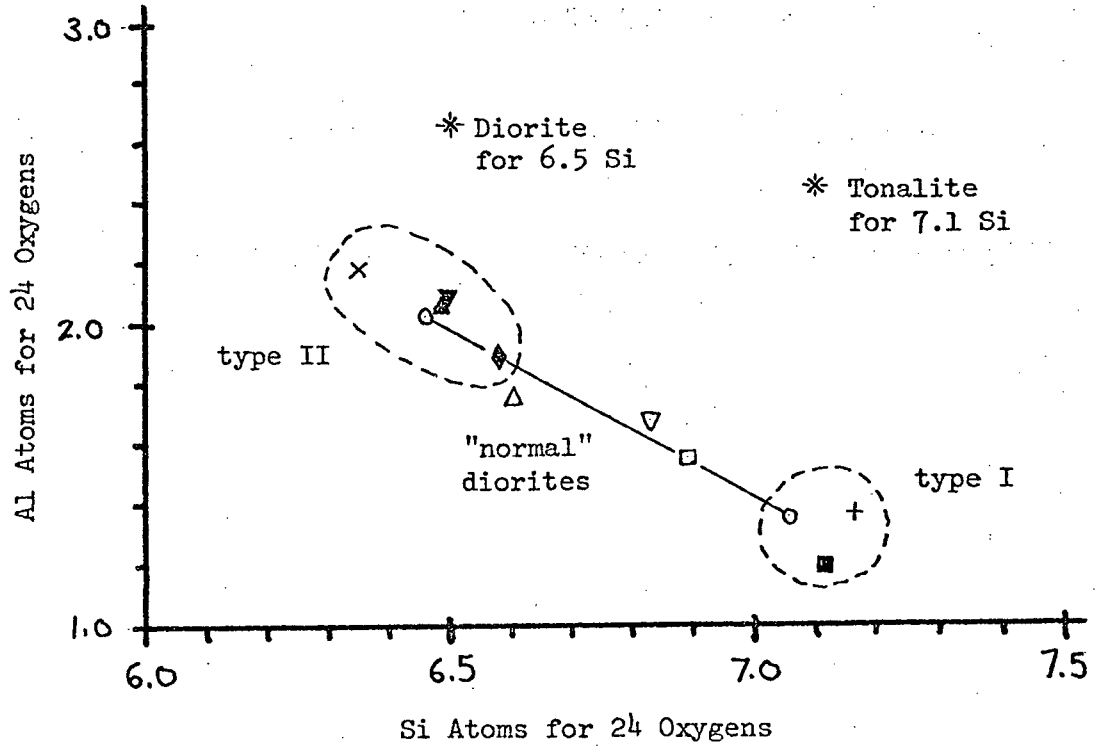

hornblende (7.1 Si). The value of Al is molar Al/Si in diorite or tonalite multiplied by the number of Si in the formula for corresponding hornblendite.

VII. ORIGIN

A. Introduction

Any hypothesis of the origin of the Spuzzum Pluton must explain the following:

(1) Chemical similarities and differences between tonalite and diorite;

(2) Mineralogical zonation from diorite to tonalite;

(3) Structural patterns in the pluton, configuration and heterogeneous distribution of phases and foliations; and

(4) Radiometric ages.

Richards (1971) suggested that dioritic magma first intruded country rocks, followed in about 20 million years by a surrounding intrusion of tonalite which formed by fractional crystallization from the same dioritic parent. Variation in mineralogy was attributed to either decrease in temperature or increase in water pressure from core to margin. Minor variation of the amounts of SiO_2 and K_2O in diorite was explained by water migration either into relatively dry diorite from country rocks, or away from the hotter plutonic core. Tonalite was interpreted to be related to diorite only by the differentiation process. He considered the domelike structure pattern to be primary foliation from diapiric emplacement of dioritic crystal mush. The northwest trending foliations in tonalite are thought to be inherited from regional deformation. He suggested that diorite is pre-orogenic whereas tonalite is synorogenic (Richards, 1971, p. 47). Radiometric ages were taken as indicating that tonalite is about 20 million years younger than diorite.

As an alternative to Richards' hypothesis, this author suggests a model of diapiric intrusion of a partly differentiated quartz diorite magma body into country rocks, producing a single zoned tongue-like pluton with a dioritic core and a tonalitic rim. Variations in chemistry and mineralogy in diorite can be explained by the same mechanism used in Richards' model. The relatively sharp distinction between tonalite and diorite respresents the boundary between magma without crystals and the same magma with accumulated crystals. Other plutons of apparent diapiric form in the Coast Plutonic Complex (and other parts of the North American Cordillera) have acidic cores and more basic rims (Hutchison, 1970; and others). The reversed distribution in the Spuzzum Pluton is explained by a mechanism of drawing up accumulated crystals.

Some of the syntectonic features of tonalite can be seen in diorite (see map in pocket and fig. 6). Regional mapping shows foliations to be heterogeneous and difficult to explain by either Richard's or this author's hypothesis. Syntectonic emplacement of a crystal mush diapir however, could be expected to produce a confusing array of internal structures.

Radiometric ages may not indicate the true age of these rocks because of the formation of secondary hornblendite in most parts of the pluton, and because of late deformation (McTaggart and Thompson, 1967). Such alteration and deformation may explain

the fact that the source of the oldest age determination (K-Ar 103 m.y.) is tonalite. Richards attempted to explain this discrepancy as contamination from diorite, its gradational contact with tonalite being 130 metres away.

B. Differentiation of Spuzzum Magma

1. Discussion

The fundamental difference between Richards' differentiation model and that of this author is illustrated graphically in fig. 14. Richards treated the dioritic core as representative of the parent magma, having been emplaced as a pre-differentiation pluton. Tonalite is later derived by removal of basic constituents of the dioritic parent magma by settling of crystals (54 per cent of its mass as 74 per cent plagioclase An 52, 13 per cent augite and hypersthene, and 13 per cent olivine) which have not been identified in the field (Richards and McTaggart, 1976). In the model proposed in the present study, diorite is considered a cumulate brought up with the rising tonalite diapir. The parent is therefore a mixture of the two. Differentiation is postulated to have been completed at depth before intrusion, thus only the products of it have risen in the Spuzzum Pluton and the parent is not seen.

In estimating the original composition of the hypothetical parent magma, the areal extent of tonalite and diorite was estimated from the map produced in this study and that of Richards and McTaggart (1976). Map areas are assumed to represent cross-sectional areas of concentric

Fig. 14

CHEMICAL RELATIONSHIPS IN SPUZZUM DIFFERENTIATION

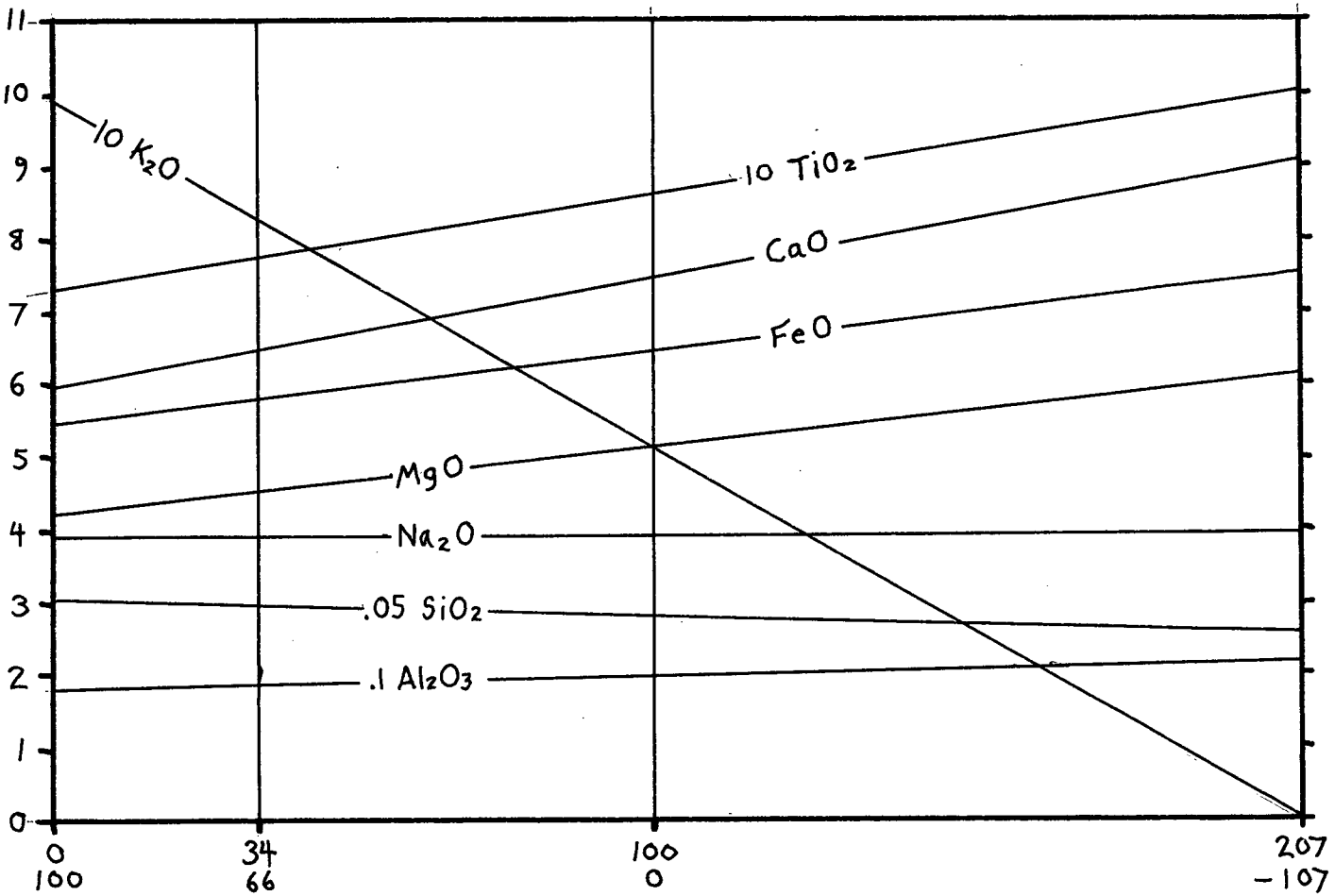

Note: FeO represents all iron.

spheres, diorite being the central one. Volume per cent of diorite is calculated thus:

$$X = \left(\frac{A1}{A2}\right)^{3/2}$$

where X = volume per cent diorite in parent magma,

A1 = area of diorite only, and

A2 = area of pluton as a whole.

Volume per cent is converted to weight per cent by the equation:

$$Y = \frac{100}{\left[1 + \frac{\rho_{ton}(100-X)}{\rho_{dio}\, X}\right]}$$

where Y = weight per cent diorite in magma

ρ_{ton} = density of tonalite, and

ρ_{dio} = density of diorite.

Approximate densities of diorite and tonalite are calculated from those of individual minerals from Robie and Waldbaum (1968) and Deer, Howie, and Zussman (1966). This calculation is carried out in table XII, and its results are consistent with densities given in Clark (1966). The mode of tonalite is the average of all twelve thin section estimated modes in Appendix I. That of diorite is the average of pyroxene diorites 15/6/75/6, 24/7/75/11, and 10/7/75/6. Calculated densities are $\rho_{ton} = 2.84$ and $\rho_{dio} = 2.93$.

This calculation of the composition of parent magma is only a crude approximation as the configuration of diorite and tonalite is not known at depth, and certainly does not conform to concentric spheres. Values of A1 and A2 from both maps each produce volume proportions of 33 per cent diorite. This is converted to 34 weight per cent diorite in parent magma.

TABLE XII

CALCULATION OF DIORITE AND TONALITE DENSITIES

Mineral	Pyroxene Diorite	Tonalite	Mineral Density	Contribution to Density	
				Diorite	Tonalite
Qz	tr	16	2.65	--	.42
Plag	69	51	50:2.68	1.85	--
(An%)	(50)	(41)	41:2.66	--	1.36
Cpx	15	--	3.35	.50	--
Opx	15	--	3.50	.53	--
Hbd	tr	22	3.2(?)	--	.70
Bio	--	10	3.0	--	.30
Opaque	1	.5	5.2	.05	.03
Chl	--	1	3.0(?)	--	.03
			TOTAL DENSITY	2.93	2.84

Mineral densities from Deer, Howie, and Zussman (1966).

Fig. 14 accurately portrays the compositions of diorite, magma, and tonalite, the line representing magma having been drawn at 34 weight per cent diorite.

2. Test of the Hypothesis

A computer program was written by the writer to test the hypothesis of Spuzzum diorite and tonalite forming from a common parent by settling of crystals into a lower fraction (diorite), leaving a crystal-depleted upper fraction (tonalite). The program, given in Appendix IV, is in BASIC and was run on a Digital PDP 11/10 desk computer. It simulates the crystallization of ilmenite, magnetite, plagioclase, orthopyroxene, and clinopyroxene from hypothetical parent magma composed of a combination of chemical analyses of Spuzzum diorite and tonalite. Oxides considered are SiO_2, Al_2O_3, TiO_2, FeO, MgO, CaO, Na_2O, and K_2O. All iron is calculated as FeO. The diorite analysis is the average of five Spuzzum diorites, and that of tonalite is the average of three Spuzzum tonalites, all given by Richards (1971, p. 35). Analyses have been normalized to 100 per cent after removal of CaO for apatite. Ilmenite and magnetite are treated as pure phases. Pyroxene compositions (table XIII) are the averages of formulas from tables Va and b of specimens 15/6/75/6, 17/6/75/15, and 24/7/75/11 (all pyroxene diorites). The composition of cumulate plagioclase is determined in the program from the composition of the magma. Plagioclase is considered to contain 1.5 molecular per cent $KAlSi_3O_8$.

The analysis of the hypothetical melt (34% diorite and 66% tonalite) is converted to a reservoir of positive ions from which formula units of the various minerals are removed. Crystallization progress is calculated for steps of one per cent of the reservoir, beginning with ilmenite and magnetite.

The operator must choose whether plagioclase should equilibrate with liquid or be shielded from it. Shielding in this case means that plagioclase crystallized during previous steps should not equilibrate with liquid during successive steps, thus preserving normal zoning. Partial equilibration is calculated later by linear interpolation between these two cases. In the case of shielding, cumulus plagioclase composition is determined at each one per cent step, whereas in the case of equilibration the composition is not determined until the end of cumulate crystallization. At a stage of crystallization (per cent atoms as crystals) determined by the operator, analyses of diorite (cumulate crystals plus some liquid) and tonalite (remaining liquid) are assembled and printed. This represents the end of cumulate crystallization, that is, when diorite and tonalite begin to crystallize independently. The amount of liquid added to crystals to form the diorite analysis is determined by the proportion of original diorite used in making the hypothetical magma.

The operator must decide at what stage of crystallization (per cent atoms as crystals) each of the major minerals should begin to crystallize. From these values the proportions of plagioclase, orthopyroxene, and clinopyroxene are determined for each one per cent step. Relative amounts of pyroxenes and plagioclase crystallizing in any step are assumed proportional to the amounts that occur in the pyroxene-richest diorites. The limiting values are averaged from thin section estimated modes of pyroxene diorites 15/6/75/6, 24/7/65/11, and 10/7/75/6. Volumes of plagioclase and combined pyroxenes are 70 and 30 per cent respectively, in accordance with the mode. The ratio of clinopyroxene over orthopyroxene is .96 by volume. Molar volumes used are for pure diopside, pure clinoenstatite (for six oxygens per formula unit), and plagioclase (An50), taken from Robie and

Waldbaum (1968).

Plagioclase compositions are determined by estimated melting relationships in the system plagioclase An 60 - enstatite - diopside at 15 kilobars dry pressure (Emslie, 1971). For this calculation only the compositions of coexisting liquid and plagioclase are needed for various bulk compositions. Temperature is of no interest. Emslie (1971) reported that plagioclase in equilibrium with pyroxenes and liquid near the pseudo-ternary piercing point at 15 kilobars has a composition of about An 65 by weight. It is assumed that liquid with normative albite, but no anorthite, will crystallize pure albite; and that liquid with normative anorthite, but no albite, will crystallize pure anorthite. This assumption is probably incorrect in detail, but it serves to simplify calculation of compositions in the middle range where the real plagioclase composition lies (that is An 40 to 60). If the liquidus is represented by a straight line, these data allow one to represent the solidus as a smooth curve, and here a hyperbolic curve is chosen for simplicity (fig. 15).

Fig. 15

CALCULATION OF PLAGIOCLASE MELTING CURVES

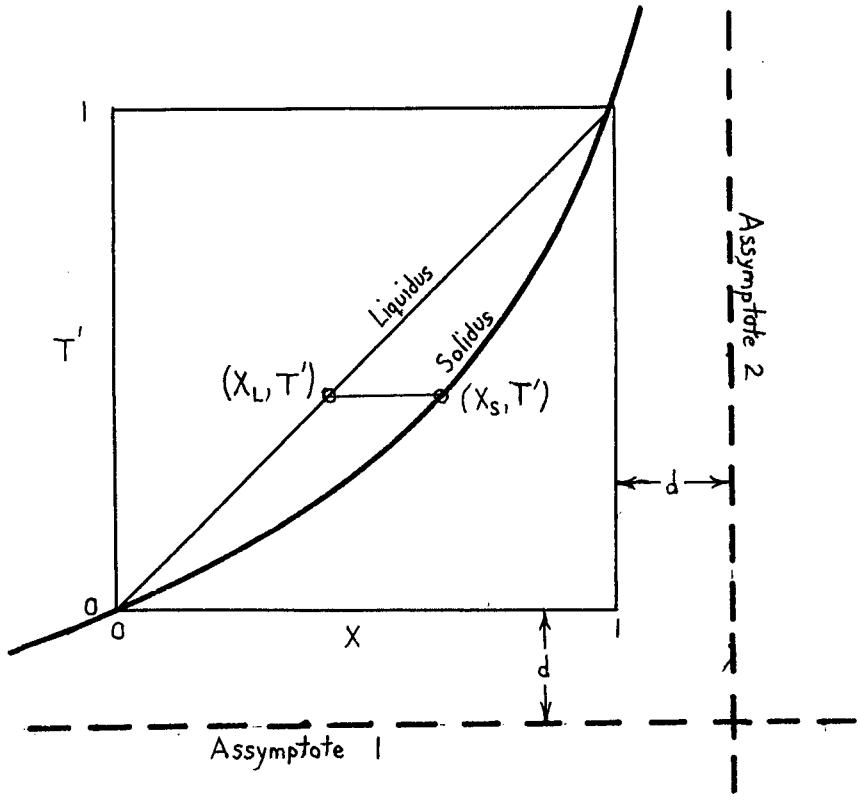

Assymptote 1: $T' = -d$

Assymptote 2: $X = 1 + d$

Liquidus: $T' = X$

Solidus: $T' = \dfrac{-k}{X - (1 + d)} - d$

where $k = d^2 + d$.

Therefore $X_S = \dfrac{-k}{X_L + d} + d + 1$

where X_S = composition of plagioclase, weight fraction An, and

X_L = weight fraction An/(An + Ab) for concentrations of An and Ab in liquid

Fig. 16

CALCULATED PLAGIOCLASE MELTING CURVES

FOR VARIOUS CONDITIONS

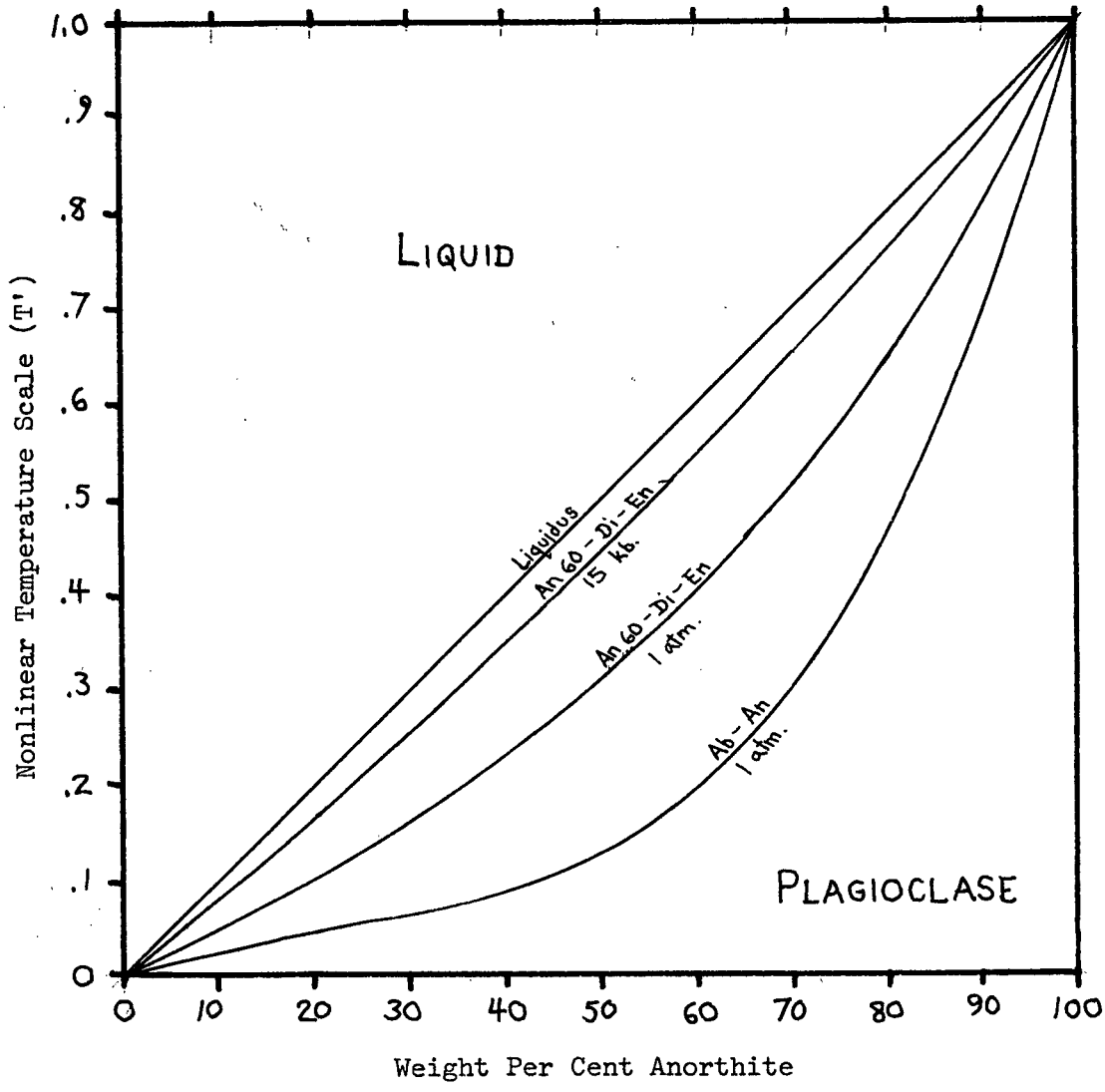

In order to specify X_L, the program calculates normative amounts of anorthite and albite in the liquid. These amounts are slightly in error, as pyroxenes contain some sodium and aluminum. For comparison, a diagram of T' (function of temperature) against weight per cent anorthite is shown in fig. 16, with the calculated curves for 15 kilobars and 1 atmosphere pressure (Emslie, 1971), and a graphically measured curve for the system albite - anorthite at 1 atmosphere (Bowen, 1913).

The output of reconstructed analyses of diorite and tonalite is accompanied by the RMS residual for all oxides in both analyses, compared with the original analyses. By varying the input parameters (crystallization sequence, amount of accessories, and end of cumulate crystallization) the RMS residual can be minimized for both shielded and equilibrated plagioclase.

3. Results

Results of the test above are shown in tables XIVa and b. Analyses of diorite and tonalite from Richards (1971) are labelled "original." Reconstructed analyses of diorite and tonalite, synthesized according to the computer program for both "equilibrated" and "shielded" plagioclase, are presented side by side with the "original" analyses. For comparison, the mixture of 34 per cent diorite and 66 per cent tonalite is shown under the title "original magma." In table XIVa the various input parameters used for the cases of "equilibrated" and "shielded" plagioclase are shown along with the resulting RMS residua. These are the minimum values of RMS residua obtained after systematically varying the input parameters during the test. For all practical purposes they are equal for the two cases for plagioclase, and in the opinion of the writer they show that the differentiation mechanism considered is consistent with chemical analyses

TABLE XIII

PYROXENE COMPOSITIONS USED IN THE DIFFERENTIATION TEST

	Mole Per Cent Anions	
Anion	Orthopyroxene	Clinopyroxene
Si	49.59	48.94
Ti	.07	.25
Al	1.32	2.38
Fe	18.50	8.06
Mg	29.70	18.62
Ca	.81	20.93
Na	.01	.81
K	.00	.00
Equivalent Oxygen	150.32	149.98

TABLE XIVa

RESULTS OF THE DIFFERENTIATION TEST:

INPUT PARAMETERS AND RMS RESIDUA

Case	Equilibrated	Shielded
RMS residual	.156	.162
Wt.% diorite	34	34
Atom% crystals	14.2	13.9
Atom% Il	.20	.20
Atom% Mt	.02	.02
Atom% xals when:		
Plag begins	1	1
Opx begins	0*	0*
Cpx begins	14.2	13

* actually calculated after removal of accessories

TABLE XIVb

RESULTS OF THE DIFFERENTIATION TEST:

COMPOSITIONS OF PHASES

	DIORITE			TONALITE			ORIGINAL MAGMA
	Original	Equil.	Shield.	Original	Equil.	Shield.	
SiO_2	56.16	56.29	56.29	60.99	60.73	60.73	59.34
TiO_2	.86	.87	.87	.73	.73	.73	.78
Al_2O_3	19.52	19.68	19.59	17.75	17.76	17.79	18.36
FeO	6.44	6.47	6.49	5.47	5.49	5.48	5.80
MgO	5.13	5.03	5.07	4.21	4.29	4.28	4.53
CaO*	7.47	7.60	7.66	5.95	5.95	5.97	6.47
Na_2O	3.91	3.47	3.43	3.91	4.11	4.13	3.91
K_2O	.51	.59	.59	.99	.93	.93	.83
Total	100.00	100.00	99.99	100.00	99.99	99.99	100.02
Norms:							
Qz	3.70	5.61	5.72	11.76	10.58	10.52	8.99
Plag	67.32	65.75	65.34	61.05	62.04	62.20	63.18
Or	3.00	3.49	3.49	5.85	5.50	5.50	4.91
Di	2.34	1.09	1.39	1.26	1.85	1.74	1.65
Hy	22.01	22.41	22.40	18.69	18.63	18.64	19.81
Il	1.63	1.65	1.65	1.39	1.39	1.39	1.48
Mg/(Mg+Fe)	.617	.611	.612	.609	.612	.612	.612
%An	49.3	53.9	54.1	44.4	42.5	42.4	46.2

* Corrected for apatite according to amount of P_2O_5

of diorite and tonalite. That is, the results of this test are consistent with the hypothesis that Spuzzum diorite is a cumulate, and that tonalite is a residual liquid, from an original quartz dioritic magma. This is not to say, however, that the Spuzzum analyses are inconsistent with any other hypothesis.

C. Origin of the Pluton

Fyfe (in Newall and Rast, 1969) discussed the initial stages in pluton formation, comparing it to a theory of formation of the core of the earth by gravitational instability in a dense liquid layer (Elsasser, 1963). This model consists of five stages of development;

(1) Melting of metal in upper layers of lower viscosity than a deeper part of the earth.

(2) Small droplets fall at decreasing velocities and build up a gravitationally unstable layer of dense liquid.

(3) Perturbations cause a bulge in the layer, which coalesces into a very large drop.

(4) The large drop eventually detaches from the layer and sinks rapidly with Stokesian behaviour.

(5) The region where the first drop formed will be a more favourable locus for further drop formation.

By considering not a dense but rather a buoyant liquid, one may invert this model and apply it to pluton formation (Fyfe, 1969; and others). A low viscosity zone of melting in the deep crust would allow small droplets of buoyant magma to form and tend to rise. Liquid would collect in a layer as droplets reach the upper part of the melting zone and are obstructed by increased viscosity. Upward bulges caused by perturbations would grow

larger spontaneously, taking in large volumes of liquid from the layer, until they could pull away as diapirs and rise.

Most of the above hypothesis can also be applied to partial melting of subducted oceanic crust. Some process is needed in this case to bring magma up from the Benioff zone at a depth of 100 kilometres or more. Marsh and Carmichael (1974) suggested that small diapirs of andesitic magma rise at intervals of about 70 kilometres along the length of a subduction zone from a narrow tube of magma collected along the loci of partial melting of oceanic crust. Their model is designed for island arc volcanism, and this magma is thought to form volcanoes immediately on arrival at the base of oceanic crust, it being thin. However, if the same small diapirs were to pass into thick and probably more viscous continental crust, it seems reasonable that in a given area they may amass to form a pocket which resembles the collected layer in the Elsasser model. With varying degrees of assimilation, the resulting mixture of crustal rocks and Benioff zone andesite may produce the wide assortment of rocks found in plutonic complexes, the majority of which perhaps being granodioritic or quartz dioritic in composition.

Studies by Ramberg (1969) into conditions that cause diapirism showed that synthetic diapirs can and do draw up their substratum as a core. Depending on the properties of materials used in an experiment and the forces applied to them, substratum cores rose to various levels within their host diapirs, in some cases reaching into the bulbous or flattened heads and appearing as though the heads were blown up like balloons. Ramberg stressed that these results applied only to materials with viscosity contrast ratios ranging from 1 to 10^3, which correspond well with pairs of different types of crystalline rocks or different magmas, but not with crystalline rock and magma together. He also experimented with an aqueous

solution and modelling clay to better simulate the supposed viscosity contrast between magma and crustal rock. Diapirs were not produced in these tests. However, little is known of the magnitude of the effective viscosity of crustal rocks at depth (Ramberg, 1969), and it may well be that rocks behave more plastically than assumed in these studies.

Depending on the physical conditions in a collected layer and on the evolution in size and shape of a bulge, a plutonic body of given composition may begin to crystallize before separating from the collected layer. Indeed, if the cause of increased thermal activity originally responsible for melting should wane, it is likely that the collected layer itself would undergo crystallization. If crystals settled in a bulge as it formed, then as it detaches it may draw up a core of crystal mush with it in a diapir-like pluton.

This is the mechanism proposed for the origin of the Spuzzum Pluton, and it is illustrated schematically in fig. 17. The conditions necessary for such a process to work include crystallization in the Elsasser bulge before its detachment, so that a cumulate layer may form at the base of the bulge. If crystallization does not begin early enough for crystals to sink through the bulge, any accumulation of crystals in the melt will not be distributed in the same fashion. For example, cooler surroundings at a higher level in the crust may cause crystallization at the margin of a pluton, but it is difficult to imagine that these crystals would collect as a cumulate core. Rather, they should form a "cumulate" margin, or perhaps sink if the magma is not too viscous and accumulate at the floor of the pluton. Once a pluton has acquired drop-like form, however, a drawn-up core (Ramberg, 1969) will be nearly impossible. The model proposed for the Spuzzum Pluton requires accumulation of a layer of crystals in the Elsasser

Fig. 17
SCHEMATIC DIAGRAM OF THE ORIGIN, RISE, AND EMPLACEMENT OF THE SPUZZUM PLUTON

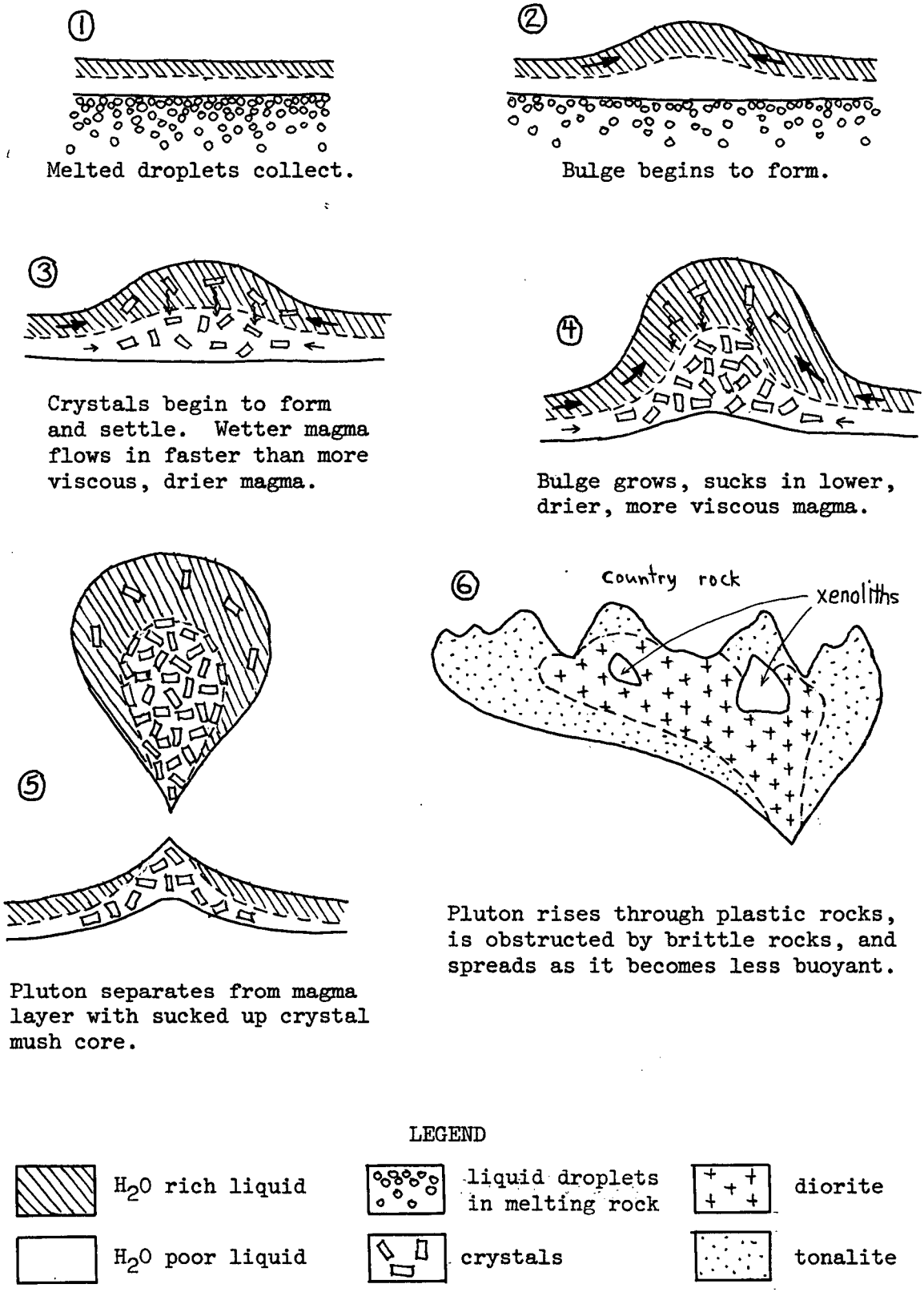

bulge, and this condition may well be rare in nature. Certainly the plutonic style characterized by a basic core with an acidic rim is rare. Most zoned plutonic bodies known have the reverse relationship. (Compare plutons of the Coast Plutonic Complex - Hutchison, 1969; Bald Rock Batholith, California - Larsen and Poldervaart, 1961; Deep Creek Stock, Idaho - White, 1973; and Guichon Batholith, British Columbia - Northcote, 1969; and Ager, et al., 1972).

D. Water in the Spuzzum Pluton

It was originally suggested by Richards (1971) that the increase in hornblende and biotite, together with the decrease in augite ($\pm$ hypersthene), from the core to the margin of Spuzzum diorite resulted from migration of water. In a more recent review of the problem (Richards and McTaggart, 1976), the authors argued that migration of water through the magma by diffusion would only be effective over a few tens of metres. As a result they proposed that the magma originally was stratified in water content, it being greatest at the highest levels of a magma chamber at depth; and the variation in water content seen at the present level is due to successive intrusions from different parts of this magma chamber.

The observed distribution of water is consistent with and perhaps better supports the single diapiric intrusion model of this study. If in a deep magma chamber (or melted layer) water were to collect in the upper parts, a diapir leaving from it could have a water-rich margin and a drier core. A collected layer with uniform temperature and water content increasing upward should be less viscous in its upper parts. An Elsasser bulge would form by relatively rapid lateral flow of water-rich magma toward the bulge, but drier magma would flow more sluggishly. As the bulge forms a pluton and detaches from the collected layer it should draw up in its core deeper

drier magma, but the majority of it would be the less viscous, wet magma.

Any crystals growing in the quartz dioritic parent magma should sink, and those in the water-rich upper portion of the bulge would sink more quickly than those in the more viscous deeper portion. This process is interpreted to be responsible for the chemical differences between tonalite and diorite. Crystals sinking through an increasing viscosity gradient could produce a relatively abrupt transition from crystal-depleted tonalite to crystal-enriched diorite below. This transition should have a strong correlation with any abrupt change in the water content (and thus viscosity) along the gradient. Such a change could be formed as water-rich magma flows laterally into the bulge from the surrounding area, forming a steepening in the viscosity gradient at the shear-like interface between faster-flowing water-rich magma and sluggish drier magma below.

The result of the foregoing processes would be a diapir of crystal-depleted water-rich tonalite magma, cored by a crystal mush of drier diorite with its water content steadily decreasing from a value less than that of tonalite (because of added anhydrous crystals) at its rim, to a very low value in the centre. Table XV shows the water contents of rocks of the Spuzzum Pluton to be consistent with this pattern. Water contents of minerals are approximated from analyses in Deer, Howie, and Zussman (1966). Densities are those used in previous sections and volumes are from averaged modes of table IIa. Fig. 17 is a schematic diagram of these processes, charting the evolution of the Spuzzum Pluton from its origin in a collected layer to its emplacement as a differentiated tongue-like pluton.

TABLE XV

CALCULATION OF WATER CONTENT OF THE SPUZZUM PLUTON

	Pyroxene Diorite	Hornblende Diorite	Tonalite	ρ min	wt% H_2O
Vol% Hbd	5.4	14.6	22.1	3.2	2
Vol% Bio	.5	6.6	9.5	3.0	4
Vol% Chl	0	0	.8	3.0	11
ρ rock	2.93	2.93	2.84		
Wt% H_2O of Hbd	.118	.319	.498		
Wt% H_2O of Bio	.020	.270	.401		
Wt% H_2O of Chl	0	0	.093		
Total wt% H_2O	.138	.589	.992		

E. Rise and Emplacement of the Pluton

A plutonic mass rises because it is less dense than its surroundings. In order for it to remain as a diapir-like body, those surrounding must behave plastically as the pluton passes through. As a pluton rises it both crystallizes and cools, becoming denser and more viscous. In turn, the rocks at higher levels in the crust are more brittle and cooler than those below. Rocks are poor thermal conductors, and the heat of crystallization of magma may largely keep pace with any drain of heat into the surroundings, so that in general a pluton will be much hotter than the rocks around it. There will therefore be a considerable thermal gradient near the margin of a pluton. Certainly stocks, plutons, and batholiths of all sizes have been emplaced hot, having produced contact metamorphism in the rocks they intrude. The ultimate depth to which a plutonic mass can rise, and its form when it arrives there, are determined by all of the above factors. If a pluton increases in density so that it no longer is buoyant, it must cease to rise as a whole (although dykes and sills may be injected higher by gas pressure effects). If surrounding rocks become too brittle, the body may rise by stoping or forceful injection along loci of weakness, and probably lose its coherent form as a diapir.

The Spuzzum Pluton appears to have been intermediate between these two cases. It has to a large extent retained its diapiric form (concentric zonation, tongue-like structure), but its shape has been influenced by the strength of its surroundings, having stoped large country rock xenoliths and flowed around massive reentrants or pendants of country rock. There is no clear evidence in the geology of the region that the pluton ever developed a volcanic pile during emplacement. It has been classified by

Richards and McTaggart (1976) as mesozonal. Contact metamorphism in a large schist reentrant indicates emplacement at a depth of about 13 kilometres or 4.5 kilobars pressure (Richards, 1971).

Fig. 18 shows the pressure-temperature environment of the Spuzzum Pluton during its evolution. Liquidi for andesite with 0% and 2% water by weight after T. Green (1972) are shown as solid lines labelled "Liq_0" and "Liq_2." The estimated position of the 0.6% water liquidus is also shown and labelled "$Liq_{.6}$." From the same source is the dry solidus shown as a dashed line labelled "Sol_0." The water saturated liquidus and solidus for quartz diorite after Piwinskii and Wyllie (1968) are labelled "Liq_{sat}" (solid line) and "Sol_2" (dashed line) respectively. The dashed line labelled "$Sol_{.6}$" is the solidus for granodiorite with a mixture of water-saturated and water-undersaturated phases (e.g. pyroxene with amphibole). This mixture corresponds with composition II of Robertson and Wyllie (1971). The short-dashed line labelled "Sat_2" represents the loci of points at which quartz diorite with 2% water by weight undergoes second boiling. Borders of the stability fields of tholeiite, garnet granulite, and eclogite after D. Green (1976) are shown as light-weight solid lines. Continental temperature gradients (normal and high) after Bailey (1969) are shown as cross-hatched solid lines.

The interpreted trajectory of the evolution of the Spuzzum Pluton through pressure-temperature space is shown in heavy dashed lines in fig. 18. The same crystallization data are used in this diagram for tonalite and all kinds of diorite; the differences in the behaviour of the various phases are thought to be controlled primarily by water content. Tonalite is considered to have contained 2% water by weight, and diorite contains between 0% and 0.6% water in hydrous minerals. The value for tonalite is arbitrarily

Fig. 18

EVOLUTION OF THE SPUZZUM PLUTON
PROJECTED IN PRESSURE-TEMPERATURE SPACE

(Refer to text for definitions and discussion)

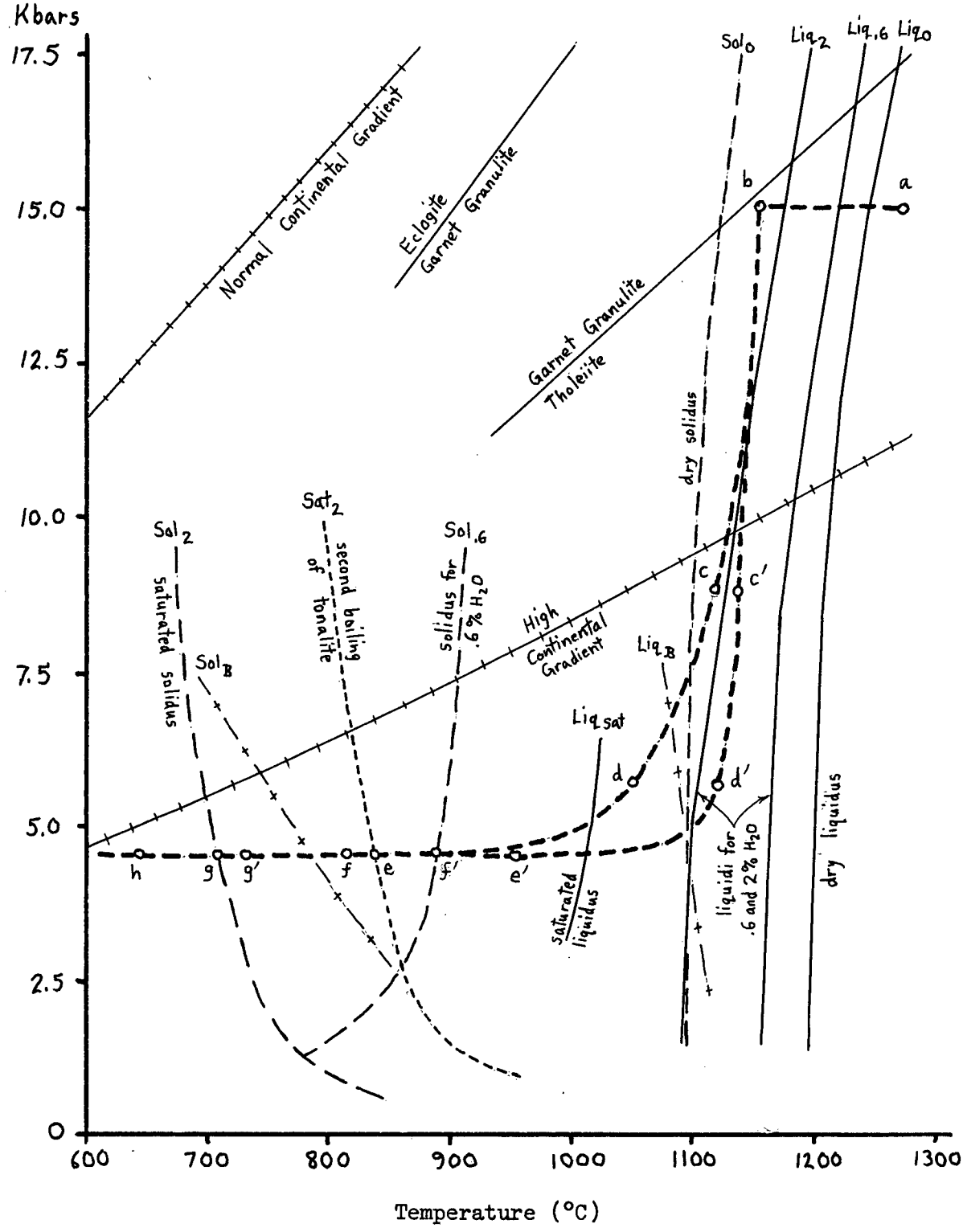

Fig. 19

SCHEMATIC DIAGRAM OF

CRYSTALLIZATION VERSUS TEMPERATURE

FOR ROCKS OF THE SPUZZUM PLUTON

AT 4.5 KILOBARS PRESSURE

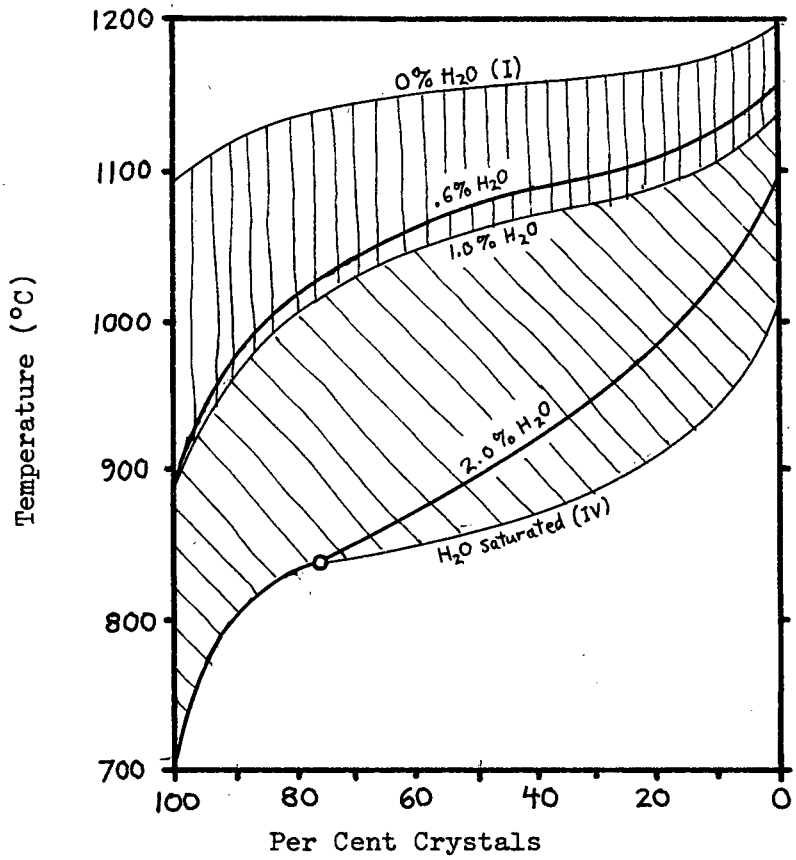

Composition II

Composition III

Roman numerals refer to compositions (bulk water contents) described by Robertson and Wyllie (1971).

chosen as a water content that would produce second boiling. The relationships of crystallization progress among these phases are illustrated in fig. 19, with temperature plotted against per cent crystals for various water contents in quartz diorite magma. The general curve shape is after a similar curve determined experimentally for water-saturated quartz diorite (Robertson and Wyllie, 1971). The various curves for undersaturated magma are placed on the temperature scale according to liquidus and solidus temperatures at 4.5 kilobars (fig. 18). The curves are labelled after the four major water content categories described by Robertson and Wyllie (1971): (I) No water is present, corresponding to the dry liquidus and solidus temperatures. (II) Water content is less than or equal to the amount necessary to saturate all solid phases. The liquidus temperature decreases steadily with increasing water content, but the solidus temperature remains nearly constant and considerably below that of I. (III) Water content is more than enough to saturate solid phases, but insufficient to saturate the liquid at some stage of crystallization. The liquidus temperature decreases steadily with increasing water content, but the solidus temperature remains constant and equal to the saturated solidus temperature. This is the only range of water contents for which magma may undergo second boiling, at which point the liquid becomes saturated and exsolves a vapour phase. The open circle in fig. 19 is the point at which tonalite undergoes second boiling, corresponding to the short-dashed line in fig. 18. (IV) Water content is greater than or equal to the amount necessary to saturate the liquid at all times. The liquidus and solidus temperatures are minimum values. When magma undergoes second boiling, it continues to crystallize along curve IV. The breaking point between compositions II and III is chosen as 1% water, which is the water content of solid tonalite (table XV).

Crystallization history of the Spuzzum Pluton can be crudely surmised from the data in fig. 18. The open circles labelled a, b, c, c', . . . depict isolated points in the history of the pluton, and are described below:

(a) A more or less arbitrary point is chosen at which original Spuzzum magma of any water content is completely liquid. This will correspond to collection of andesitic magma droplets into a layer or magma chamber (stages 1 and 2 of fig. 17). Since this may be in the deep crust or upper mantle near the crust base, a depth of about 45 kilometres is chosen as an initial depth.

(b) The incipient pluton is ready to rise, corresponding to stage 4 of fig. 17. Pyroxene diorite has formed by considerable crystallization of drier parts of the bulge, and settling of crystals from the water-richer upper parts. Hornblende diorite will eventually form from the upper, water-richer part of the accumulated crystal mush. Crystallization has occurred in all parts of the bulge by the time the pluton detaches, but the marginal parts are depleted of crystals by settling.

(c and c') The inside of the pluton retains its high temperature as it rises, whereas the marginal parts cool by conduction. Crystals may be partly resorbed as load pressure decreases.

(d and d') The pluton reaches a level where it cannot penetrate upward easily. The core is a mush of crystals and interstitial liquid, but the water-richer tonalite margin, though cooler, is dominantly liquid (fig. 19). The rim continues to cool faster than the core. The pluton spreads laterally, developing a tongue-like shape.

(e and e') Tonalite boils, producing a reactive vapour that metasomatizes country rocks and produces hornblendite. The pluton is immobile at this stage; tonalite is largely crystalline and the diorites have only small amounts of liquid left in them (fig. 19). There is a considerable difference in temperature between the core and margin of the pluton.

(f and f') Diorites are completely solid, even the most hydrated variety, yet tonalite still contains some liquid. As a result, foliations in tonalite may be locally discordant with those of diorite. The core temperature begins to approach the margin temperature.

(g and g') Tonalite is completely solid. The core temperature is nearly the same as the margin temperature.

(h) The solid pluton continues to cool, eventually reaching a temperature consistent with the geothermal gradient.

F. Origin of Hornblendite

In previous sections it has been shown that hornblendite of the Spuzzum Pluton, hornblendite rimming the Giant Mascot Ultramafic Body, and hornblendite dykelets cutting the latter, are probably chemically related to each other and to hornblende in altered diorite in contact with the ultramafite. Hornblendite in contact with tonalite (type I) differs in composition from that in contact with diorite (type II) in a manner that parallels the differences between tonalite and diorite (fig. 13). These relationships suggest (1) that hornblendite rimming the Giant Mascot Ultramafic Body originated by reaction with Spuzzum diorite and tonalite,

and (2) that hornblendite in the Spuzzum Pluton has its source in this reaction.

The idea that a reaction of this nature occurred has been discussed by Aho (1956), who believed ultramafic rocks intruded diorite. He suggested that constituents of the hornblendite rim may have been partly derived from diorite by addition of H_2O, CaO, and Na_2O to the ultramafic rocks, or that ultramafic magma may have assimilated some diorite. McLeod (1975) agreed with Aho as to the origin of the hornblendite rim, but concluded that Spuzzum diorite and tonalite intruded the ultramafic rocks which he said may have been an early phase of Spuzzum igneous activity.

The origin of hornblendite in Spuzzum diorite has been discussed by Richards (1971). He suggested that hornblendite and pyroxenite bodies formed in part by metasomatism of diorite along pre-existing fractures, either by addition of basic constituents or by subtraction of acidic constituents. He favoured their formation by subtraction of SiO_2, Al_2O_3, Na_2O and K_2O by hot water-rich fluid on the basis of experimentally determined solubilities of these components. He accounted the formation of pyroxenite rather than hornblendite to higher temperature at constant water pressure, although lower water pressure at constant temperature would produce the same result (see his fig. 19B, p. 43). If simple subtraction of acidic constituents from diorite (or tonalite) is the only mechanism in the formation of Spuzzum hornblendite, then there is no reason for the composition of this hornblendite to match that of the Giant Mascot hornblendite rim. This author believes the chemical similarities are more than coincidence, and proposes that the same reaction that produced the hornblendite rim is responsible for ultramafic bodies in the Spuzzum Pluton.

This author proposes that the hornblendite rim as well as hornblendite bodies in the Spuzzum Pluton were produced by metasomatism at its contact with ultramafic rocks in the presence of water-rich fluid during emplacement of the pluton. It seems fortuitous that hydrothermal fluid that may have metasomatized rocks at the contact of Spuzzum diorite and Giant Mascot pyroxenite should do the same to diorite five kilometres away. This process is made more plausible by the presence of fractures or shears in the nearly solid pluton, which appear to have controlled hornblendization in many places. Hornblendite bodies such as the one northwest of Odlum are more likely to be altered xenoliths of ultramafic rock analogous to the Giant Mascot Ultramafic Body, many pods of which occur in the vicinity of the Spuzzum Pluton in rocks of the Settler Schist, Hozameen Group, and Chilliwack Group (McTaggart and Thompson, 1967; and Monger, 1970). The same reaction responsible for conversion of up to 100 metres of pyroxenite to hornblendite at the mine would probably assimilate or alter beyond recognition a small pod of the same rock. Another example may be the body of hornblendite south of the fork in American Creek. Hornblendization of parts of the Spuzzum Pluton may have been by diffusion of hydrothermal fluid through diorite or tonalite or more likely along fractures, shears, and xenolith contacts, also producing small wispy pods of hornblendite common in hornblendized rocks. Pyroxenite replacement bodies (Richards, 1971) in pyroxene diorite are considered analogous to hornblendite bodies, except that they probably crystallized under conditions of lower water pressure (but equal total pressure) or higher temperature in the core of the pluton.

The character of metasomatism between Giant Mascot ultramafic rocks and the Spuzzum Pluton is shown in fig. 20. Ultramafic rocks are represented by dunite (average olivine) and pyroxenite (equal amounts of

Fig. 20

CHARACTER OF METASOMATISM BETWEEN THE SPUZZUM PLUTON AND GIANT MASCOT ULTRAMAFIC ROCKS

(Refer to text for definitions and discussion)

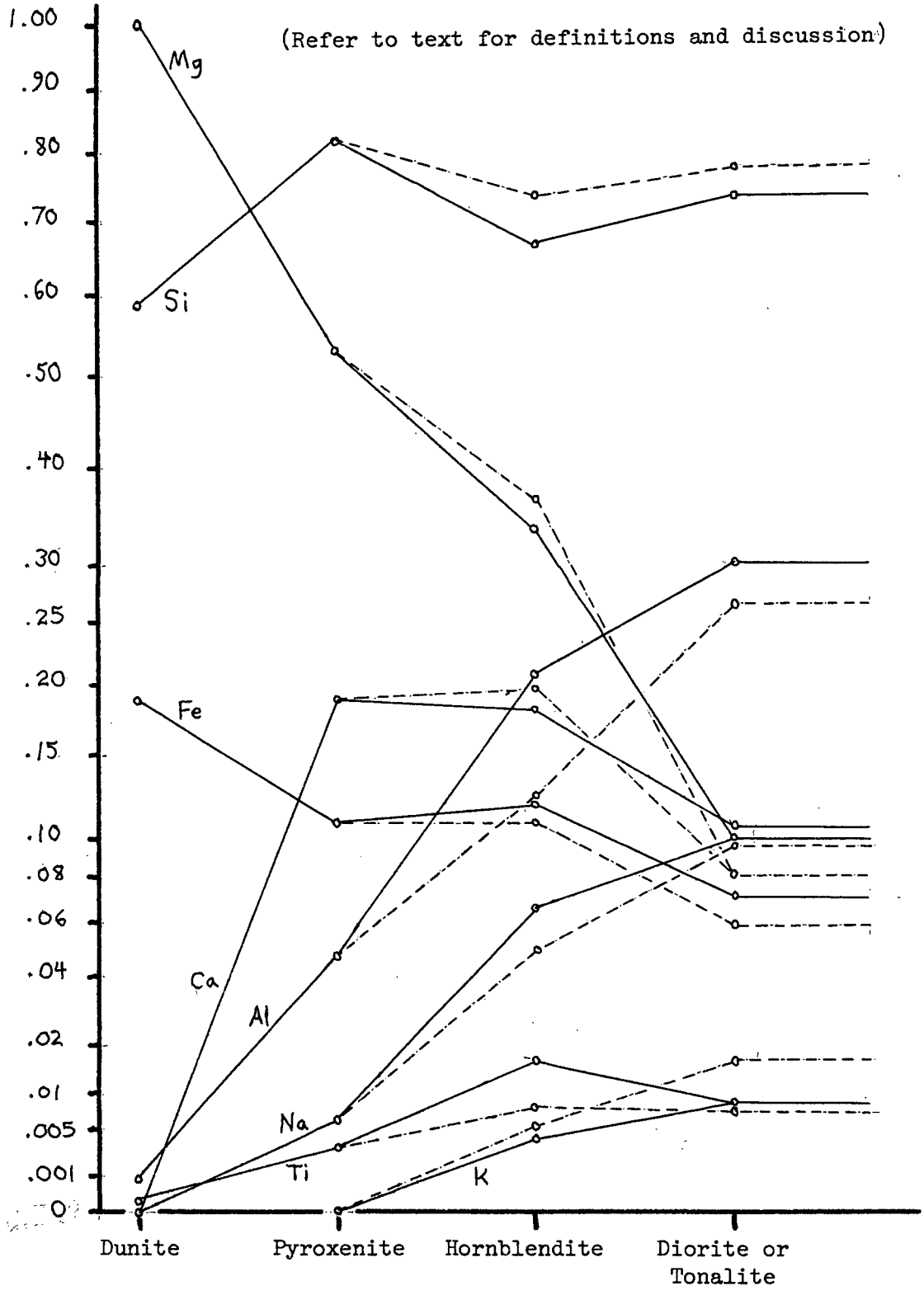

average ortho- and clinopyroxene) calculated from analyses given by McLeod (1975). Hornblendite type I is a single analysis and type II is the average of three analyses given in this study (see chemistry section). Diorite and tonalite analyses are averaged from those given in Richards (1971), after correction of CaO for apatite. The values in fig. 20 are moles of atoms for equal volumes of each rock type. Dashed lines connect type I hornblendite and tonalite, whereas type II hornblendite and diorite are connected by solid lines. Densities used are 2.93 and 2.84 for diorite and tonalite, respectively (calculated previously in this section); and 3.4, 3.2 and 3.3 for pyroxene, hornblende, and olivine, respectively. Moles of atoms are normalized so that the highest value (Mg in dunite) is equal to one. The ordinate is a nonlinear scale meant to magnify low values (K and Ti especially). Linear measure from zero along the ordinate is proportional to the square root of the actual value.

From fig. 20 it can be seen that hornblendites lie crudely in line with feldspathic rocks and pyroxenite, with some notable exceptions. Further, with the exception of Ca and Mg, the difference between hornblendites I and II for each element reflects the difference between tonalite and diorite. These relationships suggest that the composition of magma intruding pyroxenite controlled the composition of adjacent hornblendite. This supports a hypothesis of metasomatic origin of the hornblendite rim. At constant volume, diorite or tonalite can be converted to hornblendite by addition of Ti, Fe, Mg, and Ca and removal of Si, Al, Na, and K. Pyroxenite can be converted to hornblendite by addition of Ti, Al, Na, and K and removal of Si, and Mg (Fe and Ca remain nearly constant.) If both ultramafic rock and feldspathic rock contribute to conversion, hornblendite can be formed by addition of small amounts of Ti, Fe, and Ca and removal of Si.

It was shown above, page 74, that hornblendite near Odlum and that from a dykelet at the Giant Mascot Mine have compositions similar to silica-undersaturated basalt. If such a hornblendite body formed by metasomatism of ultramafic rock in a hot batholith, it could melt and be injected into its surroundings. The plausibility of such a mechanism is illustrated by the relationships of undersaturated basalt and diorite melting curves, shown in fig. 18. The water-saturated liquidus and solidus for alkali basalt (Yoder and Tilley, 1962) are shown as broken cross-hatched lines and labelled "Liq_B" and "Sol_B." Diorite liquidi and solidi for various concentrations of water are shown as solid and broken lines and further discussed above, page 101.

At 4.5 kilobars (the postulated depth of emplacement of the Spuzzum Pluton) water-saturated alkali basalt begins to melt 100 degrees below the solidus of hornblende diorite ($Sol_{.6}$), and possibly about 50 degrees below the second boiling point of tonalite (Sat_2). Certainly a hornblendite body in hot diorite would not be water saturated. In fact, it may be a mixture of hornblende and pyroxene, and therefore the melting curves of Yoder and Tilley (1962) do not apply. If tonalite were to boil as shown in fig. 18, however, water-rich vapour could follow fractures in the solid diorite and saturate any ultramafic bodies in its path (as well as any in tonalite). Coursing of water-rich fluid through fractures in pyroxene diorite produced localllized metasomatism along those fractures (plates 12 and 13). Large bodies of hornblendized diorite in pyroxene diorite (see map in pocket) evidently formed by the same process. It is conceivable that ultramafic xenoliths in tonalite and in diorite near its margin may have been converted to hornblendite and locally melted in the presence of excess water as a result of the second boiling of tonalite. Once mobilized as

a magma an ultramafic body could follow fractures, stope off slabs of diorite, or re-assimilate diorite to some degree. Diorite xenoliths in massive hornblendite near Odlum and on American Creek (plates 2, 6, and 11; fig. 5a) and hornblendite dykelets at the mine (plate 14), strongly suggest this behaviour.

The age of hornblendites, by the above hypotheses, must be somewhat younger than the age of emplacement of the Spuzzum Pluton. Diorite and tonalite must have been solid enough to fracture or shear, possibly having only interstitial liquid among interlocked crystals. Fluids may have been produced by exsolution from the last fraction of magma during the pneumatolitic stage of crystallization (for tonalite or water-richest hornblende diorite). Dry pyroxene diorite, exsolving no vapour phase with crystallization, could have been in contact with unaltered pyroxenite in such a system. This corresponds with Richards' (1971) interpretation that hornblendite and pyroxenite replacement bodies formed in diorite as it cooled. This author sees no reason why hornblendite should not have formed in tonalite as well as diorite by the same process.

LIST OF REFERENCES CITED

Ager, C. A., McMillan, W. J., and Ulrych, T. J., 1972. Gravity, magnetics, and geology of the Guichon Creek Batholith. British Columbia Dept. of Mines and Petroleum Resources Bull., v. 62.

Aho, A. E., 1956. Nickel-copper pyrrhotite deposits at the Pacific Nickel Property, southwestern British Columbia. Economic Geology, v. 51, pp. 444 - 481.

Atkins, F. B., 1969. Pyroxenes of the Bushveld Intrusions, South Africa. Journal of Petrology, v. 10, pp. 222 - 249.

Bailey, D. K., 1969. Volatile flux, heat focusing, and the generation of magma. Mechanisms of Igneous Intrusion (Newall, G., and Rast, N., eds.) Gallery Press, Liverpool, pp. 177 - 186.

Bowen, N. L., 1913. The melting phenomena of the plagioclase feldspars. American Journal of Science, series 4, v. 35, pp. 577 - 599.

Brown, G. M., 1957. Pyroxenes from the early and middle stages of fractionation of the Skaergaard Intrusion, East Greenland. Mineralogical Magazine, v. 31, pp. 511 - 543.

Cairnes, C. E., 1944. Hope area. Canada Geological Survey Map, no. 737A, scale 1 in. = 4 mi.

Clark, S. P., Jr. (ed.)., 1966. Handbook of physical constants. Geological Society of America Memoir, no. 97.

Deer, W. A., Howie, R. A., and Zussman, J., 1963. Rock-forming Minerals, v. 2, Longmans, London.

Deer, W. A., Howie, R. A., and Zussman, J., 1966. Introduction to Rock-forming Minerals, John Riley and Sons, N. Y.

Eastwood, G. E. P., 1971. NI (No. 171, Fig. E). Geology, Exploration, and Mining in British Columbia, B. C. Dept. of Mines and Petroleum Resources, pp. 258 - 264.

Elsasser, W. M., 1963. Early history of the earth. Earth Science and Meteorites, (Geiss, J., and Goldberg, E. D., eds.), North-Holland, Amsterdam, pp. 1 - 30.

Emslie, R. F., 1971. Liquidus relations and subsolidus reactions in some plagioclase-bearing systems. Annual Report of the Director, Geophysical Laboratory 1969 - 1970 (Yearbook 69), Carnegie Institution of Washington, pp. 148 - 155.

Fyfe, W. S., 1969. Some thoughts on granitic magmas. Mechanisms of Igneous Intrusion (Newall, G., and Rast, N., eds.), Gallery Press, Liverpool, pp. 201 - 216.

Green, D. H., 1976. Experimental petrology in Australia - a review. Earth-Science Review, v. 12, pp. 99 - 138.

Green, T. H., 1972. Crystallization of calc-alkaline andesite under controlled high-pressure hydrous conditions. Contributions to Mineralogy and Petrology, v. 34, pp. 150 - 166.

Hess, H. H., 1960. The Stillwater Igneous Complex, Montana. Geological Society of America Memoir, no. 80.

Hutchison, W. W., 1970. Metamorphic framework and plutonic styles in the Prince Rupert region of the central Coast Mountains, British Columbia. Canadian Journal of Earth Sciences, v. 7, pp. 376 - 405.

Hyndmann, D. W., 1972. Petrology of Igneous and Metamorphic Rocks, International Series in the Earth and Planetary Sciences, McGraw-Hill, N. Y.

Krauskopf, K. B., 1967. Introduction to Geochemistry, International Series in the Earth and Planetary Sciences, McGraw-Hill, N. Y.

Larsen, L. H., and Poldervaart, A., 1961. Petrologic study of the Bald Rock Batholith, near Bidwell Bar, California. Geological Society of America Bull., v. 72, pp. 69 - 91.

Lowes, B. E., 1971. Metamorphic petrology and structural geology of the area east of Harrison Lake, British Columbia (unpubl. Ph. D. thesis). Univ. of Washington, Seattle, U. S. A.

Marsh, B. D., and Carmichael, I. S. E., 1974. Benioff zone magmatism. Journal of Geophysical Research, v. 79, pp. 1196 - 1206.

McIver, J. R., 1972. Hornblendite from Bon Accord, Pretoria, and a possible komatiite equivalent. Transactions of the Geological Society of South Africa, v. 75, pp. 313 - 315.

McLeod, J. A., 1975. The Giant Mascot Ultramafite and its related ores (unpubl. M. A. Sc. thesis). Univ. of British Columbia, Vancouver, Canada.

McTaggart, K. C., and Thompson, R. M., 1967. Geology of part of the northern Cascades in southern British Columbia. Canadian Journal of Earth Sciences, v. 4., pp. 1199 - 1228.

McTaggart, K. C., 1970. Tectonic history of the northern Cascade Mountains. Geological Association of Canada Special Paper, no. 6, pp. 137 - 148.

McTaggart, K. C., 1971. On the origin of ultramafic rocks. Geological Society of America Bull., v. 82, pp. 23 - 42.

Misch, P., 1966. Tectonic evolution of the northern Cascades of Washington State. Tectonic History and Mineral Deposits of the Western Cordillera, spec. v. 8, Canadian Institute of Mining and Metallurgy, pp. 101 - 148.

Monger, J. W. H., 1970. Hope map-area, west half, British Columbia. Canada Geological Survey Paper, no. 69-47.

Moore, J. G., and Lockwood, P. L., 1973. Origin of comb-layering and orbicular structure, Sierra Nevada Batholith, California. Geological Society of America Bull., v. 84, pp. 1 - 20.

Morris, P. G., 1955. A petrological study of intrusive rocks along the Fraser Canyon near Hell's Gate, British Columbia. (unpubl. M. A. thesis). Univ. of British Columbia., Vancouver, Canada.

Northcote, K. E., 1969. Geology and chronology of the Guichon Creek Batholith. British Columbia Dept. of Mines and Petroleum Resources Bull., v. 56.

Pigage, L. C., 1973. Metamorphism southwest of Yale, British Columbia (unpubl. M. Sc. thesis). Univ. of British Columbia, Vancouver, Canada.

Piwinskii, A. J. and Wyllie, P. J., 1968. Experimental studies of igneous rocks: a zoned pluton in the Wallowa Batholith, Oregon. Journal of Geology, v. 76, pp. 205 - 234.

Price, R. A., and Douglas, R. J. W., 1972. Variations in tectonic styles in Canada. Geological Association of Canada Special Paper, no. 11.

Ramberg, H., 1969. Model studies in relation to intrusion of plutonic bodies. Mechanisms of Igneous Intrusion (Newall, G., and Rast, N., eds.), Gallery Press, Liverpool, pp. 261 - 285.

Read, P. B., 1960. Geology of the Fraser River valley between Hope and Emory Creek, British Columbia (unpubl. M. A. Sc. thesis). Univ. of British Columbia, Vancouver, Canada.

Richards, T. A., and White, W. H., 1970. K-Ar ages of plutonic rocks between Hope, British Columbia, and the 49th parallel. Canadian Journal of Earth Sciences, v. 7, pp. 1203 - 1207.

Richards, T. A., 1971. Plutonic rocks between Hope, British Columbia and the 49th parallel (unpubl. Ph. D. thesis). Univ. of British Columbia, Vancouver, Canada.

Richards, T. A., and McTaggart, K. C., 1976. Granitic rocks of the southern Coast Plutonic Complex and northern Cascades of British Columbia. Geological Society of America Bull., v. 87, pp. 935 - 953.

Robertson, J. K., and Wyllie, P. J., 1971. Rock-water systems, with special reference to the water-deficient region. American Journal of Science, v. 271, pp. 252 - 277.

Robie, R. A., and Waldbaum, D. R., 1968. Thermodynamic properties of minerals and related substances at 298.15°K and one atmosphere pressure and higher temperatures. United States Geological Survey Bull., v. 1259.

Roddick, J. A., and Hutchison, W. W., 1970. Northwestern part of the Hope map-area, British Columbia. Canada Geological Survey Paper, no. 69-1A, pp. 29 - 38.

Verhoogen, J., Turner, F. J., Weiss, L. E., and Wahrhaftig, C., 1970. The Earth: An Introduction to Physical Geology, Holt, Rinehart, and Winston, N. Y.

White, W. H., 1973. Flow structure and form of the Deep Creek Stock, southern Seven Devils Mountains, Idaho. Geological Society of American Bull., v. 84, pp. 199 - 210.

Wood, B. J., and Banno, S., 1973. Garnet-orthopyroxene and orthopyroxene-clinopyroxene relationships in simple and complex systems. Contributions to Mineralogy and Petrology, v. 42, pp. 109 - 124.

Yoder, H. S., and Tilley, C. E., 1962. Origin of basalt magma: an experimental study of natural and synthetic rock systems, Journal of Petrology, v. 3. pp. 342 - 532.

GUIDE TO APPENDIX I

In this appendix, modes and mineralogical data of all specimens thin-sectioned in this study are listed. Modes were measured by eye estimate in a standard petrographic microscope. Mineralogical data were estimated in the same way. Modes are presented in order of decreasing pyroxene/hornblende + biotite) for diorites (parts A and B), decreasing hornblende/ plagioclase + quartz) for hornblendized rocks (part C), decreasing biotite/hornblende for tonalites (part D), and basically in order of increasing mafic minerals for others (parts E and F).

Three specimens were borrowed from other workers: AM#2 (hornblendite) was donated by K. Nielson; 79A-2 (hornblendite) by J. McLeod; and 75-A and B (breccia) by K. C. McTaggart.

LEGEND

Qz	quartz	S/O	sulphide/oxide ratio
Plag	plagioclase	An %	% anorthite in plagioclase
Or	orthoclase	Cb	carbonate
Opx	orthopyroxene	Cz	clinozoisite
Cpx	clinopyroxene	Chb	colourless hornblende
Px	combined pyroxenes	Sn	sphene
Hbd	hornblende	Sp	spinel
Bio	biotite	Ac	actinolite
Chl	chlorite	Ol	olivine
Mu	muscovite	Tc	talc
Ep	epidote	Pr	prehnite
Gar	garnet	tr	trace
Ap	apatite	sl	slight

APPENDIX I - PART A

MODES OF PYROXENE DIORITES

SPEC. NO.	15/6 75/6	24/7 75/11	10/7 75/6	29/7 75/2	10/7 75/3	8/8 75/1	10/7 75/5b	9/7 75/11	18/7 75/5	24/7 75/12	2/7 75/10	29/7 75/10c
Qz	tr	--	1	tr	--	tr	tr	6	--	5	tr	5
Plag	66	70	70	65	60	60	65	60	70	65	66	60
Or	--	--	--	--	--	--	--	--	--	--	--	--
Opx	16	15	15	18	22	19	22	22	13	13	16	16
Cpx	16	15	13	15	15	18	9	8	13	10	8	8
Hbd	tr	tr	tr	1	1	1	2	1	3	6	8	8
Bio	--	--	tr	tr	1	1	1	2	tr	tr	--	1
Ap	tr	tr	tr	tr	--	tr	tr	tr	--	tr	--	1
Opaque	2	tr	1	1	tr	1	1	1	1	1	2	1
Others					Sn-1							Sp-tr
S/O	>>10	>>10	>>10	>>10	10	>>10	>10	>>10	>>10	>>10	>>10	>10
An%												
high	48	50	66	70	85	47	55	55	92	60	51	66
low	42	48	44	40	40	43	46	40	37	37	50	47
Opx:												
$2V_{\alpha}$	<90	70	65	65	--	60	60	60	55	55	55	60
δ	.018	.012	.016	--	.012	.012	.016	.012	.015	.012	--	.015
Cpx:												
$2V_{\gamma}$	40	60	50	45	50	60	50	35	55	45	40	50
δ	--	.033	.032	--	.032	.030	.030	.023	.031	.030	.032	.022
$\gamma \wedge c$	43	41	44	45	43	41	45	40	41	45	43	43
Hbd:												
$2V_{\alpha}$	--	--	--	85	90	85	80	85	70	80	--	80
δ	.026	.024	--	--	.027	.026	.025	--	.026	.027	.025	.022
$\gamma \wedge c$	--	--	--	20	19	17	20	--	21	21	17	19
Bio:												
$2V_{\alpha}$	--	--	--	15	--	--	--	--	--	--	--	--

APPENDIX I - PART B

MODES OF DIORITES AND TRANSITIONS TO HORNBLENDIZED ROCKS

TYPE	PYROXENE DIORITES				HORNBLENDE DIORITES					TRANSITIONS		
SPEC. NO.	1/7 75/3	18/8 75/1	27/8 75/3b	28/8 75/1a	8/8 75/5b	15/6 75/3	30/7 75/2a	25/8 75/15	8/8 75/18	7/7 75/2	20/8 75/1b	9/7 75/8
Qz	5	--	--	--	5	2	9	5	15	tr	--	5
Plag	65	65	65	60-50	60	65	60	65	52	50-60	60	55
Or	--	--	--	--	--	--	--	--	--	--	--	--
Opx	16	17	14	17-14	7	10	8	4	8	20-15	10	4
Cpx	3	5	5	3-tr	7	tr	--	2	4	0?	tr	tr
Hbd	8	13	15	20-35	8	20	9	18	14	30-25	29	25
Bio	2	--	--	--	8	3	9	6	7	--	--	1
Ap	tr	--	--	tr	tr	tr	tr	tr	tr	tr	tr	tr
Opaque	1	tr	1	tr-1	5	--	1	tr	tr	tr	1	tr
Others							CHb-4					Ac-10
S/O	>10	2	>10	2	>>10	>>10	>>10	>>10	>>10	>10	>>10	10
An%:												
high	49	85	79	51	47	55	60	57	50	71	82	56
low	43	64	46	46	44	40	41	39	42	52	52	35
Opx:												
$2V_{\alpha}$	--	65	67	60	70	80	55	--	55	65	65	55
δ	.012	.013	.012	.013	.013	.018	.011	--	.011	.014	.016	.013
Cpx:												
$2V_{\gamma}$	--	--	--	40	40	--	--		50	--	55	--
δ	.023	.027	.031	.029	.025	.035	--	--	.030	--	.030	--
$\gamma \wedge c$	35	--	39	40	35	38	--	--	40	--	--	--
Hbd:												
$2V_{\alpha}$	--	80	85	--	75	$\approx$90	90	--	80	--	85	80
δ	.021	.025	.027	--	.022	.031	.026	--	.025	.023	.028	.027
$\gamma \wedge c$	--	18	18	--	--	--	16	--	18	18	18	21
Bio:												
$2V_{\alpha}$	--	--	--	--	0	10	5	--	--	--	--	--

APPENDIX I - PART C

MODES OF HORNBLENDIZED ROCKS

SPEC. NO.	25/6 75/4	25/8 75/4	29/7 75/3a	19/6 75/5	2/7 75/2	20/8 75/3	18/8 75/12	25/8 75/3	28/8 75/1b	25/8 75/8	6/8 75/15	29/7 75/3b
Qz	--	--	--	--	tr	--	2	tr	5	--	tr	--
Plag	40-tr	40-tr	50	50-tr	50	55	53	60	54	60	60	65-tr
Or	--	--	--	--	--	--	--	--	--	--	--	--
Px	--	--	--	--	tr	tr	--	--	--	--	--	--
Hbd	60-100	60-100	50	50-100	47	44	37	40	40	38	35	35-100
Bio	--	--	tr	--	2	--	6	--	--	1	3	tr
Chl	--	--	--	--	tr	--	tr	tr	--	tr	tr	--
Ap	tr	tr	tr	tr	tr	tr	1	tr	tr	tr	tr	tr
Opaque	tr	tr	1	tr	1	1	1	tr	1	1	2	tr
Others	Sn-tr Cz-tr											
S/O	>10	2	--	>>10	>10	10	>10	5	>10	>>10	>>10	--
An%:												
high	?	79	60	78	58	80	53	82	65	53	48	?
low	?	75	0	60	37	53	30	55	47	48	18	?
Hbd:												
$2V_{\alpha}$	80	--	83	78	--	85	75	--	--	--	75	80
δ	.026	--	.022	.027	.029	.028	--	--	.025	--	.024	.021
$\gamma \wedge c$	18	--	21	20	17	17	--	--	18	--	17	21
Bio:												
$2V_{\alpha}$	--	--	--	--	0	--	0	--	--	--	--	--
Chl:												
$2V_{\gamma}$	--	--	--	--	0	--	--	--	--	--	15	--

APPENDIX I - PART D

MODES OF TONALITES

SPEC. NO.	20/8 75/4	21/8 75/10	19/6 75/2	24/7 75/1	15/6 75/1	7/7 75/8	19/8 75/3	17/6 75/1	6/8 75/7	25/8 75/11	24/7 75/6	18/7 75/2
Qz	25	18	20	14	15	20	15	12	13	15	10	11
Plag	55	50	60	50	55	50	55	53	52	50	40	45
Or	--	--	--	--	--	--	--	--	--	--	--	--
Hbd	6	10	10	20	15	20	19	27	28	27	40	40
Bio	14	20	10	15	8	10	9	7	7	4	10	tr
Chl	--	tr	tr	--	7	--	tr	--	--	3	tr	--
Ep	--	2	tr	--	--	--	1	tr	--	tr	--	--
Ap	tr	tr	tr	tr	tr	tr	tr	tr	tr	tr	tr	tr
Opaque	1	tr	tr	1	--	--	1	1	tr	1	--	1
Others		To-tr Sn-tr	Mu-tr Sn-tr		Pr-tr	Opx-tr	Mu-tr	Ac-tr		Mu-tr		CHb-3
S/O	>10	>>10	>10	>>10	>10	5	>>10	>10	10	>>10	>>10	>10
An%:												
high	74	38	46	59	55	52	51	41	56	41	50	48
low	23	25	28	30	40	26	36	38	31	38	33	46
Hbd:												
$2V_{\alpha}$	90	70	66	72	--	70	80	70	85	--	85	90
δ	.023	.023	.018	.025	.019	--	.020	.022	.025	--	.028	.026
$\gamma \wedge c$	17	16	20	19	14	22	18	19	17	--	17	17
Bio:												
$2V_{\alpha}$	0	0	--	0	--	--	0	--	0	--	0	--
Chl:												
$2V_{\gamma}$	--	0	--	--	--	--	25	--	--	--	--	--

APPENDIX I - PART E
ULTRAMAFIC ROCKS AND ASSOCIATES

TYPE	DIORITE		GIANT MASCOT ULTRAMAFIC ROCKS							HORNBLENDIC ROCKS				
	27/8	27/8	27/8	8/8	24/8	24/8	27/8	8/8	24/8	13/9	24/8	13/9	AM#2	79A-2
NO.	75/2a	75/2c	75/2b	75/13	75/7c	75/7b	75/2a	75/4a	75/7a	75/2	75/9	75/1a		
Qz	--	tr	2	tr	--	--	tr-1	--	--	--	--	--	--	--
Plag	75	50-80	43	35	tr	--	tr-39	3	--	50	24	8	--	--
Or	--	--	--	--	--	--	--	--	--	sl-tr	--	--	--	--
Opx	20	20-10	20	25	15	18	30-15	35	40	--	--	--	--	--
Cpx	--	15-8	15	14	5	7	30-15	30	35	--	--	12	--	tr-2
Hbd	5	15-2	20	25	80	75	40-20	30	10	50	75	80	90	99-97
Bio	--	--	tr	--	--	tr	--	--	--	--	--	--	--	--
Chl	--	--	--	--	tr	--	--	--	--	tr	1	--	1	--
Ap	--	--	--	--	--	--	--	--	--	--	tr	tr	--	--
Opaque	tr	tr	tr	tr	tr	tr	tr	2	tr	tr	tr	tr	tr	1
Others			Cb-tr		Cb-tr	Tc-tr Cb-tr		Sn-tr	01-15	Mu-tr		Sn-tr		
S/O	10	>10	>>10	>>10	>>10	>>10	10	>>10	>>10	10	5	3	>>10	--
An%:														
high	80	80	61	72	--	--	90	79	--	71	85	--	--	--
low	55	52	41	57	--	--	71	74	--	62	68	42	--	--
Opx:														
$2V_\alpha$	80	85	85	70	90	90	85	85	90	--	--	--	--	--
δ	.010	.014	.014	.015	.012	.010	.011	.013	.011	--	--	--	--	--
Cpx:														
$2V_\gamma$	--	70	60	60	65	60	60	65	60	--	--	70	--	--
δ	--	.032	.029	.030	.030	.030	.027	.033	.027	--	--	.031	--	--
$\gamma \wedge c$	--	40	39	41	41	41	40	40	44	--	--	37	--	--
Hbd:														
$2V_\alpha$	--	90	85	80	90	90	--	90	≈80	--	90	85	80	90
δ	.025	.030	.027	.027	.027	.026	.024	.027	.024	.021	--	.027	.026	.025
$\gamma \wedge c$	16	19	18	18	18	18	17	18	18	17	--	18	17	18
Chl:														
2V	--	--	--	--	--	--	--	--	--	≈0	≈0	--	--	--

APPENDIX I - PART F

MISCELLANEOUS ROCKS

TYPE	MAFIC DYKES				BRECCIA	APLITES		XENOLITHS		GRANOFELS
SPEC. NO.	8/8 75/5b	20/8 75/3	27/8 75/3a	28/8 75/1a	75-A,B	24/6 75/3b	23/7 75/3	1/7 75/3	6/8 75/15	2/7 75/4b
Qz	tr	--	--	--	--	30	37	60	--	25
Plag	60	34-29	48	19	40	58	48		70	25
Or	--	--	--	--	--	--	--	--	--	--
Opx	28	--	--	tr	--	--	--	4	--	10
Cpx	10	--	--	--	--	--	--	--	--	--
Hbd	--	65-70	50	80	60	--	--	35	tr	--
Bio	tr	--	tr	--	--	7	12		28	15
Mu	--	--	--	--	--	3	1	--	--	--
Gar	--	--	--	--	--	2	1	--	--	20
Ap	--	tr	tr	--	--	tr	tr	--	--	--
Opaque	2	1	2	1	tr	tr	tr	1	1	5
Others						Sn-tr	Cz-1		Chl-1	
S/O	>>10	5	>>10	1	--	>10	>10	>10	>>10	>>10
An%:										
high	73	82	69	78	65	59	58	--	47	58
low	45	48	47	69	40	32	32	--	34	40
Opx:										
$2V_{\alpha}$	75	--	--	<90	--	--	--	--	--	65
δ	.014	--	--	--	--	--	--	--	--	.012
Cpx:										
$2V_{\gamma}$	≈50	--	--	--	--	--	--	--	--	--
δ	.032	--	--	--	--	--	--	--	--	--
$\gamma \wedge c$	42	--	--	--	--	--	--	--	--	--
Hbd:										
$2V_{\alpha}$	--	--	90	90	80	--	--	--	75	--
δ	--	--	.021	.026	.027	--	--	--	.024	--
$\gamma \wedge c$	--	--	15	17	17	--	--	--	17	--

APPENDIX II

KEY TO PYROXENE ANALYSES

NO.	REF.	TYPES	LOCALITY OR OCCURRENCE
SA 660	Atkins, 1969	Diop./Bronz.	Bushveld gabbro, Critical Series
SA 722	"	Diop./Bronz.	Bushveld gabbro, Critical Series
SA 733	"	Aug./Bronz.	Bushveld gabbro, Main Zone a
SA 738	"	Aug./Inv.Pig.	Bushveld gabbro, Main Zone b
SA 616	"	Aug./Inv.Pig.	Bushveld ferrogabbro, Upper Zone a
7493	Hess, 1960	Aug./Inv.Pig.	Bushveld gabbro, Main Zone b
EB 41	"	Aug./Inv.Pig.	Stillwater Complex, gabbro
EB 43	"	Aug./OPX	Stillwater Complex
4526	Brown, 1957	CPX/OPX	Skaergaard gabbroic picrite
4385A	"	CPX/OPX*	Skaergaard olivine gabbro
4341	"	CPX/OPX*	Skaergaard gabbro (middle)
4430	"	CPX/OPX*	Skaergaard ferrogabbro

* formula suggests these are inverted pigeonite

Note: Formulas given are for six oxygens

APPENDIX II - PART A

CALCIUM-RICH CLINOPYROXENES

REF.	Atkins, 1969					Hess, 1960				Brown, 1957		
NO.	SA660	SA722	SA733	SA738	SA616	7493	EB41	EB43	4526	4385A	4341	4430
SiO_2	52.90	52.93	52.17	51.74	50.35	51.39	51.86	51.83	51.17	50.66	51.26	50.58
TiO_2	.37	.26	.29	.41	.36	.41	.55	.49	.97	1.30	.84	.61
Al_2O_3	2.41	2.40	2.47	2.45	2.21	2.45	2.33	3.07	3.22	2.45	1.98	2.20
Cr_2O_3	.26	.27	.02	<.01	--	--	.01	--	.42	--	<.01	<.01
Fe_2O_3	1.03	1.07	1.10	1.33	1.69	1.26	1.60	1.38	1.53	1.33	1.25	1.57
FeO	5.10	4.61	6.15	9.73	16.18	11.63	9.45	7.21	4.54	11.24	14.49	15.53
MgO	16.18	16.55	16.04	14.50	11.15	14.21	14.50	16.00	16.68	14.25	12.85	12.60
MnO	.16	.15	.20	.26	.37	.32	.24	.17	.13	.29	.35	.28
CaO	21.46	21.55	21.14	19.48	17.93	18.12	5.13	19.21	20.54	18.01	16.91	16.40
Na_2O	.34	.33	.26	.32	.23	.27	.23	.27	.65	.36	.26	.24
K_2O	.02	.02	.01	.04	.03	.02	.00	.02	.05	.08	.02	.03
Others	.02	.03	.03	.03	.02	--	--	.58	--	--	--	--
Total	100.25	100.17	99.88	100.29	100.52	100.18	100.17	100.23	99.90	99.97	100.21	100.04
Si	1.9370	1.9363	1.9267	1.9279	1.9253	1.9278	1.9370	1.9175	1.8829	1.9047	1.9395	1.9269
Ti	.0102	.0072	.0081	.0115	.0104	.0116	.0155	.0136	.0268	.0368	.0239	.0175
Al	.1040	.1035	.1075	.1076	.0996	.1083	.1026	.1339	.1397	.1086	.0883	.0988
Cr	.0075	.0078	.0006	.0	.0	.0	.0003	.0	.0122	.0	.0	.0
Fe+3	.0284	.0295	.0306	.0373	.0486	.0356	.0450	.0384	.0424	.0376	.0356	.0450
Fe+2	.1562	.1410	.1900	.3032	.5174	.3649	.2952	.2231	.1397	.3534	.4585	.4948
Mg	.8806	.8999	.8804	.8030	.6337	.7923	.8050	.8798	.9123	.7963	.7226	.7132
Mn	.0050	.0047	.0063	.0082	.0120	.0102	.0076	.0053	.0041	.0092	.0112	.0090
Ca	.8420	.8447	.8366	.7778	.7347	.7283	.7572	.7615	.8099	.7256	.6856	.6695
Na	.0241	.0234	.0186	.0231	.0171	.0196	.0167	.0194	.0464	.0262	.0191	.0177

APPENDIX II - PART B

ORTHOPYROXENES AND PIGEONITES

REF.	Atkins, 1969					Hess, 1960				Brown, 1957		
NO.	SA660	SA722	SA733	SA738	SA616	7493	EB41	EB43	4526	4385A	4341	4430
SiO_2	54.32	54.82	53.26	51.47	48.90	51.40	52.81	53.20	53.60	50.35	50.90	50.50
TiO_2	.25	.21	.20	.29	.50	.37	--	.26	.50	.55	.50	.40
Al_2O_3	1.83	1.87	1.79	1.56	1.50	1.78	1.65	2.24	2.30	2.23	1.80	1.30
Cr_2O_3	.12	.14	.01	<.01	--	--	--	.10	.30	--	--	--
Fe_2O_3	1.28	1.22	1.35	1.42	2.10	1.40	1.13	.83	1.30	1.14	.70	.70
FeO	13.44	11.49	15.25	21.72	28.70	20.68	18.13	15.15	10.80	21.12	25.10	27.00
MgO	27.56	28.71	26.30	21.68	13.80	19.37	19.81	24.58	28.70	20.03	16.40	15.50
MnO	.29	.28	.36	.52	.60	.38	.38	.32	.30	.38	.30	.20
CaO	1.18	1.44	1.10	1.45	3.60	4.07	5.13	2.61	2.00	4.50	4.20	4.10
Na_2O	.05	.07	.07	.07	.20	.11	.05	.06	.20	--	.10	.20
K_2O	.02	.02	.02	.03	.00	--	.00	.01	.00	--	.00	.10
Others	.01	.02	.02	.02	--	--	--	.58	--	--	--	--
Total	100.35	100.29	99.73	100.23	99.90	100.00	100.16	99.94	100.00	100.30	100.00	100.00
Si	1.9446	1.9470	1.9377	1.9279	1.9221	1.9426	1.9700	1.9447	1.9129	1.8960	1.9484	1.9540
Ti	.0067	.0056	.0055	.0082	.0148	.0085	.0104	.0072	.0134	.0156	.0144	.116
Al	.0772	.0783	.0768	.0689	.0695	.0748	.0726	.0965	.0968	.0990	.0812	.0593
Cr	.0034	.0039	.0003	.0	.0	.0	.0	.0029	.0085	.0	.0	.0
Fe+3	.0345	.0326	.0370	.0400	.0621	.0398	.0317	.0228	.0349	.0323	.0202	.0204
Fe+2	.4024	.3413	.4640	.6804	.9435	.6536	.5656	.4632	.3224	.6651	.8036	.8737
Mg	1.4664	1.5155	1.4221	1.2069	.8062	1.0880	1.0983	1.3355	1.5223	1.1210	.9331	.8914
Mn	.0088	.0084	.0111	.0165	.0200	.0154	.0120	.0099	.0091	.0121	.0097	.0066
Ca	.0453	.0548	.0429	.0582	.1516	.1648	.2051	.1022	.0765	.1816	.1723	.1700
Na	.0035	.0048	.0049	.0051	.0152	.0081	.0036	.0043	.0138	.0	.0074	.0150

APPENDIX III

KEY TO HORNBLENDE ANALYSES

NO.	LOCALITY OR OCCURRENCE
27	Tonalite, Idaho
5	Hornblendite, Austria
14	Hornblendite, Sweden
6	Actinolite-Chlorite Schist, South Africa
7	Amphibolite, Australia
30	Amphibolite, Japan
32	Charnockite, Norway
11	Gabbro, Pennsylvania

Analyses from Deer, Howie and Zussman (1963) pp. 274-281.

Note: Formulas are calculated according to the scheme described in the text, and are for 22 oxygens and 2 OH.

APPENDIX III

HORNBLENDE ANALYSES AND FORMULAS

Number	27	5**	14	6	7	30	32	11
SiO_2	44.99	51.63	42.80	52.78	50.08	45.62	42.24	48.71
TiO_2	1.46	tr	3.80	.43	.36	1.13	2.76	.32
Al_2O_3	11.21	7.39	12.71	5.77	9.42	8.87	10.47	9.48
Fe_2O_3	3.33	2.50	1.85	2.45	1.14	2.85	4.04	2.33
FeO	13.17	5.30	10.70	6.61	6.89	16.09	16.06	9.12
MgO	10.41	18.09	14.24	17.43	16.00	10.13	9.22	14.43
MnO	.31	.17	.15	.17	.33	.32	.28	.23
CaO	12.11	12.32	11.36	11.90	12.53	11.42	11.23	11.93
Na_2O	.97	.61	1.34	.68	1.09	1.27	1.44	1.16
K_2O	.76	--	.54	.07	.21	.33	.89	.15
H_2O	1.52	2.31	.28	2.26	1.49	2.08	.72	1.83
Others	.17	--	--	.03	--	--	.05	.23
Total	100.41	100.32	99.77	100.58	99.54	100.11	99.40	99.92
Alkali Site	.358	.119	.493*	.055	.269	.349	.481	.237
K	.142	.0	.099	.013	.038	.063	.171	.027
Na	.216	.119	.374	.042	.231	.286	.310	.210
Cubic Site	2	2	2	2	2	2	2	2
Na	.059	.047	.0	.142	.067	.081	.109	.113
Ca	1.902	1.847	1.730	1.786	1.894	1.824	1.808	1.831
Mn	.038	.020	.018	.020	.039	.040	.036	.028
Fe^{+2}	.0	.086	.251	.052	.0	.055	.047	.028
Octahedral Site	4.943	5	5	5	4.955	5	5	5
Mg	2.268	3.761	3.044	3.629	3.354	2.244	2.059	3.072
Fe^{+2}	1.615	.534	1.036	.723	.813	1.951	1.971	1.064
Fe^{+3}	.367	.263	.200	.258	.121	.320	.457	.251
Al	.532	.442	.310	.345	.629	.358	.201	.578
Ti	.161	tr	.411	.045	.038	.127	.312	.034
Tetrahedral Site	8	8	8	8	8	8	8	8
Al	1.405	.777	1.845	.607	.937	1.200	1.653	1.023
Si	6.595	7.223	6.155	7.393	7.063	6.800	6.347	6.977

* includes .020 Ca
** analyses includes 1.2% epidote

APPENDIX IV

COMPUTER PROGRAM USED IN THE DIFFERENTIATION TEST

This appendix is provided so that the reader may verify that the method used to calculate Spuzzum differentiation phenomena is correct. The program was run on a PDP 11/10 desk computer owned by the Department of Geological Sciences, University of British Columbia.

```
NONAME   14-SEP-76   BASIC/CAPS   V01-01

1 REM: DATA FOR DIORITE FIRST, THEN TONALITE; LINES 20-25
2 REM:   LIST SIO2,TIO2,AL2O3,FE2O3,FEO,MGO,CAO,NA2O,K2O.
5 DIM A(8),B(8),C(8),D(8),M(8),N(8),W(8)
10 PRINT "SPUZZUM DIFFERENTIATION MODEL"
11 PRINT
15 PRINT "RESTART AT LINE 150 OR 180."
20 DATA 55.4,.348,19.26,1.04,5.42,5.06,7.37,3.36,.5
21 DATA 59.77,.717,17.4,1.1,4.37,4.13,5.83,3.83,.97
30 READ A(2),A(3),A(4),A(0),A(1),A(5),A(6),A(7),A(8)
31 READ B(2),B(3),B(4),B(0),B(1),B(5),B(6),B(7),B(8)
32 PRINT
35 DATA 79.85,71.85,60.09,79.9,50.98,40.43,56.08,30.991,47.096
40 READ W(0),W(1)
41 LET A(1)=A(1)+A(0)*W(1)/W(0)
42 LET A(0)=0
43 LET B(1)=B(1)+B(0)*W(1)/W(0)
44 LET B(0)=0
45 LET S0=A(1)+A(2)+A(3)+A(4)+A(5)+A(6)+A(7)+A(8)
46 LET S1=B(1)+B(2)+B(3)+B(4)+B(5)+B(6)+B(7)+B(8)
50 FOR I=1 TO 8
55 IF I>=2 THEN READ W(I)
56 LET A(I)=100*A(I)/S0
57 LET B(I)=100*B(I)/S1
58 NEXT I
60 DATA .3221,.7367,1.956,1.975,.0101,2.30000E-03,.095,.0527
61 DATA .7443,1.103,.3365,.0321,.0324,3.00000E-04,0,0
65 FOR I=1 TO 8
66 READ C(I),D(I)
67 NEXT I
69 LET D(0)=0
70 LET C(0)=0
71 LET W1=W(6)+2*(W(4)+W(2))
72 LET W2=W(7)+W(4)+3*W(2)
75 LET S0=C(1)+C(2)+C(3)+C(4)+C(5)+C(6)+C(7)+C(8)

READY
```

```
76 LET S1=D(1)+D(2)+D(3)+D(4)+D(5)+D(6)+D(7)+D(8)
80 FOR I=1 TO 8
85 LET C(I)=100*C(I)/S0
86 LET D(I)=100*D(I)/S1
90 NEXT I
95 DATA 1.5795,1.5043,2.4046
96 READ V0,V1,V2
100 GO TO 2000
110 LET S0=3.48/V2+.6188/V1+.594/V0
115 LET Q0=.594/(V0*S0)
116 LET Q1=.6188/(V1*S0)
117 LET Q2=3.48/(V2*S0)
120 PRINT
150 PRINT "PLAGIOCLASE EQUILIBRATES WITH LIQUID (0), OR"
151 PRINT "   IS SHIELDED (+1)";
160 INPUT Z
170 PRINT
180 LET U=0
200 PRINT "WT. % DIORITE";
201 INPUT X
205 LET S0=0
206 LET S1=0
210 FOR I=1 TO 8
215 LET M(I)=(X*A(I)/100+(1-X/100)*B(I))/W(I)
216 LET S1=S1+X*A(I)/(100*W(I))
220 LET S0=S0+M(I)
221 LET N(I)=0
225 NEXT I
228 LET S1=S1/S0
230 FOR I=1 TO 8
235 LET M(I)=M(I)*100/S0
236 NEXT I
240 PRINT
250 PRINT "BEGIN GROWTH"
251 PRINT "PLAG";
252 INPUT P2
255 PRINT "CPX ";
256 INPUT P1
260 PRINT "CPX ";
261 INPUT P0
263 PRINT
270 PRINT "BEGIN PRINTING";
271 INPUT E
272 PRINT
273 LET E=E/100
280 LET P=0
290 LET S=100
295 GOSUB 900
298 PRINT
300 IF P0*P1*P2>0 GO TO 317
301 IF P0+P1+P2=0 GO TO 360
302 IF P0+P1=0 GO TO 320
303 IF P0+P2=0 GO TO 322
304 IF P1+P2=0 GO TO 324
305 IF P0=P1 GO TO 326

READY
```

```
306 IF P0=P2 GO TO 328
307 IF P1=P2 GO TO 330
308 IF (P1-P0)*P0>0 GO TO 340
309 IF (P0-P1)*P1>0 GO TO 343
310 IF (P2-P0)*P0>0 GO TO 346
311 IF (P0-P2)*P2>0 GO TO 349
312 IF (P2-P1)*P1>0 GO TO 352
313 IF (P1-P2)*P2>0 GO TO 355
314 PRINT "I GOOFED"
315 STOP
317 PRINT "INVALID CRYSTALLIZATION SEQUENCE"
318 GO TO 240
320 IF 100-S<P2 GO TO 330
321 GO TO 360
322 IF 100-S<P1 GO TO 335
323 GO TO 360
324 IF 100-S<P0 GO TO 390
325 GO TO 360
326 IF 100-S<P0 GO TO 365
327 GO TO 360
328 IF 100-S<P0 GO TO 370
329 GO TO 360
330 IF 100-S<P1 GO TO 375
331 GO TO 360
340 IF 100-S<P0 GO TO 365
341 IF 100-S<P1 GO TO 385
342 GO TO 360
343 IF 100-S<P1 GO TO 365
344 IF 100-S<P0 GO TO 390
345 GO TO 360
346 IF 100-S<P0 GO TO 370
347 IF 100-S<P2 GO TO 380
348 GO TO 360
349 IF 100-S<P2 GO TO 370
350 IF 100-S<P0 GO TO 390
351 GO TO 360
352 IF 100-S<P1 GO TO 375
353 IF 100-S<P2 GO TO 380
354 GO TO 360
355 IF 100-S<P2 GO TO 375
356 IF 100-S<P1 GO TO 385
360 LET R0=00
361 LET R1=01
362 LET R2=02
363 GO TO 400
365 LET R0=0
366 LET R1=0
367 LET R2=1
368 GO TO 400
370 LET R0=0
371 LET R1=1
372 GO TO 382
375 LET R0=1
376 LET R1=0
377 GO TO 382

READY
```

```
380 LET R0=Q0/(Q0+Q1)
381 LET R1=1-R0
382 LET R2=0
383 GO TO 400
385 LET R0=Q0/(Q0+Q2)
386 LET R1=0
387 LET R2=1-R0
388 GO TO 400
390 LET R0=0
391 LET R1=Q1/(Q1+Q2)
392 LET R2=1-R1
400 IF S=100 THEN IF T=1 THEN  GOSUB 900
402 FOR I=1 TO 8
405 LET M(I)=M(I)-.01*(R0*C(I)+R1*D(I))
406 LET N(I)=N(I)+.01*(R0*C(I)+R1*D(I))
410 NEXT I
420 LET X3=(M(4)-M(7)-M(8))/(M(4)-M(8))
421 LET X=X3/(X3+(1-X3)*W2/W1)
430 IF Z=0 GO TO 455
434 LET D0=4.2
435 LET Y=1+D0-(D0↑2+D0)/(X+D0)
436 LET Y=Y/(Y+(1-Y)*W1/W2)
440 LET M(2)=M(2)-R2*(9.00000E-03+.591*(1-Y)+.394*Y)
441 LET N(2)=N(2)+R2*(9.00000E-03+.591*(1-Y)+.394*Y)
442 LET M(4)=M(4)-R2*(3.00000E-03+.197*(1-Y)+.394*Y)
443 LET N(4)=N(4)+R2*(3.00000E-03+.197*(1-Y)+.394*Y)
444 LET M(6)=M(6)-R2*.197*Y
445 LET N(6)=N(6)+R2*.197*Y
446 LET M(7)=M(7)-R2*.197*(1-Y)
447 LET N(7)=N(7)+R2*.197*(1-Y)
448 LET M(8)=M(8)-R2*3.00000E-03
449 LET N(8)=N(8)+R2*3.00000E-03
455 LET P=P+R2
460 LET S=S-1
461 LET S0=1-S/100
465 LET U=U+1
470 IF U+.1<100*E GO TO 300
480 IF Z>0 GO TO 745
500 LET L1=-.032
505 LET X=X-L1
510 LET X=X+L1
520 LET D0=4.2
521 LET Y=1+D0-(D0↑2+D0)/(X+D0)
530 LET Y4=Y/(Y+(1-Y)*W1/W2)
531 LET X4=X/(X+(1-X)*W1/W2)
540 IF ABS((X3-X4)/(Y4-X4)-.985*P/(M(4)-M(8)))<=5.00000E-04 GO TO 66
545 IF (X3-X4)/(Y4-X4)>.985*P/(M(4)-M(8)) GO TO 550
546 GO TO 510
550 LET X=X-L1
551 LET L1=L1/2
560 GO TO 510
660 LET M2=M(2)-P*(9.00000E-03+.591*(1-Y4)+.394*Y4)
661 LET N2=N(2)+P*(9.00000E-03+.591*(1-Y4)+.394*Y4)
662 LET M4=M(4)-P*(3.00000E-03+.197*(1-Y4)+.394*Y4)
663 LET N4=N(4)+P*(3.00000E-03+.197*(1-Y4)+.394*Y4)
664 LET M6=M(6)-P*.197*Y4

READY
```

```
665 LET N6=N(6)+P*.197*Y4
666 LET M7=M(7)-P*.197*(1-Y4)
667 LET N7=N(7)+P*.197*(1-Y4)
668 LET M8=M(8)-P*3.00000E-03
669 LET N8=N(8)+P*3.00000E-03
745 PRINT
746 PRINT
751 PRINT "  "U" % CRYSTALS"
770 PRINT
771 PRINT "OXIDE","DIORITE","TONALITE"
772 LET U0=0
773 LET T0=0
774 LET T1=0
777 IF Z=0 GO TO 800
780 FOR I=1 TO 8
785 LET T0=T0+W(I)*(N(I)+(S1-S0)*M(I))
786 LET T1=T1+W(I)*(1-S1)*M(I)
787 NEXT I
790 FOR I=1 TO 8
792 LET U0=U0+(W(I)*(N(I)+(S1-S0)*M(I))*100/T0-A(I))↑2
793 LET U0=U0+(W(I)*(1-S1)*M(I)*100/T1-B(I))↑2
795 PRINT I,
796 PRINT INT(10000*W(I)*(N(I)+(S1-S0)*M(I))/T0+.5)/100,
797 PRINT INT(10000*W(I)*(1-S1)*M(I)/T1+.5)/100
798 NEXT I
799 GO TO 840
800 LET T0=W(1)*(N(1)+(S1-S0)*M(1))+W(2)*(N2+(S1-S0)*M2)
801 LET T0=T0+W(3)*(N(3)+(S1-S0)*M(3))+W(4)*(N4+(S1-S0)*M4)
802 LET T0=T0+W(5)*(N(5)+(S1-S0)*M(5))+W(6)*(N6+(S1-S0)*M6)
803 LET T0=T0+W(7)*(N7+(S1-S0)*M7)+W(8)*(N8+(S1-S0)*M8)
810 LET T1=W(1)*M(1)+W(2)*M2+W(3)*M(3)+W(4)*M4
811 LET T1=T1+W(5)*M(5)+W(6)*M6+W(7)*M7+W(8)*M8
812 LET T1=(1-S1)*T1
820 PRINT 1,INT(10000*W(1)*(N(1)+(S1-S0)*M(1))/T0+.5)/100,
821 PRINT INT(10000*W(1)*(1-S1)*M(1)/T1+.5)/100
822 PRINT 2,INT(10000*W(2)*(N2+(S1-S0)*M2)/T0+.5)/100,
823 PRINT INT(10000*W(2)*(1-S1)*M2/T1+.5)/100
824 PRINT 3,INT(10000*W(3)*(N(3)+(S1-S0)*M(3))/T0+.5)/100,
825 PRINT INT(10000*W(3)*(1-S1)*M(3)/T1+.5)/100
826 PRINT 4,INT(10000*W(4)*(N4+(S1-S0)*M4)/T0+.5)/100,
827 PRINT INT(10000*W(4)*(1-S1)*M4/T1+.5)/100
828 PRINT 5,INT(10000*W(5)*(N(5)+(S1-S0)*M(5))/T0+.5)/100,
829 PRINT INT(10000*W(5)*(1-S1)*M(5)/T1+.5)/100
830 PRINT 6,INT(10000*W(6)*(N6+(S1-S0)*M6)/T0+.5)/100,
831 PRINT INT(10000*W(6)*(1-S1)*M6/T1+.5)/100
832 PRINT 7,INT(10000*W(7)*(N7+(S1-S0)*M7)/T0+.5)/100,
833 PRINT INT(10000*W(7)*(1-S1)*M7/T1+.5)/100
834 PRINT 8,INT(10000*W(8)*(N8+(S1-S0)*M8)/T0+.5)/100,
835 PRINT INT(10000*W(8)*(1-S1)*M8/T1+.5)/100
836 GOSUB 970
840 PRINT "RMS RESID="SQR(U0/16)
845 PRINT
850 GO TO 300
900 PRINT "ACCESSORIES (<=1%)"

READY
```

```
901 PRINT "ILMN";
902 INPUT Z0
903 PRINT "MAGN";
904 INPUT Z1
910 LET S=S-Z0-Z1
920 LET M(1)=M(1)-Z0/2-Z1
921 LET N(1)=N(1)+Z0/2+Z1
925 LET M(3)=M(3)-Z0/2
926 LET N(3)=N(3)+Z0/2
930 LET R0=(1-Z0-Z1)*R0
931 LET R1=(1-Z0-Z1)*R1
932 LET R2=(1-Z0-Z1)*R2
940 RETURN
950 PRINT
951 PRINT
952 PRINT
953 PRINT
960 GO TO 180
970 FOR I=1 TO 5 STEP 2
975 LET U0=U0+(W(I)*(N(I)+(S1-S0)*M(I))*100/T0-A(I))↑2
976 LET U0=U0+(W(I)*(1-S1)*M(I)*100/T1-B(I))↑2
977 NEXT I
980 LET U0=U0+(W(2)*(N2+(S1-S0)*M2)*100/T0-A(2))↑2
981 LET U0=U0+(W(4)*(N4+(S1-S0)*M4)*100/T0-A(4))↑2
982 LET U0=U0+(W(6)*(N6+(S1-S0)*M6)*100/T0-A(6))↑2
983 LET U0=U0+(W(7)*(N7+(S1-S0)*M7)*100/T0-A(7))↑2
984 LET U0=U0+(W(8)*(N8+(S1-S0)*M8)*100/T0-A(8))↑2
990 LET U0=U0+(W(2)*(1-S1)*M2*100/T1-B(2))↑2
991 LET U0=U0+(W(4)*(1-S1)*M4*100/T1-B(4))↑2
992 LET U0=U0+(W(6)*(1-S1)*M6*100/T1-B(6))↑2
993 LET U0=U0+(W(7)*(1-S1)*M7*100/T1-B(7))↑2
994 LET U0=U0+(W(8)*(1-S1)*M8*100/T1-B(8))↑2
995 RETURN
1000 STOP
2000 PRINT
2005 PRINT "ORIGINAL ANALYSES:"
2006 PRINT "OXIDE","DIORITE","TONALITE"
2010 FOR I=0 TO 8
2020 PRINT I,A(I),B(I)
2025 NEXT I
2030 PRINT
2034 PRINT "PYROXENE FORMULAS:"
2035 PRINT "ELEMENT","ORTHO.","CLINO."
2040 FOR I=0 TO 8
2050 PRINT I,D(I),C(I)
2055 NEXT I
2060 PRINT
2070 PRINT "MOLAR VOLUMES:"
2075 PRINT "PLAG  "V2
2076 PRINT "OPX   "V1
2077 PRINT "CPX   "V0
2080 PRINT
2090 PRINT "REMOVE LINE 100 AND RESTART."
3000 END

READY
```

GUIDE TO APPENDIX V

The purpose of this appendix is to relieve cluttering in the map produced in this study. Instead of plotting station locations on the map, they are tabulated in the appendix.

The tables are organized thus:

Column 1: Station number.

Column 2: Longitude as minutes and seconds west of 121°W (min.-sec.).

Column 3: Latitude as minutes and seconds north of 49°N (min.-sec.).

Column 4: Elevation in metres

Column 5: Rocktype

S	schist	HPX	hornblende pyroxenite
T	tonalite	OPX	olivine pyroxenite
HD	hornblende diorite	HB	hornblendite
PD	pyroxene diorite	UB	ultrabasic rocks
PHD	transition PD to HD	AP	aplite
HZ	hornblendized rocks	Grfs	granofels
HZD	transition HZ to PD or HD	CGn	Custer Gneiss
SCB	schist contact intrusive breccia	Cgl	conglomerate

Columns 6 and 7: Attitude, foliation open and lineation in parentheses.

Col. 6: Azimuth or strike (degrees true).

Col. 7: Plunge or dip (degrees).

Column 8: Quality of attitude data

VG	very good	FP	fairly poor
G	good	P	poor
FG	fairly good	W	too weak to measure
F	fair	D	directionless

Column 9: Notes about specimen or station

S	Specimen thin sectioned
P	Specimen microanalyzed

APPENDIX V

CATALOGUE OF FIELD DATA

1 Number	2 Longitude	3 Latitude	4 Elevation	5 Rocktype	Attitude 6 Azim.	Attitude 7 Inclin.	8 Q.	9 Notes
15/6/75/1	27-27.6	23-30.0	88	T	--	--	--	S
/2	28-19.1	11.4	91	HD	--	--	--	
/3	40.8	22-57.6	88	HD	--	--	--	S
/4	29-40.4	40.4	82	PHD	--	--	--	
/5	30-17.3	36.3	76	PD+S	--	--	--	
/6	31-39.0	21-49.8	91	PD	--	--	--	S,P
17/6/75/1	29-30.9	28-05.1	792	T	130	78NE	F	S
/2	39.8	03.3	792	HPX	--	--	D	
/3	27.7	06.1	792	T	(315)	(50)	P	
/4	22.8	07.3	792	T	100	65NE	P	
/5	19.8	08.6	792	T	80	50N	G	
/6	29.6	03.7	771	T	160	61NE	G	
					(350)	(45)	P	
/7	31.1	02.6	762	HZ	100	55N	G	
/8	22.2	27-58.3	774	T	--	--	--	
/9	16.7	58.7	789	T+S	60	58NW	F	
/10	07.5	57.2	792	T	25	40NW	F	
/11	04.8	57.0	792	T+S	110	80NE	G	
/12	02.1	57.1	792	T	165	90	P	
/13	28-59.9	57.6	792	T+S	(325)	(40)	G	
/14a	32.4	28-03.8	792	T	--	--	D	
/14b	40.1	03.3	786	T+AP	--	--	D	
/15	29-47.3	27-58.9	805	PD	35	65NW	G	P
19/6/75/1a	27-39.1	29-32.1	506	S	70	35NW	G	
/1b	38.5	28.6	503	HPX	--	--	D	
/2	28-08.5	25-38.5	390	T	(0)	(40)	P	
/3	29-19.9	34.8	610	T	105	50NE	P	
					(330)	(43)	G	
/4	30-22.1	41.5	655	T	15	50NW	F	
/5	31-10.7	11.7	707	HZ	--	--	D	S

APPENDIX V

CATALOGUE OF FIELD DATA

1 Number	2 Longitude	3 Latitude	4 Elevation	5 Rocktype	Attitude 6 Azim.	Attitude 7 Inclin.	8 Q.	9 Notes
20/6/75/1a	27-17.3	25-34.8	320	Cgl	--	--	--	
/1b	07.2	35.0	320	Cgl	--	--	--	
/2	28-59.7	34.6	546	T	150	70NE	G	
/3	29-05.1	15.4	701	T	110	50NE	F	
/4	44.2	24-35.0	802	HZD	60	80NW	P	
/5	49.7	22.6	835	HZ	110	60NE	G	
/6	30.0	52.0	829	HZD	120	53NE	G	
/7	00.6	25-02.6	747	T	105	60NE	F	
21/6/75/1	27-12.9	28-54.2	411	S	140	65NE	G	
					(335)	(43)	G	
/2	11.2	29-04.5	402	S	--	--	D	
/3	12.9	28.2	457	S	10	54W	G	
					(285)	(48)	G	
/4	16.4	19.6	457	S	145	38NE	G	
					(35)	(34)	FG	
/5	14.5	02.6	427	S	5	65W	G	
					(0)	(13)	G	
/6	20.4	28-46.7	427	S	40	22NW	G	
					(320)	(21)	G	
/7	26.5	51.0	457	S+UB	130	40NE	FG	
					(330)	(24)	FG	
/8	44.6	45.7	488	S	0	35W	FG	
					(325)	(11)	G	
/9	10.7	47.4	344	S	--	--	--	
/10	29.1	37.9	372	S	110	40NE	G	
					(315)	(17)	G	
24/6/75/1	27-48.7	28-39.3	518	S	0	30W	FG	
					(320)	(22)	G	
/2	52.5	32.1	524	S	175	53W	G	
					(330)	(22)	G	
/3a,b	59.2	31.5	533	S	0	60W	G	S(ofA)
					(330)	(25)		

APPENDIX V

CATALOGUE OF FIELD DATA

1 Number	2 Longitude	3 Latitude	4 Elevation	5 Rocktype	Attitude 6 Azim.	Attitude 7 Inclin.	8 Q.	9 Notes
24/6/75/4	28-15.3	28-30.0	573	S	170	60W	G	
					(340)	(18)	G	
/6a	22.9	28.4	600	S	0	47W	G	
					(315)	(38)	G	
/6b	25.4	28.0	610	T	(330)	(44)	G	
/6c	27.3	26.9	613	T	25	38NW	G	
					(290)	(34)	G	
25/6/75/1	28-31.4	28-25.1	625	S	20	65NW	G	
					(320)	(58)	G	
/2	36.5	22.8	637	S	(335)	(35)	G	
/3a	40.9	20.5	640	S	(320)	(35)	G	
/3c	42.5	19.7	640	S	(330)	(45)	G	
/4	44.7	18.7	640	HZ	(335)	(27)	G	S
/5	29-05.3	10.4	695	T	--	--	--	
/6	23.9	02.8	728	T	--	--	--	
1/7/75/1	27-17.0	26-14.7	518	CGn	--	--	--	
/2	31-28.1	24-57.1	789	HD	--	--	--	
/3	55.2	39.9	927	PD+S	130	20NE	FG	S
/4	37.9	32.1	1009	PD	110	35NE	FG	
/5b	31.2	44.3	957	PD+HB	--	--	--	
/6	44.2	43.4	942	PD	100	14NE	FG	
/7	32-48.5	53.6	1131	HZ	130	20NE	F	
/8	39.4	57.1	1097	HZ	25	40NW	FG	
/9	41.0	25-04.3	1088	HD	170	40W	G	
/10a	24.0	06.6	1036	Grfs	--	--	--	
/10b	16.1	10.5	1021	HD	5	35W	FG	
2/7/75/1	31-58.9	25-18.7	978	HD	0	45W	G	
/2	55.3	25.5	994	HZ	--	--	--	S
/3	32-10.4	39.8	1021	PD	(30)	(50)	FG	
/4a,b	03.8	36.4	1012	Grfs+PD	45	50NW	G	data in PD,S
/5	01.0	32.1	1006	HZ	5	35W	FG	

APPENDIX V

CATALOGUE OF FIELD DATA

1 Number	2 Longitude	3 Latitude	4 Elevation	5 Rocktype	Attitude 6 Azim.	Attitude 7 Inclin.	8 Q.	9 Notes
2/7/75/6	32-35.5	26-18.2	924	PD	--	--	D	
/7a	31.0	20.6	914	PD	30	45NW	G	
/7b	15.2	28.6	884	PD	--	--	--	
/8	31-49.0	20.2	850	PD	50	40NW	G	
/9	40.8	12.8	850	PD	--	--	D	
/10	36.7	09.6	841	PD	55	40NW	FG	S
7/7/75/1	31-19.4	25-09.1	698	HD	--	--	--	
/2	21.6	17.1	701	HZD	--	--	--	S
/3	21.8	27.8	701	HD	25	45NW	F	
/4	19.3	39.8	704	HD	30	50NW	G	
/5	10.4	48.2	716	HD+S	50	55NW	G	data in HD
/6	05.7	52.8	716	HD+S	--	--	--	
/7	13.9	26-01.4	725	S	10 (240)	50W (40)	G P	
/8	16.8	05.8	725	T	40	45NW	G	S
/9	06.3	06.7	786	T	25	45NW	G	
/10	30-45.7	08.9	860	UB	--	--	--	
9/7/75/1	30-23.7	25-35.3	732	T+S	--	--	D	
/2	31-54.3	02.2	853	PHD	0	30W	G	
/3	42.0	12.3	811	HD	25	30NW	FG	
/4	40.7	24.9	817	HD	10	30W	G	
/5	38.2	33.8	847	HD	--	--	--	
/6	37.0	43.3	881	HD	20	40NW	FG	
/7	47.7	40.0	930	PHD	20	35NW	FG	
/8	17.4	26-37.1	942	HZD	--	--	D	S
/9	34.8	39.8	914	HD	--	--	D	
/10	40.8	42.9	893	Grfs	--	--	D	
/11	52.5	42.7	884	PD	105	25SW	P	S
/12	44.6	29.5	792	PD	(55)	(35)	F	

APPENDIX V

CATALOGUE OF FIELD DATA

1 Number	2 Longitude	3 Latitude	4 Elevation	5 Rocktype	Attitude 6 Azim.	Attitude 7 Inclin.	8 Q.	9 Notes
10/7/75/1	31-56.1	26-26.8	844	HZ	110	10SW	FG	
/2	33-12.1	03.3	780	PD	--	--	D	
/3	32-51.9	16.7	844	PD	--	--	D	S
/4a	58.2	22.0	850	PD	175	55W	G	
/4b	51.0	26.6	847	PD	25	45NW	VG	
/4c	47.5	28.9	850	PD	20	50NW	VG	
/4d	44.3	30.7	850	PD	15	40NW	VG	
/4e	41.2	32.6	850	PD	15	35NW	VG	
/5a	37.7	34.6	856	PD	20	40NW	VG	S
/5b	31.7	37.2	863	PD	175	35W	VG	
/6	40.5	24.8	847	PD	--	--	D	S
/7a	24.4	36.9	850	PX	--	--	D	
/7b	27.6	34.7	847	PD	--	--	D	
/8	14.9	36.9	838	PD	75	20NW	F	
16/7/75/1	29-12.6	28-12.3	792	T	80	55N	G	
/2	07.8	14.8	792	T	60	50NW	G	
/3	02.1	17.6	792	T	55	60NW	G	
/4	28-57.1	20.5	792	T	30	60NW	G	
/5	48.2	23.4	789	T	10	70W	G	
					(355)	(50)	G	
/6	47.6	27.4	826	T	--	--	--	talus
/7	37.7	38.3	832	HZ+T	--	--	--	talus
/8	32.2	41.6	838	S+T	150	80NE	G	data in S
/9	25.4	44.2	835	S	155	60SW	G	
/10	10.5	44.7	753	S	160	55SW	G	
/11	27.1	39.1	774	S	155	50SW	G	
16/7/75/12	32.7	35.2	783	HZ	--	--	D	
/13	39.5	30.2	789	T	10	90	G	
18/7/75/2	31-07.2	28-23.0	1414	T?	--	--	D	S
/3	30-53.6	27.4	1402	HD	135	70NE	FG	
/5	39.1	30.4	1433	PD	--	--	--	talus,S,P

APPENDIX V

CATALOGUE OF FIELD DATA

1 Number	2 Longitude	3 Latitude	4 Elevation	5 Rocktype	Attitude 6 Azim.	Attitude 7 Inclin.	8 Q.	9 Notes
18/7/75/7a	30-39.1	28-03.4	1106	HB	--	--	--	P
23/7/75/1a	28-56.8	27-41.2	1091	T+HB	170	45E	G	data in T
/1b	50.1	43.2	1094	S	150	75SW	G	
/2a	44.1	43.7	1103	T+HB	--	--	--	
/2b	45.4	41.1	1113	S	75	60NW	G	
/3	36.2	41.7	1091	S	30	40NW	G	
/4	41.6	42.6	1097	T	65	45NW	G	
/5	53.6	38.8	1134	T+AP	70	35NW	G	data in T, S
/6a	50.0	31.1	1173	S	60	50NW	G	
/6b	54.1	27.3	1204	S	65	50NW	G	
/6c	29-00.2	23.6	1234	S	95	70N	G	
23/7/75/7	29-02.1	27-27.4	1219	S	135	65NE	G	
					(150)	(40)	G	
/8	12.3	14.3	1375	S	110	55NE	G	
/9	32.2	00.9	1341	S	70	25NW	G	
/10	42.6	26-31.8	1372	S+T	5	45W	G	data in S
24/7/75/1	29-55.6	26-36.7	1408	S+T	170	65W	FG	data in S, S
/2	30-17.7	41.5	1301	S+T	110	50NE	FG	
/3	37.1	47.5	1341	S	145	45NE	FG	
/4	47.4	27-08.7	1387	S	55	40NW	G	
/5	59.4	15.3	1338	HZ	5	80W	G	
/6	31-02.9	17.2	1332	T	--	--	D	S
/7	08.6	21.1	1341	HD	--	--	--	
/8	22.8	17.0	1353	HD	110	45SW	F	
/9	32.0	14.5	1341	PHD	150	45SW	FG	
/10	44.3	18.6	1402	PD	160	35SW	G	
/11	52.2	22.5	1433	PD	110	60SW	G	S,P
/12	53.5	27.7	1384	PD	120	40SW	G	S

APPENDIX V

CATALOGUE OF FIELD DATA

1 Number	2 Longitude	3 Latitude	4 Elevation	5 Rocktype	Attitude 6 Azim.	Attitude 7 Inclin.	8 Q.	9 Notes
24/7/75/13	31-45.6	27-38.6	1341	PD	125	50SW	G	
/14	32.7	47.9	1372	PD	75	45SE	P	
/15	23.3	58.5	1402	HD	130	60SW	G	
29/7/75/1	32-35.2	26-50.1	1030	PD	40	30NW	G	
/2	34.1	45.8	960	PD	20	30NW	G	S
/3a,b	43.7	39.0	945	HZ	175	35W	G	S(3a,b)
/4	37.4	41.7	945	HZ	30	45NW	G	
/5a	22.2	43.7	927	PD	80	20N	G	
/5b	17.5	42.7	908	HZ	100	35N	FG	
/6	10.2	43.1	893	HZ	50	40NW	G	
/7	02.9	40.7	850	PD	155	20NE	G	
/8	31-49.8	41.1	863	HZ	--	--	--	
/9	59.4	40.3	853	HZD	--	--	D	
/10a	39.9	36.5	850	HD	--	--	D	
/10b	33.2	35.5	850	HD	--	--	D	
/10c	26.9	33.8	853	PD	45	45NW	F	S
30/7/75/1	30-46.8	26-19.2	1030	S	60	45NW	G	
/2a	50.6	15.8	981	HD	55	40NW	G	S
/3	31-05.4	25.2	930	SCB	--	--	D	
/4	04.5	40.7	1030	HD	30	90	P	
/5	09.2	42.9	1042	HD	35	65NW	G	
/6	16.6	44.4	1058	HD	20	90	P	
/7	19.6	46.1	1094	HD	--	--	D	
/8	17.6	48.3	1113	HD	140	60SW	G	
/9	04.8	49.9	1128	PD	140	65SW	G	
/10a	30-57.5	46.2	1128	SCB	--	--	--	
/10b	53.4	40.4	1128	S	45	75NW	FG	
/10c	31-00.1	49.4	1128	HD	150	60SW	FG	
31/7/75/1	30-13.7	27-59.9	933	HZ	70	90	F	
/3	12.1	28-01.9	927	HB	--	--	D	
/4	09.5	02.0	911	HZ	--	--	--	

APPENDIX V

CATALOGUE OF FIELD DATA

1 Number	2 Longitude	3 Latitude	4 Elevation	5 Rocktype	Attitude 6 Azim.	Attitude 7 Inclin.	8 Q.	9 Notes
6/8/75/1	30-03.2	29-52.2	607	T	--	--	D	
/2	32-17.3	28-26.9	811	HZ	70	70NW	FG	
/3	23.0	03.0	890	PD	65	65NW	G	
/4	18.8	27-54.1	924	PD	80	90	G	
/5	17.3	28-02.6	927	PHD	--	--	D	
/6	13.0	05.4	960	HD	55	75NW	FG	
/7	06.2	27-56.6	997	T	150	50NE	F	S
/8	01.5	28-15.8	1042	T	165	60NE	VG	
/9	02.6	12.7	1042	T	70	55NW	G	
/10	08.1	10.4	1015	HPX	--	--	D	hi.gr.ore
/11a	53.5	26-53.0	945	PD	--	--	D	
/11b	45.3	27-06.2	948	PD	--	--	D	
/12	42.2	14.1	966	PD	65	50SE	G	
/13	38.7	20.7	969	PD	(220)	(40)	FG	
/14	35.9	28.9	972	PD	75	60SE	VG	
/15	35.1	40.7	960	HZ	90	80S	G	S
/16	30.9	53.9	924	PD	90	70S	VG	
/17	27.2	28-01.1	881	PD	80	70NW	VG	
8/8/75/1	32-26.4	28-12.2	838	PD	75	90	FG	S
/2a	33-10.1	07.5	884	HD	120	60SW	G	
/2b	00.3	09.1	878	PHD	95	85S	FG	
/3a	32-54.0	10.1	872	PD	--	--	--	
/3b	45.1	12.7	872	PD	80	80N	F	
/4a	17.0	12.1	914	HPX	--	--	D	S
/5a	17.6	16.0	908	HD	--	--	D	
/5b	13.4	27-43.0	972	HD	110	55SW	G	S
/6	10.3	52.7	1006	HD	75	55SE	FG	
/7	06.8	56.6	1030	HD	80	70S	G	
/8	04.1	28-03.6	1045	HD	75	90	G	
/9	01.8	07.9	1061	HD	70	90	G	

APPENDIX V

CATALOGUE OF FIELD DATA

1 Number	2 Longitude	3 Latitude	4 Elevation	5 Rocktype	Attitude 6 Azim.	Attitude 7 Inclin.	8 Q.	9 Notes
8/8/75/10	31-38.8	28-03.1	850	UB	--	--	D	
/13	43.4	04.0	893	UB+HD	100	45S	G	data in HD, S
/15	47.9	04.4	908	HD	90	65S	G	
/16	53.2	04.2	927	HD	110	75SW	G	
/17	55.8	03.8	1030	HD	130	80SW	G	
/18	57.0	27-59.9	945	HD	120	90	G	S
18/8/75/1	29-48.3	27-50.6	856	PD+HZ	--	--	--	S
/2a	42.0	47.1	884	S	170	90	F	
					(-)	(90)	FG	
/2b	54.9	30.0	1042	S	140	55NE	G	
/3	30-04.9	20.1	1097	S+UB	--	--	--	
/4	09.5	18.4	1113	HPX	--	--	D	
/5	14.2	18.0	1128	S	--	--	W	
/6	19.1	17.2	1161	T	150	60SW	FG	
/7	34.5	10.4	1262	S	(135)	(35)	G	
/8	41.1	14.9	1250	S	--	--	W	
/9	46.8	18.0	1250	S	--	--	W	
/10	51.2	20.5	1250	S	--	--	W	
/11a	55.3	23.2	1250	S	--	--	W	
/11b	57.7	21.7	1274	S	--	--	W	
/12	31-04.5	22.6	1292	HZ	--	--	W	S
19/8/75/1	32-57.3	26-37.2	887	HD	55	35NW	F	
/2	33-10.1	32.6	899	HZ	--	--	D	
/3	18.7	30.7	887	T	110	80NE	VG	S
20/8/75/1a	30-23.4	27-39.0	875	HPX	--	--	D	
/1b	25.9	39.9	905	HZD	--	--	D	S
/2	30.7	38.7	920	HZ	--	--	D	
/3	34.8	36.6	945	HZ	--	--	--	S
/4	36.0	33.4	960	T	120	90	G	S

APPENDIX V

CATALOGUE OF FIELD DATA

1 Number	2 Longitude	3 Latitude	4 Elevation	5 Rocktype	Attitude 6 Azim.	Attitude 7 Inclin.	8 Q.	9 Notes
20/8/75/5	30-33.4	27-29.9	960	T	130	90	G	
/6	29.1	27.3	975	T	130	80NE	F	
/7	23.9	26.5	966	T	135	90	FG	
/8	19.1	25.6	981	T	170	90	FG	
/9	10.4	43.9	826	PD	--	--	--	
21/8/75/1a	28-45.6	28-59.1	1152	S	150	75SW	G	
/1b	50.7	58.8	1152	S	30	75NW	G	
					(340)	(65)	G	
/2	53.5	56.7	1189	T	145	90	G	
/3	29-01.1	50.2	1247	T	140	70NE	G	
/4	05.1	50.5	1305	T	145	70NE	G	
/5	11.1	51.5	1359	T	140	70NE	G	
/6	21.4	52.3	1417	T	155	90	G	
/7	31.5	52.7	1469	T	150	90	G	
/8	38.5	51.5	1506	T	150	75SW	G	
/9	45.8	52.7	1487	T	130	90	G	
/10	53.0	54.0	1570	T	125	80NE	G	S
/11	30-02.2	50.9	1463	T	140	90	FG	
/12	09.8	51.7	1436	T	135	80NE	FG	
/13	13.4	47.6	1457	T	160	80SW	G	
/14	21.2	45.7	1433	T	145	65NE	G	
24/8/75/1	31-18.8	28-02.6	1387	HPX	--	--	D	
/2	16.5	03.7	1402	S+HZ	80	55N	G	data in HZ
/3	17.5	05.9	1448	S+HZ	--	--	--	
/4	13.9	09.4	1445	S+HZ	--	--	--	
/5	09.4	10.2	1439	HD	--	--	--	
/6a	30-42.6	27-59.7	1137	PD	--	--	--	
/6b	(see 18/7/75/7a)			PD	70	70NW	G	

APPENDIX V

CATALOGUE OF FIELD DATA

1 Number	2 Longitude	3 Latitude	4 Elevation	5 Rocktype	Attitude 6 Azim.	Attitude 7 Inclin.	8 Q.	9 Notes
24/8/75/7a	29-58.7	28-10.0	1027	OPX	--	--	D	S
/7b	Giant Mascot dump pile			HB	--	--	D	S
/7c	Giant Mascot dump pile			HB	--	--	D	S
/8a	29-39.7	28-11.9	985	HD	100	90	G	
/8b	37.4	11.0	951	HD	110	75NE	G	
/8c	41.9	09.8	948	HD	150	55NE	G	
/8d	45.1	09.0	945	HD	40	50NW	G	
/9	30-06.7	27-56.4	853	HB	--	--	D	
25/8/75/1	31-15.1	28-06.1	1436	S+HZ	110	90	FG	data in HZ
/2	16.5	09.9	1436	HZ	40	90	FG	
/3	16.5	12.2	1439	S+HZ	60	90	G	data in HZ, S
/4	16.3	14.5	1443	HB+HZ	50	90	F	S
/5	16.6	17.6	1457	HD	75	65N	G	shears
/6	19.6	16.4	1469	HD	120	70NE	G	
/7	24.7	15.9	1457	HD	--	--	W	
/8	18.0	23.5	1393	HZ	--	--	--	S
/10	30-58.6	25.7	1430	HD	110	90	F	
/11	41.1	29.5	1362	T	--	--	D	S
/12	39.5	34.8	1433	T+UB	--	--	W	
/13	39.5	38.1	1417	T	(-)	(90)	G	
25/8/75/14a	30-32.6	28-39.7	1442	T	120	80NE	G	
/14b	30.4	41.4	1448	T	130	75NE	G	
/15	35.6	35.0	1466	HD	--	--	D	S
/16	23.7	32.3	1372	HPX	--	--	--	
27/8/75/2a,b, c	29-41.2	27-55.2	792	PD+UB	--	--	--	S(2a,b,c), P(2a,c)
/3a,b	(see 20/8/75/1b)			HD+UB	--	--	--	S(mafic dyke)
28/8/75/1a,b	30-54.0	28-02.2	1274	PD+UB	--	--	--	S(1a,b)
13/9/75/1	29-28.5	28-10.2	853	T+HB	--	--	--	S

APPENDIX V

CATALOGUE OF FIELD DATA

1 Number	2 Longitude	3 Latitude	4 Elevation	5 Rocktype	Attitude 6 Azim.	Attitude 7 Inclin.	8 Q.	9 Notes
								S
13/9/75/2	30-02.4	27-59.6	869	UB	--	--	--	
15/9/75/1a	33-43.0	25-57.3	707	PD	(220)	(25)	FP	
/1b	34-06.4	49.3	698	PD	45	25NW	FG	
/2	42.1	45.6	732	PD	165	50NE	VG	
/3	35-10.5	35.0	796	PD	155	40NE	VG	
/4	13.6	13.4	588	PD	170	45E	FG	
/5	42.7	45.8	683	PD	170	55E	VG	
15/9/75/6	36-14.7	26-17.5	716	PD	10	55E	VG	
/7	29.6	27-06.0	789	HD	35	65SE	FG	
/8	35-59.5	20.3	954	HD	70	90	VG	
/9	36-16.3	31.4	893	HD	70	75SE	G	
/10	10.9	40.1	942	HD	50	80SE	G	
/11	33-35.8	26-01.7	744	PD	145	25SW	FG	
/12	24.4	05.4	860	PD	120	45SW	VG	
/13	31-02.4	06.0	796	T	125	25NE	G	
/14	19.6	21.7	792	HD	165	?	P	
AM#2	29-04.8	22-50.5	122	HB	--	--	D	S,P
2600	30-06.3	27-55.6	853	HB	--	--	D	P

GEOLOGY BETWEEN THE FRASER RIVER AND EMORY CREEK, NORTHWEST OF HOPE, B. C.

by Mark R. Vining, 1977

LEGEND

EOCENE

- Conglomerate and sandstone

UPPER CRETACEOUS

- Hornblendized tonalite or diorite
- Tonalite
- Hornblende diorite
- Pyroxene diorite

CRETACEOUS (?)

- Giant Mascot Body: Hornblendite, pyroxenite, peridotite, and dunite

UPPER PALEOZOIC

- Chilliwack Group: Pelite, greenstone, and minor limestone

AGES UNKNOWN

- Gabbro, hornblendite, and pyroxenite
- Settler Schist: Pelitic schist; minor marble, quartzite, and calc silicate rock
- Custer Gneiss: Gneiss, migmatite, and amphibolite

FAULT

- thrust
- high angle

Position known approx. uncertain

CONTACT

Position known approx. uncertain

Metamorphic Foliation

Igneous Foliation

MINERALOGICAL ZONATION IN THE SPUZZUM PLUTON

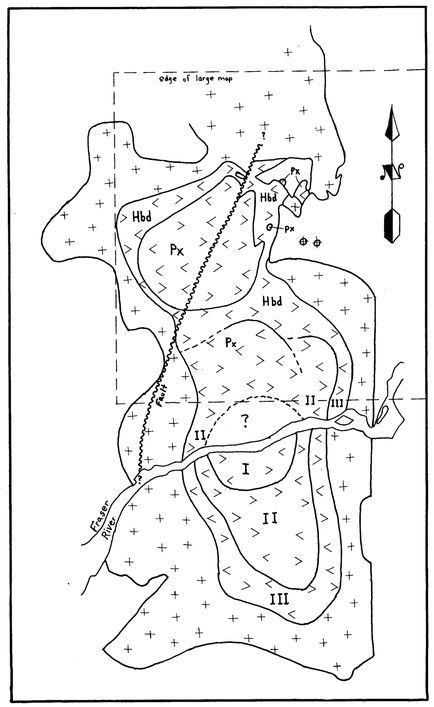

SCALE 1:125,000

KILOMETRES 0 2 4 6 8

Diorite undivided

Tonalite

Geology after Richards and McTaggart (1976) and this study

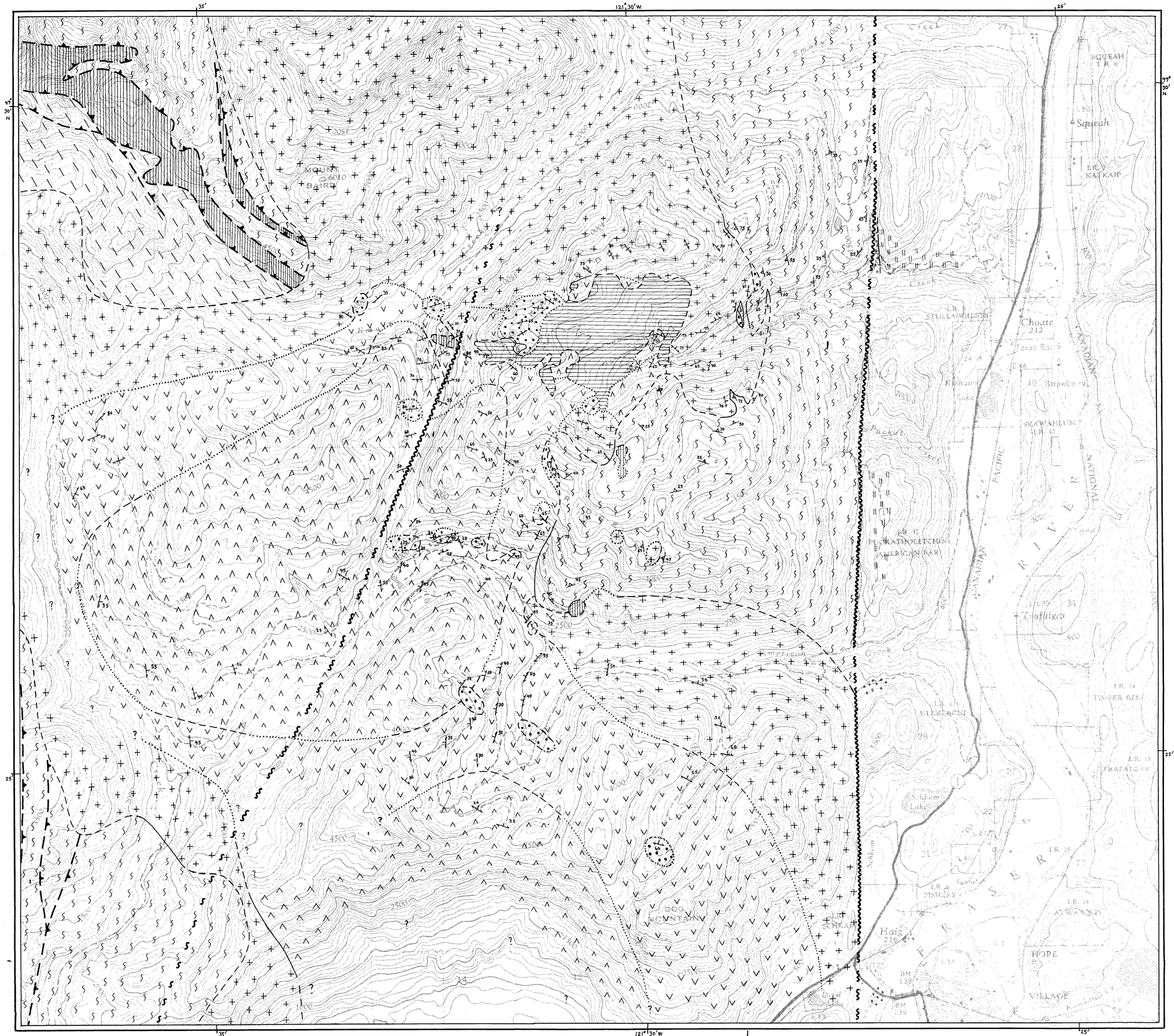

Geology in outlying areas after: Monger (1970), Richards (1971), Lowes (1971), and Pigage (1973)

SCALE 1: 25,000

tenths 0 MILES 1 2

tenths 0 1 2 3 KILOMETRES

Base map modified after National Topographic Series Maps:

Sheet 92 H/5 — Harrison Lake
Sheet 92 H/6 — Hope
Sheet 92 H/12 — Mount Urquhart
Sheet 92 H/11 — Spuzzum